6-2007

# Laboratory Based Chemical and Isotopic Investigations on Biotic (Microbial) and Abiotic Reduction of Iron and Oxidation of Organic Compounds

Tsigabu Asmelash Gebrehiwet
*Western Michigan University*

# LABORATORY BASED CHEMICAL AND ISOTOPIC INVESTIGATIONS ON BIOTIC (MICROBIAL) AND ABIOTIC REDUCTION OF IRON AND OXIDATION OF ORGANIC COMPOUNDS

by

Tsigabu Asmelash Gebrehiwet

A Dissertation
Submitted to the
Faculty of The Graduate College
in partial fulfillment of the
requirements for the
Degree of Doctor of Philosophy
Department of Geosciences

Western Michigan University
Kalamazoo, Michigan
June 2007

This dissertation is dedicated to my beloved younger brother, Habtom Asmelash Gebrehiwet, whom my family and I lost on March 5, 1999.

## ACKNOWLEDGMENTS

First and foremost I would like to thank my advisor Prof. R.V. Krishnamurthy for his day to day encouragement and help from start to finish of this dissertation. I would also like to thank Dr. Carla Koretsky, Dr. Eliot Atekwana and Dr Johnson Haas for their invaluable insight during this research and for being my dissertation committee. The help and generosity of the Microbial Aqueous Geochemistry, Biogeochemistry and Thermodynamics (MAGBAT) Laboratory of Dr. J. Haas, and Aqueous Biogeochemistry Laboratory of Dr. C. Koretsky at WMU is highly appreciated. Thanks to Elizabeth Semkiw for her help in running HPLC and GC instruments; the Water Quality Laboratory of Dr. M. Barcelona for letting me to use HPLC and GC instruments.

This work and my career development would not have been possible without the patience, understanding, encouragement and support of my parents, sisters, brothers, and my fiancée, Saba Tesfazghi. Dr. Ahmed Murad and Dr. Loago Molwalefhe are highly appreciated for showing me the ins and outs of the Stable Isotope Geochemistry Laboratory. I would like also to thank Kathy Wright, Elizabeth Steele, Nathaniel Barnes, Steve Beukema, and Haile Mengistu for their help at various stages. My appreciation continues to all friends in the department and around the world for their moral support during my study.

I am so grateful to the Faculty Research and Creative Activities Support Fund (FRACASF), the Monroe Brown Life Science Graduate Research Award, the Graduate College and Department of Geosciences at WMU for the financial support.

Tsigabu Asmelash Gebrehiwet

# LABORATORY BASED CHEMICAL AND ISOTOPIC INVESTIGATIONS ON BIOTIC (MICROBIAL) AND ABIOTIC REDUCTION OF IRON AND OXIDATION OF ORGANIC COMPOUNDS

Tsigabu Asmelash Gebrehiwet, Ph.D.

Western Michigan University, 2007

Studies using chemical and isotopic techniques have been conducted to investigate experimental microbial (biotic) iron reduction and abiotic redox processes. In the microbially mediated study Fe(III) reduction and lactate oxidation at circum-neutral pH and anaerobic conditions were used to characterize the metabolic pathways followed by dissimilatory $Fe^{+3}$-reducing bacterium *Shewanella putrefaciens strain 200R*. Iron (II), Iron (III), dissolved inorganic carbon (DIC) and carbon isotope ratios were measured under bicarbonate and phosphate buffered conditions. Carbon isotope disproportionation among organic carbon substrate (lactate), biomass and respired carbon dioxide at the lag to stationary phase of the microbial growth curve showed that bicarbonate buffered system has an enhancing effect in the reduction process compared to the phosphate system. Both buffered systems resulted in carbon isotope fractionations between the lactate substrate and DIC that could be modeled as a Rayleigh type process. The biomass produced under both buffer conditions was depleted on average by ~2 ‰ relative to the substrate and enriched by ~5 ‰ relative to the DIC. This translates to an overall isotopic fractionation of 10 – 12 ‰ between the biomass and respired $CO_2$ in both buffering systems and could explain the depleted isotopic signatures reported by previous workers during the serine metabolic pathway.

Abiotic oxidation of organic compounds as a function of electron acceptors, media composition, and pH in the presence and absence of fluorescent light was investigated. Sample collections and analytical techniques were similar to the biotic experiments. Abiotic results showed that HFO media resulted in the generation of

more DIC compared to ferric citrate containing media. Type of buffer showed little effect on the redox process. Light and pH had major roles in the oxidation of citrate and lactate in the presence of ferric iron. Under dark conditions in the presence or absence of Fe (III) the DIC produced was very low in all pH conditions. The slower redox processes observed in our abiotic study, compared to previous studies, could be due to inhibiting effect of chloride ions on photochemical reactions. Chloride and bicarbonate ions have a scavenging effect on the hydroxyl radical. Isotopic results of both bicarbonate and phosphate buffered systems, at neutral pH condition, approached the $\delta^{13}C$ values of citrate/lactate used. Rayleigh type process in the bicarbonate buffered abiotic media was modified due to the involvement of bicarbonate in the scavenging of the hydroxyl radicals in the system.

TABLE OF CONTENTS

Table of Contents—continued

CHAPTER

Table of Contents—continued

Table of Contents—continued

APPENDICES

LIST OF TABLES

LIST OF FIGURES

# CHAPTER I

# INTRODUCTION

## Statement of the Problem

Microorganisms are an integral part in the biogeochemical cycling of metals (toxic and non-toxic) and organic compounds including contaminants in the natural and engineered environments. Understanding their metabolic pathways has been the subject of different interdisciplinary studies from molecular to field scale. Since the pioneering work by Lovely and Phillips (1988), two of the most studied microbes in the field of bioremediation of toxic metals and organic compounds have been *Geobacter* and *Shewanella* species. These have been studied extensively based on genomic analyses and conventional chemical analyses. The application of stable isotopic fractionation based studies in metal ion reducing bacteria coupled with oxidation of organic compounds is relatively recent compared to genomic and conventional chemical transformation studies (e.g. Teece et al., 1999, Zhang et al, 2003). Distinct signatures of isotope fractionation between biomass and synthesized fatty acids (Teece et al., 1999, Zhang et al, 2003) and biomass and respired $CO_2$ (this study) could differentiate the predominant metabolic pathways followed by different microbes.

Abiotic photooxidation of organic compounds and reduction of metals has been a subject of interest among a wide range of scientific communities due to its

importance in the fields of waste water treatment, understanding atmospheric chemistry, *in situ* degradation of those contaminants which are hard to degrade microbially, and the role they play in wetland organic matter oxidation (e.g. Deng et al., 1998; Hornibrook et al., 2000; Minero et al., 2005; Li et al., 2006; Vione et al., 2006; Zhang et al., 2006).

## Objective of the Study

The main objectives of this study are 1) gain a mechanistic understanding of the metabolic pathways followed by microbial organisms at the molecular level and (2) investigate the factors controlling abiotic photochemical oxidation of organic compounds; Experimental methodological approaches employed include chemical analyses of redox-sensitive species (Fe(II), Fe(III), oxidation products (dissolved organic carbon (DIC)), remaining lactate, pH and stable carbon isotopes of the DIC. Correlation of chemical and isotopic results would be used to addressing the question concerned. .

## Significance of Study

Organic carbon source, biomass, respired carbon dioxide are the three carbon reservoirs in the oxidation-reduction process. Since studies related to the third reservoir, especially in terms of isotope systematic, have been limited, obtaining fundamental data would give an added dimension to our understanding of the reduction process involved. The preferential uptake of lighter carbon isotopes by the microorganisms during the synthesis of their fatty acids is the key to the isotopic application in this kind of study. The use of carbon isotope fractionation in

differentiating the various carbon dioxide fixation pathways could have implications for understanding of bioremedial strategies and in the quest for alternative energy cultivation. This research will investigate stable carbon isotope fractionation between respired carbon dioxide and bacterial biomass and provide additional information in characterizing the metabolic pathway followed by *Shewanella putrefaciens* used as model bacteria. This will be discussed and presented in detail in the third chapter of this thesis.

The controlling factors in abiotic photooxidation of organic compounds are media compositions; sensitizing agents (e.g. Fe (III)); and pH. Previous research was focused on the photooxidation of organic compounds at low pH (<5) conditions. This research will compare and contrast qualitatively the effect of the controlling factors at a wider range of pH (5<pH<9) and anaerobic conditions.

# CHAPTER II

# METHODS OF INVESTIGATION

## Sample Collection

Data presented in the current study were based on experiments designed in the laboratory. Laboratory experiments comprised time series analysis of samples collected in microbially mediated and abiotic systems. Microbial mediated experiments were carried out to investigate the effect of buffering compounds on the reduction rate of ferric iron and associated carbon isotope fractionation using *Shewanella putrefaciens,* commonly found microbial species, as a model bacterium. Abiotic experiments were conducted the effect of pH, buffering compounds and ferric iron on the oxidation of organic compounds under fluorescent light exposed and anaerobic conditions. All the data are presented in Appendix C (microbial based study), D (Abiotic experiments).

## Media Preparation and Bacterial Cultures

All experiments other than the DIC extraction and isotopic analysis were carried out in the Microbial Aqueous Geochemistry, Biogeochemistry and Thermodynamics (MAGBAT) and Aqueous Biogeochemistry Laboratories of Dr. Johnson Haas and Dr. Carla Koretsky. *S. putrefaciens* strain 200R bacterium was used to perform two parallel batch experiments using two different buffering compounds with ferric citrate as electron acceptor and sodium lactate as electron donor. The bacteria were maintained

in an autoclaved Luria Bertani (LB) growing medium containing Trypton (10 g/L), yeast extract (5 g/L) and NaCl (10 g/L) (Difco Laboratories, Detroit, MI) at 30 °C for 24 hours to facilitate their growth to the mid log phase. The microbes were harvested and washed three times with 0.1 M NaCl to remove the likely interference from the LB media in the subsequent isotopic analyses.

Microbial based experiments were carried out using BD vacutainer serum tubes (Vacutainer© serum tubes Becton Dickson and Company, Franklin Lakes, NJ) of volume 15 ml/L/L containing 8ml/L/L medium in a $CO_2$ free anaerobic glove box puffed with >95 % $N_2$ and ~4 % $H_2$ (Coy Laboratories, Inc., Grass Lake, MI). In each case 10 - 12.5 µl/ml of aerobically grown and re-suspended in 0.1 M NaCl supernatant solution *strain 200R* were inoculated into a defined medium resulting in a cell density of 2 - 4 . $10^8$ cells/ml (Haas et al., 2001). The medium was dispensed into the air-tight and sterilized vacuutainer tubes using syringe and needle within the anaerobic chamber after spurging with nitrogen gas to exclude dissolved oxygen and carbon dioxide. A defined circum neutral pH medium was prepared with components containing: $NH_4Cl$ (4.7 mM), $NaH_2PO_4.H_2O$ (4.4 mM), and KCl (1.4 mM), vitamins (0.1 ml/L), Wolfe's minerals (1 ml/L), sodium lactate (35 mM), ferric citrate (50 mM), and sodium bicarbonate ($NaHCO_3$, 30 mM) or potassium phosphate ($KH_2PO_4.3H_2O$, 50 mM). Lists of the components of the whole medium, Wolfe's minerals and vitamins solutions can be referred from Appendix A. Ferric citrate (500 mM) stock solution was prepared using autoclaved double-dionized water (R~ 17.6 MΩ cm) amended with reagent-grade ferric citrate (Fischer Chemical ®, Pittsburgh,

PA) and 10 N NaOH (Haas et al., 2001). The stock solution was stirred for 24 hours and heated for one hour while adding NaOH and pH was adjusted to ~7. Prior to adding the vitamins, Wolfe's trace minerals, and electron acceptors inside the glove box, the rest of the media components were autoclaved. Biotic experiments were done by shaking (50 rpm) at 30°C until extraction and subsequent chemical and isotope analyses.

Sampling was done at various stages along the microbial growth curve (Figure 2.1). The experiments were continued for about 350 hours. During each sampling period duplicate samples were taken under fluorescent light exposed and dark conditions.

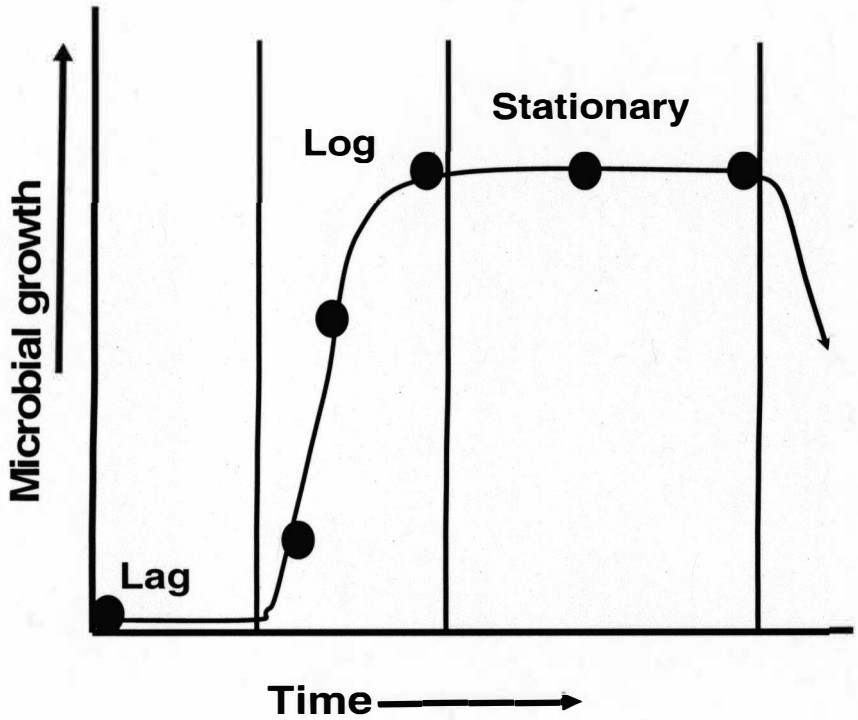


Figure 2.1 Schematics of temporal sampling in the microbial mediated experiments. The lag phase represents adaptation period of the microbes with the media prepared; The log (exponential) phase is curve at which the maximum growth of the microbial population takes place and The stationary phase represents period of no substantial growth in the microbial population as a result of various limiting factors such as maximum cell density, used up electron acceptor/donor, nutrients and so on. Black circles represent relative sampling frequencies at the different growth stages.

Abiotic Media Preparation

Media preparation in the abiotic experiments was similar to the ferric citrate based biotic experiments discussed above. For the abiotic systems, an additional experiment was carried out using HFO (70 mM) as electron acceptor and potassium phosphate as a buffering compound. Solid HFO (2-ferrihidryite) was added, which

was prepared using the method discussed by Schwertmann and Cornell (2000), into each vacuutainer tube. Briefly, Fe $(NO_3)_3.9H_2O$ (80 g/L) dissolved in a DDIW with 330 ml/L of 1 M KOH and pH was adjusted to ~7.7. The prepared solution was stirred for 1 hour before repeated centrifuging for 5 min at 1500 rpm to remove any impurities. Then the solution was filtered using 0.2 μm sized filters before freeze-drying. HFO looses its structure on heating above 80 °C, so to preserve its structure HFO was added in the anaerobic chamber after autoclaving the rest of the media components. The pH of abiotic media was maintained between 5 and 9 based on the objective of the experiment as discussed below.

Media Complexity Eight 500 ml/L Pyrex bottles were autoclaved and filled with defined salt media by omitting one media component at a time ($NH_4Cl$, $NaH_2PO_4.H_2O$, KCl, vitamins, wolf's minerals, sodium lactate, ferric citrate, or the buffering agent $KH_2PO_4.3H_2O$) from each bottle. Each bottle was set to pH of approximately 7.1 by adding HCl drop wise. All respective media components with the exception of minerals and vitamins were added before autoclaving. For each experimental setup 6 vacutainer tubes of 15 ml/L volume were loaded with 8 ml/L solution of the media within the anaerobic chamber after spurging each with nitrogen for an hour. All samples were taken in duplicates and a pair of samples from each Pyrex bottle was taken before starting to shake to know the starting values. These set of experiments continued for about 2900 hours (~ 121 days).

Fe(III) Compounds Set of experiments with ferric citrate and HFO as Fe(III) containing compounds were used to examine the effect of ferric iron-complex compounds on the oxidation of the organic compounds under our experimental

conditions.

Buffer Type The effect of two buffering compounds, $NaHCO_3$ and $KH_2PO_4.3H_2O$, on the generation of carbon dioxide and soluble ferrous iron were compared under both dark (wrapped by aluminum foil) and fluorescent light conditions. Each sample from both conditions was treated similarly and the experiments were carried out for pH 5 and 7 to check the relative importance of two of the controlling factors, pH and fluorescent light.

Effect of pH The effects of pH on the photooxidation of ferric citrate and sodium lactate was investigated in the presence of light for pH varying from acidic (pH ~5) to alkaline pH (pH ~9) conditions for both bicarbonate and phosphate buffered systems.

Photoreaction System Photooxidation of organic compounds were investigated in the presence and absence of light and Fe(III) in the acidic (pH ~5) to neutral (pH ~7) pH conditions for both bicarbonate and phosphate buffered systems. This portion of the experiment was done to compare and contrast the effect of pH, Fe(III) and light on the redox process.

## Analytical Methods

### Chemical Analyses

Time series sampling for aqueous Fe(II)/Fe(III) concentration was done by sacrificing one sample tube at a time. Samples were filtered through 0.2 μm nylon filter to measure the dissolved $Fe^{+2}$ and total iron. Iron concentration was determined using UV/VIS spectrophotometer absorbance wavelength of 562 nm by the ferrozine

method under anaerobic conditions and is reported in mg/l of Fe (II)/Fe(III) (Viollier et al., 2000). Calibration curves were prepared in each experiment using five point standards with the Ferrozine method by preparing known standards. See Figure A1 in Appendix A for a typical calibration curve and measured data. The pH of each sample was determined using a portable pH/mV meter (Fisher Scientific®, Pittsburgh, PA). Time series oxidation of lactate was monitored using High Performance Liquid Chromatography (HPLC) on samples preserved in 3 N HCl following pH and soluble iron measurements. Twenty micro liters of sample was injected into the HPLC port manually to determine the concentrations of remaining lactate, acetate, and citrate. The resulting retention times of the respective samples were compared with standards prepared in the water quality laboratory of Dr. Michael Barcelona, chemistry department, Western Michigan University (Result of the analysis is shown in Appendix A, Table A1).

X-ray Diffraction

Samples for X-ray diffraction (XRD) were prepared from precipitates formed in the phosphate-buffered reduction experiments by smearing the slurry on glass slides within the anaerobic chamber. The slides were dried using acetone, and kept in the glove box till the time of analysis. XRD patterns of the selected samples with precipitate were determined using Rigaku® in the geochemistry lab. The XRD patterns were compared with known mineral standards (International Center for Diffraction Data) to determine the mineralogical composition of the precipitates.

Stable Carbon Isotope Analyses

Biotic Experiments Aliquots of samples were analyzed for DIC and stable carbon isotope ratios (Krishnamurthy et al., 1997, Atekwana & Krishnamurthy, 1998). The carbon isotopic composition of sodium lactate, sodium acetate, ferric citrate and bacterial biomass was determined from $CO_2$. Dry weighed samples of these organic compounds were loaded to 9 mm O.D. quartz tube for combustion with ~1 g CuO at 900 °C. Total biomass for carbon isotopic analysis was determined from *S. putrefaciens* harvested in 40 ml/L of the media according to the method described in Zhang et al. (2003). The stable carbon isotopic ratio of sodium bicarbonate used as a buffering agent was analyzed by reacting with 85 % phosphoric acid (Krishnamurthy et al., 1997).

Carbon isotope measurements were made using a VG IRMS (Isotope Ratio Mass Spectrometer) and the results are reported in the traditional δ notation relative to Vienna PeeDee Belemnite (V-PDB) standard:

$$\delta^{13}C\ ‰ = (R_{Sample} / R_{Standard} - 1)*1000 \quad \text{.....} \quad (2.1)$$

Where: $R_{Sample}$ and $R_{Standard}$ represent the $^{13}C/^{12}C$ ratio of the sample and standard respectively. The overall precision of the analytical processes are better than 0.1 ‰ for $\delta^{13}C$, $\delta^{13}C_{org}$, $\delta^{13}C_{Inorg;}$ and 1 % for carbon dioxide measurements.

Abiotic Experiments All abiotic samples were treated with cupric oxide at ~900 °C to purify other gases produced during the photochemical reactions before subsequent isotope ratio measurements. This purification resulted in much cleaner isotope ratio traces.

# CHAPTER III

## ISOTOPIC AND CHEMICAL INVESTIGATIONS OF FE (III) REDUCTION BY *SHEWANELLA PUTREFACIENS STRAIN 200R*

### Introduction

Facultative microbial species respire and perform their metabolic processes under aerobic and anaerobic conditions depending on the available sources of energy (Myers & Myers 1997; Haas & DiChristina 2002; Nealson et al., 2002). Most bacteria in the subsurface (e.g. *Shewanella)* metabolize anaerobically, offering clues that under anaerobic and circum-neutral pH conditions, they could utilize metals (e.g. $Fe^{+3}$, $Mn^{+4}$, $Cr^{+6}$, $U^{+6}$) as sole terminal electron acceptors in their respiratory processes (Haas et al., 2001). *S. putrefaciens* is a facultative gram negative bacterium commonly found in the subsurface environment at the oxic-anoxic interface (e.g. DiChristina & Delong, 1994; Teece et al., 1999). Dissimilatory metal reducing bacteria in general and *S. putrefaciens* in particular play vital roles in the biogeochemical cycling of metals, carbon and other redox sensitive elements within the sedimentary environment and groundwater systems (Nealson et al., 2002; Roden, 2004).

Iron, the $4^{th}$ most naturally occurring element, is a significantly utilized transition metal in the sedimentary environment (Schwertmann & Cornell, 2000; Kappler & Straub, 2005). Reduction of iron at circum-neutral pH is facilitated by

anaerobic microbial metabolism (Romanek et al., 2003). In most natural waters $Fe^{+3}$ and $Mn^{+4}$ are insoluble at near neutral pH, which makes it a more challenging respiration processes for the microbes compared to soluble electron acceptors such as oxygen and nitrate (Zachara et al., 1998; Haas et al., 2001; Haas & DiChristina, 2002; Luu & Ramsay, 2003; Fredrickson et al., 2003). The kinetics and thermodynamics of the chemical transformations during microbial reduction of environmentally significant metals coupled with oxidation of lactate, acetate, or $H_2$ has been documented under different experimental conditions (Lovley & Phillips, 1988; Lovley, 1991, 1993; Fredrickson et al., 1998; Zachara et al., 1998; Haas et al., 2001; Zhang et al., 2001; Romanek et al., 2003; Roden, 2003, 2004). Isotopic studies related to these environmentally significant biogeochemical cycling processes are limited.

Recent isotopic studies associated with biogeochemical processes have provided clues in understanding the fate of contaminants, metabolic pathways of microorganisms and in reconstructing earth's evolutionary history (e.g. Teece et al., 1999; Zhang et al., 2001; Romanek et al., 2003; Zhang et al., 2003; Somsamak et al., 2006). Studies of Zhang et al. (2001) and Romanek et al. (2003) focused on isotopic fractionation during the formation of iron carbonate during microbial respiration of carbon dioxide. However, the formation of precipitate, which depends on the dominant electron acceptor and buffering compounds in a system, is not always the case (Frederickson et al., 1998; Romanek et al., 2003). Teece et al. (1999) and Zhang et al. (2003) studied the carbon isotope fractionation between microbial biomass and fatty acids synthesized. In addition to the carbon source and biomass, respired carbon

dioxide and other oxidation products (e.g. acetate, formate) constitute important carbon reservoirs in the oxidation-reduction process.

Additional data from studies focusing on the carbon isotope fractionation between the respired carbon dioxide and bacterial biomass during microbial metabolism would improve our understanding of the metal reduction process involved. The main objective of this study was to investigate carbon isotope fractionation between respired carbon dioxide and carbon substrate (lactate) during the reduction of iron by of *S. putrefaciens* (200R). Towards this, total DIC produced was used as a proxy for the time-dependent consumption of lactate according to the following generalized enzymatically (lactate dehydrogenase, $NAD^+$) mediated reaction (3.1), which was further verified by measuring the remaining lactate in the media using HPLC techniques.

$$\underset{\text{(Lactate)}}{NaCH_3CH_2OCHOO(aq)} + 4FeC_6H_5O_7(s) + 2H_2O + NAD^+ \rightarrow HCO_3^-(aq) + 4Fe^{2+}(aq) + \underset{\text{(Citrate)}}{4C_6H_5O_7^{-3}(aq)} + \underset{\text{(Acetate)}}{NaCH_3COO(aq)} + NADH + 5H^+ \quad (3.1)$$

Additionally, this research was aimed at comparing the effects of bicarbonate and phosphate buffering agents on the carbon isotope signatures during anoxic reduction of Fe(III), given their widespread occurrence in the natural environment. An understanding of the reduction process at molecular levels might shed light on mechanistic pathways and likely have environmental implications for natural and engineered remediation strategies of contaminated sites dealing with fate and transport of organic and inorganic contaminants (Fredrickson et al., 2003).

# Results and Discussion

## Iron Reduction and Variation in pH

The results of $Fe^{2+}$ and pH measurements are shown in Table 1. The reduction of iron and oxidation of lactate occurred in both the bicarbonate and phosphate buffered media. However, the reduced form of iron was lower than the theoretically calculated values based on the lactate to total iron reduced ratio of 1:4 (Fredrickson et al., 1998; Roden, 2004). In this study, we measured the aqueous form of Fe (II)/Fe(III) which could be responsible for the observed discrepancy in both buffered systems (Fredrickson et al., 2003). In addition, reduced iron could also be present in the form of precipitates and adsorbed onto bacterial and other surfaces.

We observed that a greater degree of reduction of ferric iron and DIC generation occurred in the bicarbonate-buffered system consistent with previous studies (Zhang et al., 2001). Also, there should be generally a linear relationship between the concentrations of reduced form of iron and the production of carbon dioxide (Zhang et al., 2001). Both the bicarbonate- and phosphate-buffered experiments showed relatively low regression ($r^2$=0.5) value between soluble Fe (II) and DIC likely due to the formation of precipitates in the phosphate-buffered system and the adsorption of the metal ions on bacterial surfaces in the bicarbonate system (Liu et al., 2001). This was supported by the observation where in the phosphate-buffered media, dissolved iron concentrations decreased with time, coinciding with the formation of precipitates whereas in the case of the bicarbonate-buffered media no such process was observed. The formation of precipitates was observed visually

after about 129 hours, the time when the aqueous $Fe^{+2}$ values started to decrease (Figure 3.1). Based on XRD analysis the precipitate in the phosphate buffered system was identified as a mineral similar to vivianite ($Fe_3 (PO4)_2.8H_2O$). In the bicarbonate system no detectable precipitation was observed, which was probably due to the chelating of soluble ferrous iron by the dissolved citrate (Frederickson et al., 2003; Romanek et al., 2003). However, visual inspection indicated dark green coatings (probably green rust) on the rubber septum of the serum tubes in the bicarbonate-buffered system (Zachara et al., 2002). The amount of coating was observed to increase with time.

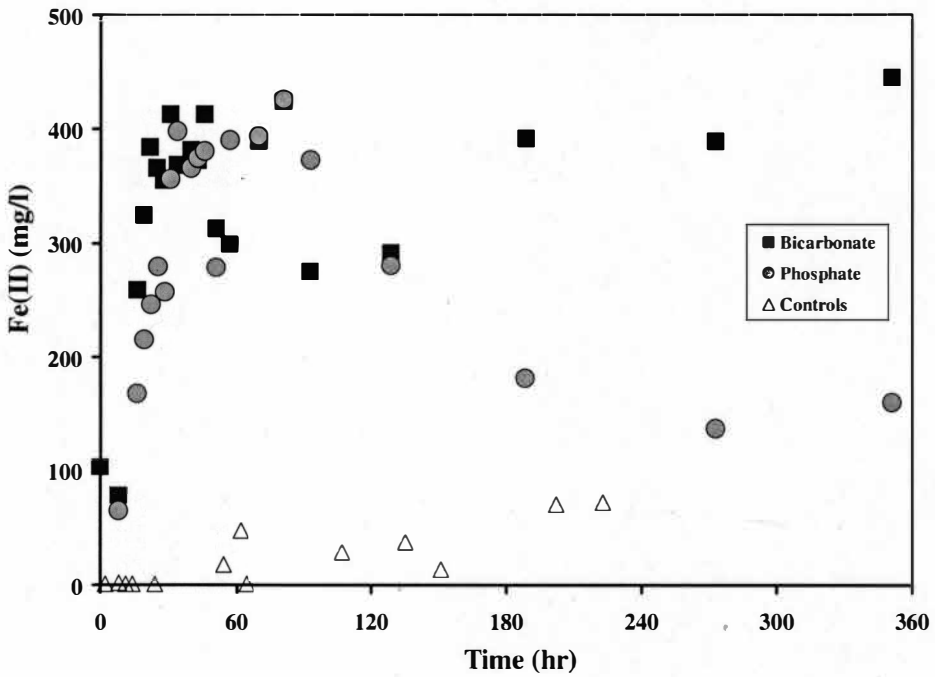


Figure 3.1 Aqueous $Fe^{2+}$ produced during the reduction process as a function of time for the bicarbonate (black squares), phosphate (shaded circles) buffered systems and control samples (open triangles).

Dissolved Inorganic Carbon, Biomass and Lactate Oxidation

In calculating the DIC yield and carbon isotope values for the samples containing bicarbonate media, corrections of the DIC and isotopic values were made for the initial added bicarbonate. Acidification of lactate, acetate and ferric citrate resulted in negligible $CO_2$ yield, suggesting that these compounds did not contribute any $CO_2$ to DIC produced during acidification of samples. Comparing the two buffered systems, the bicarbonate-buffered media was observed to generate higher DIC, indicating a faster and higher rate of lactate oxidation (Figure 3.2). Moreover, there was near complete oxidation of lactate in the bicarbonate media, whereas ~10 % of the lactate still remained in the phosphate system at the end experiment (Figures 3.2 & 3.3, Table 3.1). Both the DIC (Figure 3.2) and lactate (Figure 3.3) data support our argument that a greater degree of oxidation of lactate took place in the bicarbonate system. The total biomass yield also indicates that more bacterial growth occurred in the bicarbonate buffered system (Table 3.2, Figure 3.4).

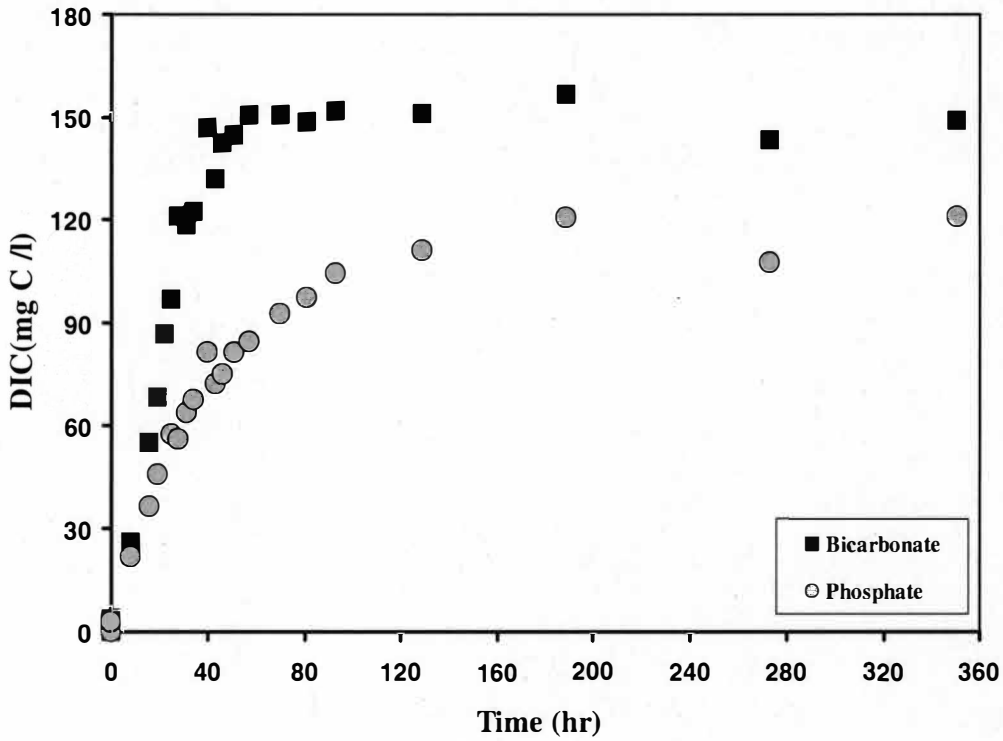


Figure 3.2 DIC versus time of reaction during the reduction process for both bicarbonate (black squares) and phosphate (shaded circles) buffered systems. The bicarbonate-buffered experiments are corrected for initial DIC.

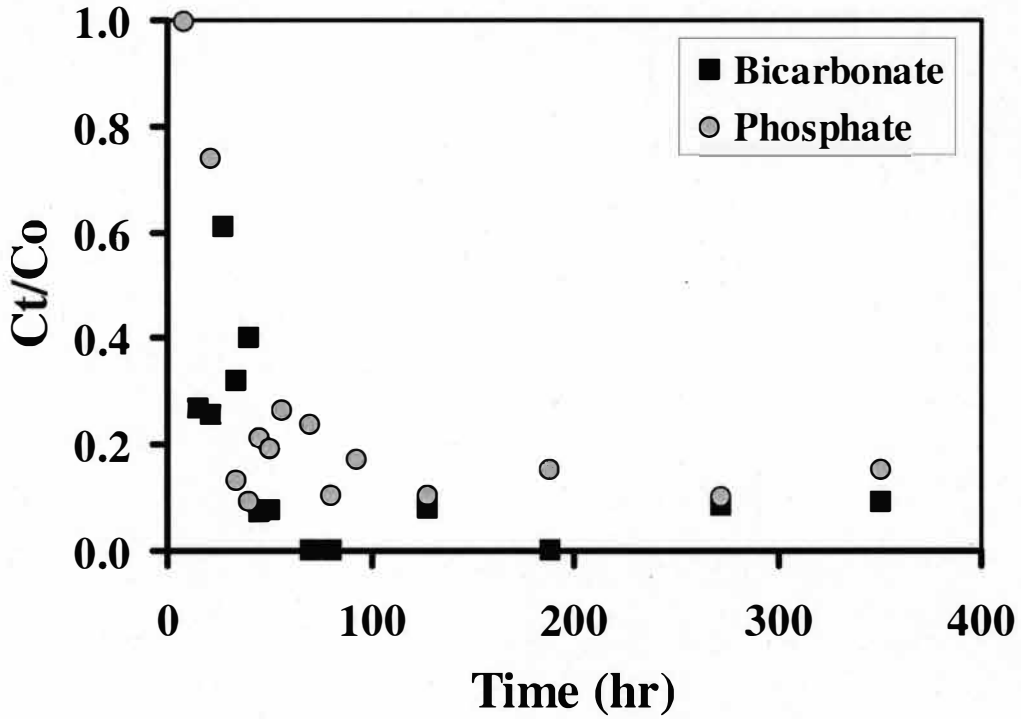


Figure 3.3 Ratios of remaining lactate at time t ($C_t$) to initial lactate ($C_0$) as a function of reaction time during the reduction process for the bicarbonate- (black squares) and phosphate- (shaded circles) buffered systems.

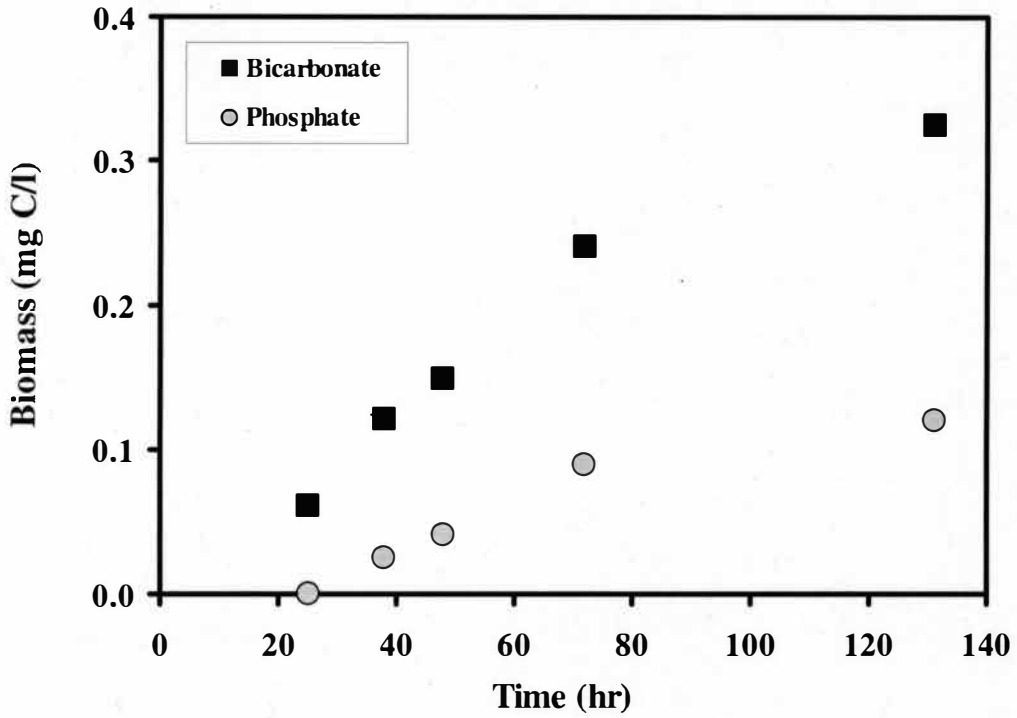


Figure 3.4 $\delta^{13}C$ values of microbial biomass as a function of remaining lactate fraction for the bicarbonate- (black squares) and phosphate- (shaded circles) buffered systems.

Table 3.1

Time (hr) series measurements of pH, Fe (II)(mM), DIC (mM), Lactate remaining (ppm) and $\delta^{13}C_{DIC}$ (‰) for bicarbonate- and phosphate-buffered conditions (ND Not detected, NA Not measured). SPFe21: stands for SP (*S. putrefaciens*), Fe for iron reduction experiment and 21 time series sample number.

| Buffer | Sample | Time | pH | $Fe(II)_{aq}$ | DIC | Lactate | $\delta^{13}C_{DIC}$ |
|---|---|---|---|---|---|---|---|
| | SPFe61 | 0 | 7.3 | 7.53 | 0.3 | 2124.8 | -29.0 |
| | SPFe62 | 8 | 7.4 | 5.72 | 2.2 | NA | -29.8 |
| | SPFe63 | 16 | 7.5 | 18.97 | 4.6 | 936.1 | -28.5 |
| | SPFe64 | 19 | 7.4 | 23.86 | 5.7 | NA | -27.8 |
| | SPFe65 | 22 | 7.9 | 28.16 | 7.2 | 895.7 | -27.3 |
| | SPFe66 | 25 | 7.9 | 26.81 | 8.1 | NA | -27.1 |
| | SPFe67 | 28 | 7.8 | 26.09 | 10.1 | 1334.9 | -27.0 |
| | SPFe68 | 31 | 7.8 | 30.19 | 9.9 | ND | -27.2 |
| | SPFe69 | 34 | 7.8 | 27.01 | 10.2 | 1110.6 | -27.2 |
| | SPFe70 | 40 | 7.9 | 27.99 | 12.2 | 1395.9 | -26.4 |
| | SPFe71 | 43 | 7.8 | 27.34 | 11.0 | ND | -27.1 |
| $NaHCO_3$ | SPFe72 | 46 | 7.8 | 30.19 | 11.8 | 245.0 | -26.7 |
| | SPFe73 | 51 | 7.8 | 22.98 | 12.0 | 271.6 | -26.5 |
| | SPFe74 | 57 | 7.8 | 21.96 | 12.5 | ND | -26.2 |
| | SPFe75 | 70 | 7.8 | 28.55 | 12.5 | ND | -26.4 |
| | SPFe76 | 81 | 7.8 | 31.11 | 12.4 | ND | -26.4 |
| | SPFe77 | 93 | 7.8 | 20.25 | 12.6 | ND | -26.4 |
| | SPFe78 | 129 | 7.9 | 21.40 | 12.6 | 282.0 | -25.7 |
| | SPFe79 | 189 | 7.9 | 28.72 | 13.0 | ND | -26.2 |
| | SPFe80 | 273 | 7.9 | 28.55 | 11.9 | 291.4 | -26.9 |
| | SPFe81 | 351 | 7.9 | 32.62 | 12.4 | 315.0 | -26.6 |
| | SPFe21 | 25 | 7.6 | 15.34 | 6.04 | NA | -26.5 |
| | SPFe21 | 38 | 7.8 | 43.74 | 8.90 | NA | -28.0 |
| | SPFe21 | 48 | 8.2 | 46.54 | 9.39 | NA | -28.0 |
| | SPFe21 | 72 | 8.3 | 45.97 | 10.13 | 303.6 | -26.3 |
| | SPFe21 | 131 | 8.3 | 13.01 | 9.59 | 46.4 | -26.1 |
| | SPFe82 | 0 | 7.0 | 7.30 | 0.3 | 3473.2 | -32.5 |
| | SPFe83 | 8 | 7.0 | 4.74 | 1.8 | 3462.1 | -29.5 |
| | SPFe84 | 16 | 7.0 | 12.32 | 3.0 | NA | -28.0 |
| | SPFe85 | 19 | 7.0 | 15.79 | 3.8 | NA | -27.8 |
| | SPFe86 | 22 | 7.1 | 18.06 | 1.3 | 2568.6 | -26.6 |
| | SPFe87 | 25 | 7.1 | 20.48 | 4.8 | NA | -26.9 |
| | SPFe88 | 28 | 7.0 | 18.84 | 4.7 | NA | -26.9 |
| | SPFe89 | 31 | 7.1 | 26.16 | 5.3 | NA | -26.6 |

Table 3.1- Continued

| | | | | | | | |
|---|---|---|---|---|---|---|---|
| | SPFe90 | 34 | 7.1 | 29.18 | 5.6 | 453.7 | -27.1 |
| $KH_2PO_4$ | SPFe91 | 40 | 7.1 | 26.85 | 6.8 | 314.8 | -26.8 |
| | SPFe92 | 43 | 7.1 | 27.44 | 6.0 | NA | -27.0 |
| | SPFe93 | 46 | 7.1 | 27.90 | 6.2 | 744.9 | -27.1 |
| | SPFe94 | 51 | 7.2 | 20.45 | 6.8 | 666.0 | -26.6 |
| | SPFe95 | 57 | 7.2 | 28.62 | 7.1 | 920.5 | -25.7 |
| | SPFe96 | 70 | 7.1 | 28.81 | 7.7 | 823.9 | -26.5 |
| | SPFe97 | 81 | 7.2 | 31.24 | 8.1 | 367.3 | -26.5 |
| | SPFe98 | 93 | 7.3 | 27.37 | 8.7 | 604.9 | -26.4 |
| | SPFe99 | 129 | 7.3 | 20.58 | 9.3 | 356.3 | -26.6 |
| | SPFe10 | 189 | 7.2 | 13.30 | 10.1 | 525.0 | -26.8 |
| | SPFe10 | 273 | 7.3 | 10.05 | 9.0 | 350.3 | -26.5 |
| | SPFe10 | 351 | 7.2 | 11.73 | 10.1 | 525.4 | -26.4 |
| | SPFe22 | 25 | 6.5 | 4.09 | 3.32 | NA | -27.8 |
| | SPFe22 | 38 | 6.7 | 7.10 | 2.96 | NA | -27.0 |
| | SPFe22 | 48 | 6.7 | 12.90 | 5.28 | 504.7 | -27.1 |
| | SPFe22 | 72 | 7.0 | 17.78 | 5.70 | 330.1 | -26.6 |
| | SPFe22 | 131 | 6.9 | 35.76 | 6.55 | 322.5 | -26.9 |

The initial pH in both buffered media was identical about 7. However, the pH in both the systems increased with increasing DIC and reduction of iron (III) (Figure 3.1, Table 3.1), the increase being higher in the bicarbonate system (Figure 3.5). In the bicarbonate-buffered media the pH increased by about 0.6 units in the first 22 hours and then continued at a lower rate until the end of the experiment (t=350 hrs). In the phosphate-buffered system the pH increments continued at nearly constant rate throughout the experiment. As mentioned above, the stoichiometric relationship between lactate oxidation and reduced form of iron concentration is lower than expected. One possible reason for the lower Fe (II) in concentration could be its re-oxidation to ferric iron in the bicarbonate-buffered experiment as pointed out by Straub et al. (2001). Another possible reason could be an increase in the chargeability

of cell wall of microbial organisms with increasing pH, which could in turn increase the metal binding capacity of *S. putrefaciens* (Sokolov et al., 2001). In addition, the distinct differences in Fe (II) production as reflected by the DIC data (Figure 3.2) is not so well defined in the dissolved iron measurements (Figure 3.1). This could be due to the formation of also precipitates in the phosphate-buffered conditions in combination with the arguments presented above.

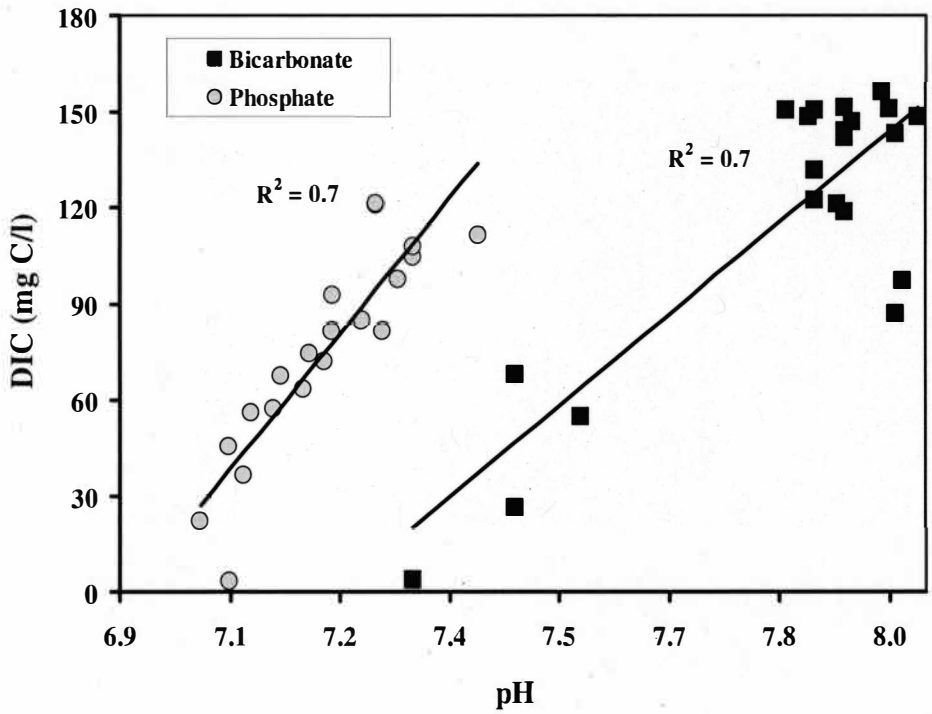


Figure 3.5 DIC versus pH variation during the reduction process for the bicarbonate- (black squares) and phosphate- (shaded circles) buffered systems.

Carbon Isotopes

The $\delta^{13}C$ values of the various starting materials used are: sodium lactate (-

24.8 ‰), acetate (-32.9 ‰), ferric citrate (-24.7 ‰), bicarbonate (+10‰) and bacterial biomass (-24.5 ‰). In the bicarbonate-buffered system the isotopic values, when not corrected for the initial bicarbonate, showed the sequential time-dependent contribution of carbon from lactate oxidation to the DIC pool (Figure 3.6). With time the contribution from the bicarbonate became less dominant and the isotopic values of DIC approached that of the starting lactate/citrate isotopic values (~-25 ‰). When corrected for the initial bicarbonate, the isotopic values of both the systems showed similar trends eventually approaching that of the starting lactate as shown Figure 3.7 and Table 3.1. The stable carbon isotope ratios of the microbial biomass in both systems were determined for both systems at selected times and are shown in Table 3.2.

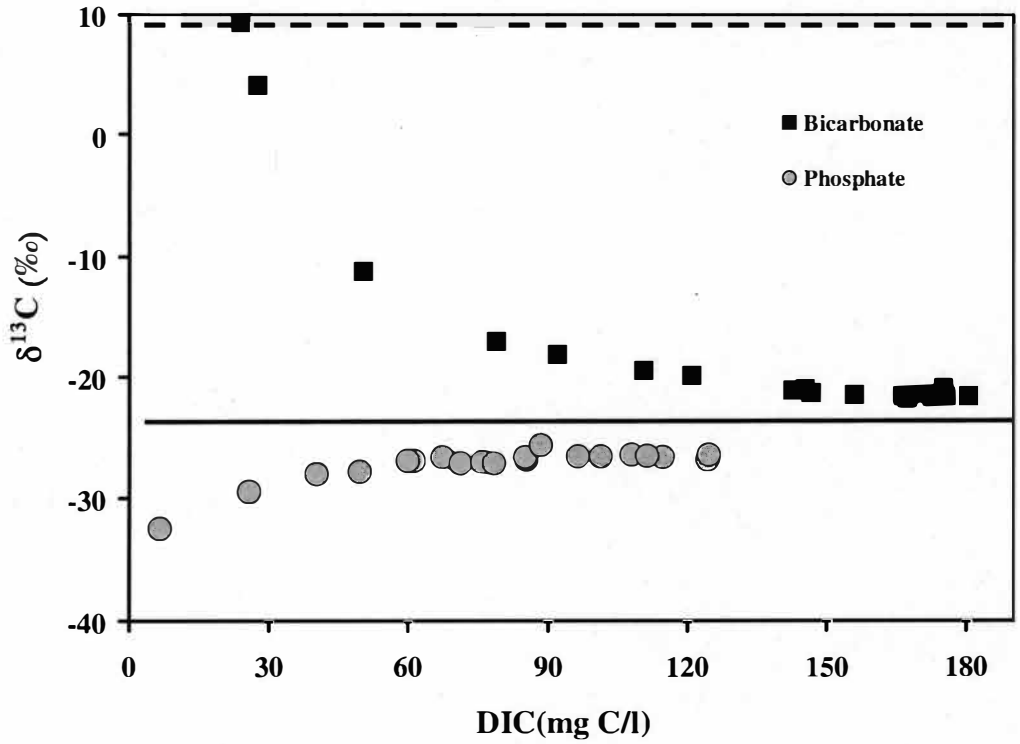


Figure 3.6 Carbon isotope ratios of DIC as a function of DIC produced during the reduction process for the bicarbonate- (black squares) and phosphate- (shaded circles) buffered systems. Dashed line indicates initial values for the added bicarbonate and solid line shows the initial value for the lactate. DIC was not corrected for initial bicarbonate in the bicarbonate system.

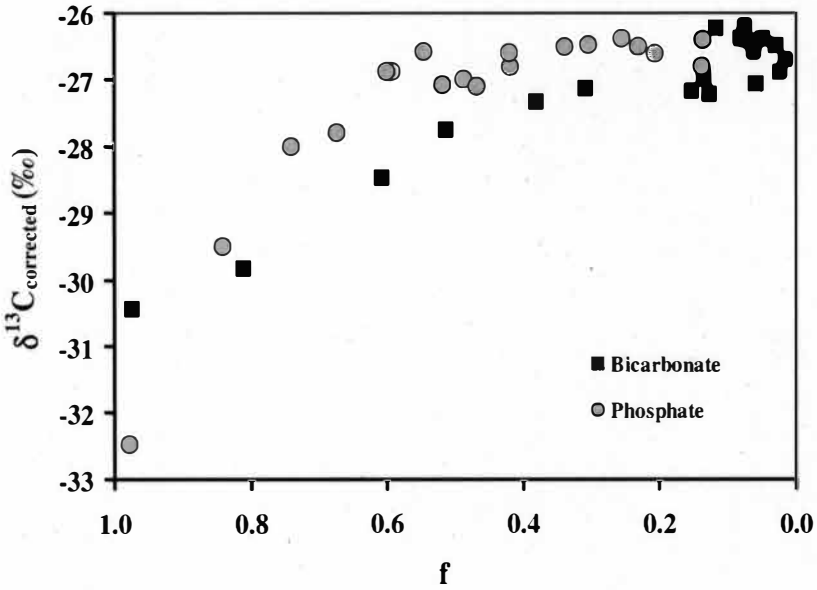


Figure 3.7 $\delta^{13}C$ values of DIC versus remaining lactate fraction for the bicarbonate- (black squares) and phosphate- (shaded circles) buffered systems.

Table 3.2

Time series measurements of $\delta^{13}C$ of the biomass for the bicarbonate and phosphate-buffered conditions. (N.D. = Not detected)

| Buffer | Sample | Time (hr) | Biomass (mg C) | $\delta^{13}C(‰)_{Biomass}$ |
|---|---|---|---|---|
| | SPFe211 | 25 | 0.06 | -26.7 |
| $NaHCO_3$ | SPFe212 | 38 | 0.12 | -26.8 |
| | SPFe213 | 48 | 0.15 | -26.9 |
| | SPFe214 | 72 | 0.24 | -26.6 |
| | SPFe215 | 131 | 0.32 | -26.6 |
| Average | | | 0.18 | -26.7 ± 0.1 |
| | SPFe221 | 25 | N.D. | N.D. |
| $KH_2PO_4$ | SPFe222 | 38 | 0.03 | -26.9 |
| | SPFe223 | 48 | 0.04 | -26.4 |
| | SPFe224 | 72 | 0.09 | -26.6 |
| | SPFe225 | 131 | 0.12 | -26.7 |
| Average | | | 0.07 | -26.7 ± 0.2 |

Rayleigh Fractionation Model for Lactate Oxidation

The carbon isotope values (Table 3.1) were used to examine if the process of lactate oxidation was amenable to modeling. In order to do this, we assumed that carbon came solely from lactate oxidation and not from citrate and acetate oxidations was used. This assumption was based on the information that *S. putrefaciens* does not use citrate and acetate as a carbon source in the presence of lactate (DiChristina et al., 2002). Separate experiment to verify whether *S. putrefaciens* used acetate to reduce iron was conducted and showed negligible DIC production associated with iron reduction. This observation suggests that there was negligible isotope interference

from acetate with the DIC pool. Based on this observation, the isotopic fractionation in the bicarbonate- and phosphate-buffered systems was examined to check if the oxidation of lactate coupled with ferric iron reduction might follow Rayleigh distillation type fractionation (Detail background of Rayleigh-type process is presented in Appendix B). DIC was taken as a proxy for the oxidation of lactate and direct measurements of the remaining lactate in the media using HPLC was used to verify the lactate consumption values estimated based on DIC measurements. Figure 3.8 shows the correlation between the calculated and measured fraction of lactate in solution ($f_t/f_0$) for both the bicarbonate and phosphate systems.

The isotopic value of the lactate remaining in solution at any time was calculated using equation 3.2 (Mariotti et al., 1981):

$$\delta_{react} = [\delta_{o-react} - ((1-f) * \delta_{prod-reservoir})]/f \qquad (3.2)$$

Where: $\delta_{react} = \delta^{13}C$ of lactate remaining at time t
$\delta_{o-react} = \delta^{13}C$ of initial lactate
$\delta_{product-reservoir} = \delta^{13}C$ of DIC produced at time t corrected for initial DIC and $\delta^{13}C$ of bicarbonate
f= fraction of lactate remaining at time t

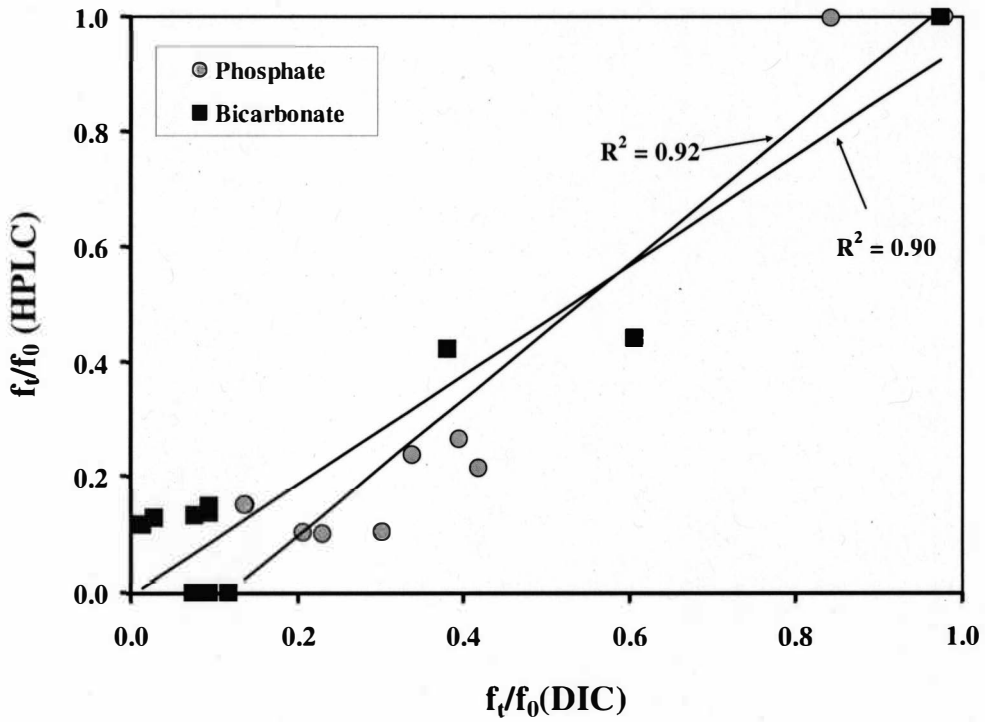


Figure 3.8 Cross plot of the ratio of remaining lactate at any time t ($f_t$) to initial lactate ($f_0$) determined by HPLC and estimated from DIC measurements for bicarbonate- (black squares) and phosphate- (shaded circles) buffered systems.

Figure 3.9 shows the isotopic values of lactate as a function of remaining lactate fraction for both buffered systems. As shown in Figure 3.7 with respect to DIC, there is a kinetically controlled fractionation until 85% of the lactate was consumed. This occurred in the first 45 and 93 hours in the bicarbonate- and phosphate- buffered systems respectively (Figure 3.2). The fractionation factor for the two buffered systems representing the kinetically controlled phase of the reduction process could be estimated according to equation 3.3, treating both systems as a closed system (Mariotti et al., 1981, & Somsamak et al., 2006):

$$\delta_{react} = \delta_{o-react} + \varepsilon \ln f \qquad (3.3)$$

Where: $\delta_{react}$= $\delta^{13}C$ of lactate remaining at time t,

$\delta_{o-react}$= $\delta^{13}C$ of initial lactate,

$\varepsilon$= average equilibrium fractionation between lactate and DIC, which is related to $\alpha$ (fractionation factor) by: $\varepsilon = (\alpha - 1)*1000$

f= remaining fraction of lactate at time t

Figure 3.10 shows the $\delta^{13}C$ values vs. the natural logarithm of the remaining lactate fraction in the bicarbonate-buffered system and in the phosphate-buffered system. The $R^2$ values of ~0.9 suggest that both buffered systems could be approximated to a Rayleigh-type fractionation model, with the slope of the regression line indicating an isotopic fractionation ($\varepsilon$) between the lactate consumed and the carbon dioxide of ~6.6 ‰ in the bicarbonate buffered media and ~4.6 ‰ for the phosphate-buffered media. The slight difference in fractionation factors between the two buffered systems could be attributed to the differences in carbon reservoir surrounding the microbial membrane.

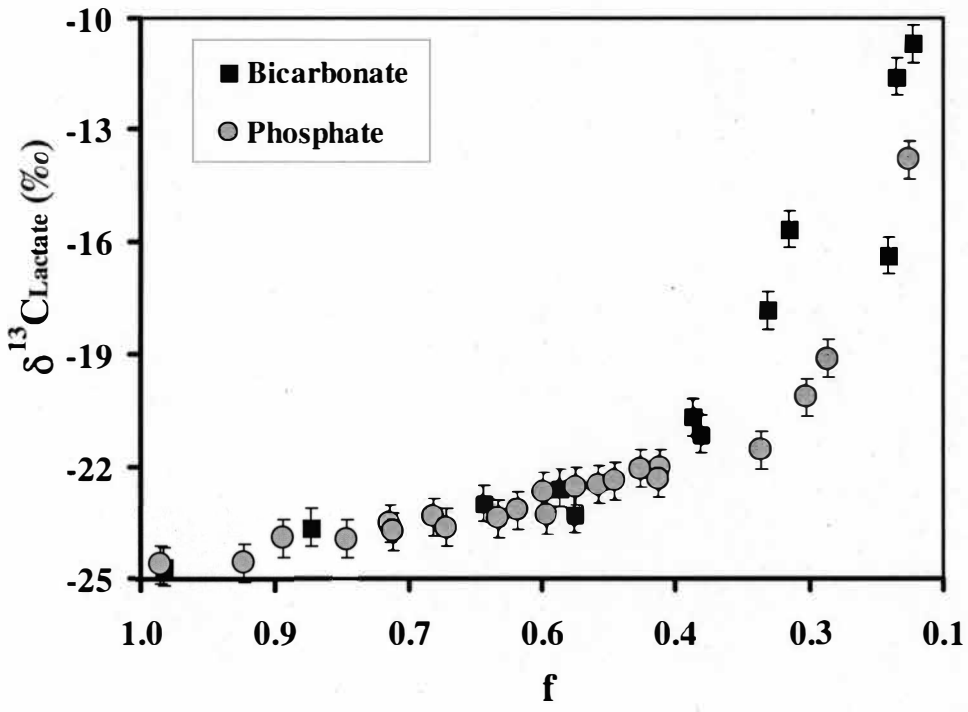


Figure 3.9 $\delta^{13}C$ values of remaining lactate as a function of remaining lactate fraction for the bicarbonate- (black squares) and phosphate- (shaded circles) buffered systems.

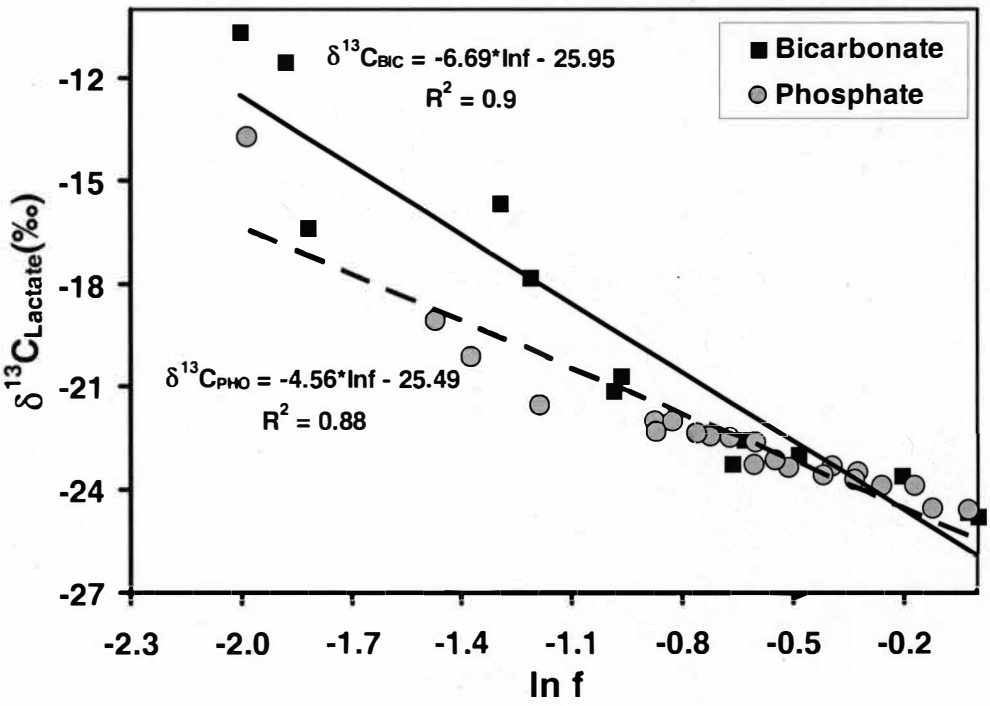


Figure 3.10 Semi-logarithmic plot of $\delta^{13}C$ values of the lactate as a function of remaining lactate fraction (lnf) for bicarbonate- (black squares) and phosphate- (shaded circles) buffered experiments. Slope of the regression lines were used to estimate equilibrium fractionation (ε).

Teece et al. (1999), in their study comparing aerobic vs. anaerobic (nitrate as electron acceptor) microbial growth, reported that isotope fractionation associated with anaerobically synthesized fatty acids is significantly larger than those synthesized under oxic condition. They proposed that under anaerobic conditions, the metabolic activity of *S. putrefaciens* (Strain MR-4) followed the serine pathway as opposed to the tricarboxylic acid (TCA) cycle under oxic conditions. The former is facilitated by hydroxypyruvate reductase enzyme with formate being the key intermediate which involves exchange of $CO_2$ between the internal cell and the

aqueous DIC pool. Zhang et al. (2003), using *Shewanella algae strain BrY* and *Geobacter metallireducens GS-15* under anaerobic (iron reducing) conditions, found similar results with regards to the pathway followed by *Shewanella* under anaerobic conditions (Teece et al., 1999). These authors further pointed that out the likelihood of incorporation of $CO_2$ in the serine pathway from the DIC in the buffered systems. As observed in our study the slightly larger fractionation in the bicarbonate-buffered system might therefore be attributed to the larger DIC reservoir in the system. This possibility needs more investigation.

The computed fractionation factors using the Rayleigh model between the DIC and lactate in both systems were used to infer the fractionation between biomass and respired carbon dioxide using equilibrium fractionation between gaseous $CO_2$ and DIC at 30°C (Mook et al., 1974). In studies dealing with the isotopic ratios of fatty acids synthesized by *Shewanella* under anaerobic conditions, Teece et al. (1999) and Zhang et al. (2003) reported comparable isotopic values ranging -38 ‰ to -44 ‰ for the fatty acids synthesized during nitrate and iron reduction, respectively. The respective computed fractionation factor values averaged -8.3 ‰ and -13 ‰ between the fatty acids and total biomass during the oxidation of lactate. These authors attributed the large fractionation during fatty acid synthesis to the carboxylation involved in the serine pathway. Under similar bicarbonate-buffered conditions, our study estimated a fractionation factor of ~7 ‰ between oxidized lactate and DIC. The average isotopic value of the biomass (-26.7 ‰) was depleted by ~2 ‰ with respect to the starting isotopic values of the lactate oxidized (-24.8 ‰) and enriched by ~5 ‰ with respect to the DIC (-31.8 ‰). Assuming that the DIC was in isotopic

equilibrium with gaseous $CO_2$, and using the a fractionation factor of ~7 ‰ at 30 °C (the experimental temperature of reaction) an average isotopic value of ~ -39 ‰ for the gaseous $CO_2$ likely involved in the fatty acid synthesis can be estimated. Incorporation of this $CO_2$ during the synthesis of fatty acids via a serine pathway may account for the depleted isotopic values of fatty acids (Teece et al., 1999; Zhang et al., 2003). Respired $CO_2$ with a $\delta^{13}C$ value of ~ -39 ‰ also yields a fractionation of ~12 ‰ between bacterial biomass and respired $CO_2$.

## Conclusions

Experiments were conducted using *S. putrefaciens* strain 200R under two most commonly occurring buffering conditions bicarbonate and phosphate, to characterize the effect of media composition on the iron reduction coupled with lactate oxidation. Larger lactate oxidation in the $NaHCO_3$ media compared to the $KH_2PO_4$ media was observed which was consistent in the differences in DIC between the two buffered systems, which were further verified using direct measurements of the remaining lactate and bacterial biomass. Along the exponential phase of the growth curve, the DIC and aqueous iron (II) concentration in the bicarbonate system was twice as high as that of the phosphate-buffered system. The DIC yield showed significant differences between the two buffering systems compared to the concentration of ferrous iron. Possible causes in the observed differences include re-oxidation of ferrous iron to ferric iron in the bicarbonate-buffered media and an increase in the binding energy of *S. putrefaciens* with increasing pH.

Based on the assumption that lactate served as the sole carbon source during

the course of the reduction process and hence approximating DIC as a proxy for the lactate consumed (verified by time series HPLC measurements) iron reduction might be modeled as a Rayleigh-type process. Bicarbonate appeared to induce a slightly larger fractionation between lactate and DIC compared to phosphate (6.6 ‰ vs. 4.6 ‰). This might be due to the reservoir effect, which is larger in the bicarbonate buffered system due to the initial added bicarbonate and a greater degree of lactate oxidation.

The biomass was depleted by ~2 ‰ compared to the lactate, in agreement with previous studies. Further, based on this Rayleigh model, a fractionation of ~12 ‰ was estimated between biomass and the respired $CO_2$, with the estimated $\delta^{13}C$ of the respired $CO_2$ itself being ~ -39 ‰. Incorporation of this $CO_2$ in the synthesis of fatty acids via the serine pathway could account for isotopically depleted fatty acids as reported previously by other researchers.

# CHAPTER IV

# CHEMICAL AND ISOTOPIC INVESTIGATION OF ABIOTIC OXIDATION OF ORGANIC COMPOUNDS UNDER CIRCUMNEUTRAL ANAEROBIC CONDITIONS

## Introduction

The fate, mobility, and bioavailability of inorganic and organic compounds in the environment are heavily influenced by various geochemical processes including sorption, precipitation, dissolution and electron transfer (Grundil and Sparks, 1998; Li et al., 2006; Pignatello et al., 2006). Investigating these different geochemical processes and their reaction mechanisms would add to our understanding of natural systems and the fates of inorganic and organic compounds in pristine and contaminated environment. Electron transfer processes could be either enzymatically mediated microbial metabolism or abiotically controlled.

Abiotic electron transfer processes have drawn much attention in many fields including waste water treatment, enhancing *in situ* degradation of organic and inorganic compounds, cycling of nutrients in wetland ecosystems, and in atmospheric chemistry in investigating sources and sinks of chemicals in the troposphere (e.g. Kormanen et al., 1989; Abrahamson et al., 1994; Deng et al., 1998; Grundil and Sparks, 1998; Wu and Deng, 2000; Cornell and Schwertmann, 2003; Chatterjee and Dasgupta, 2005; Minero et al., 2005; Li et al., 2006; Meeroff et al., 2006; Pignatello et al., 2006; Li et al., 2006; Vione et al., 2006; Zhang et al., 2006).

Abiotic reactions are electron transferring processes, which take place either by direct or indirect (chemically or sensitized) photolysis. Direct photolysis is a process in which the organic compound absorbs light and as result of light absorption it undergoes photochemical transformation. With some organic compounds, exposure to light source alone does not result in electron transferring reactions (Kormanen et al., 1989; Wu and Deng, 2000; Chatterjee and Dasgupta, 2005). Such organic compounds undergo oxidation via indirect photolysis. Indirect photolysis takes place either due to energy transfer from another excited species (sensitized photolysis) or chemical reactions (e.g. Fenton like reactions) of (nonexcited) compounds. The non-excited compounds possess short-lived but very reactive species (e.g. OH- and peroxy- radicals, singlet oxygen) formed in the presence of light due to reactions of excited compounds (e.g. citrate, lactate). Sensitizing agents (e.g. Fe(III) and other transitions metals) act as geocatalysts (acting as catalyzing agents) in natural ecosystems assisting photochemical reactions to transform pollutants. One of these catalysts is ferric iron, which acts as a photosensitizer and participates in the formation of oxidants via photo initiated transformations (Li et al., 2006; Meeroff et al., 2006). Under our experimental conditions, $Fe^{+3}$ form complexes with polycarboxylic compounds (e.g. ferric citrate) and oxyhydroxides (e.g. HFO). Photochemical dissociation of ferric citrate complexes in aqueous solutions have been reported to involve the reduction of ferric iron to ferrous iron coupled with the oxidation of citrate producing acetone and carbon dioxide represented by the general reaction shown below (reaction 4.1) (Abrahamson et al., 1994; Deng et al., 1998; Zhang et al., 2006). Along with microbial metabolism, photochemical processes, and

Fenton-like reactions enhance the reduction of metals and oxidation of organic compounds (e.g. Howsawkeng et al., 2001; Ndjou'ou and Cassidy, 2006; Northup and Cassidy, 2007).

$$\underset{\text{(Citrate)}}{C(OH)(COOH)(CH_2COOH)_2}+2Fe^{+3}\xrightarrow{h\nu}\underset{\text{(Acetone)}}{CH_3COCH_3}+2Fe^{+2}+3CO_2+2H^{+} \qquad (4.1)$$

Where: $h\nu$ ➔ photons or quanta, h =Planck constant, 6.63 x 10-34 J.s, $\nu$= frequency

Recent studies have reported that the photochemical reaction of ferric citrate and ferric oxyhydroxides results in the formation of hydroxyl radical as an intermediate product. The intermediate process involved is modified Fenton-like reaction (Deng et al., 1998; Northup and Cassidy, 2007). Fenton chemistry ($Fe^{+2}$ + $H_2O_2 \rightarrow Fe^{+3}$ +·OH) plays role in photochemical transformations of organic compounds in two ways. One is producing hydroxyl radical that attack the covalent bonds of the organic materials. The radical in turn attacks organic compounds, such as citrate and lactate, mineralizing them to lower molecular weight carbon compounds such as carbon dioxide, both aerobically and anaerobically (Deng et al., 1998; Minero et al., 2005; Li et al., 2006; Vione et al., 2006; Zhang et al., 2006). Second, this (Fenton chemistry) oxidizes ferrous to ferric iron, an excited species, for further sensitized photooxidation of the organic compounds. Under anaerobic conditions, the presence of anions such as chloride inhibits abiotic reduction-oxidation couplings by forming halogenated compounds and by scavenging the hydroxyl radicals (Calza et al., 2005; Vione et al., 2005).

Iron is the fourth most common naturally occurring element (Schwertmann and Cornell, 2000, Kappler and Straub, 2005). It is very reactive in near surface

environments and its two most common oxidation states (ferric and ferrous) can form stable compounds (Li et al., 2006). The oxyhydroxides of iron are common on the crust and can function as geocatalysts in the speciation of organic and inorganic pollutants in the subsurface environment (Cornell and Schwertmann, 2003). Recent studies have shown the importance of dissolved organic compounds and iron ions involved in the photochemical formation of hydrogen peroxide and other photooxidants in degrading natural and anthropogenic inorganic and organic compounds (Kormanen et al., 1989; Abrahamson et al., 1994; Deng et al., 1998; Grundil and Sparks, 1998; Wu and Deng, 2000; Cornell and Schwertmann, 2003; Chatterjee and Dasgupta, 2005; Li et al., 2006; Meeroff et al., 2006; Pignatello et al., 2006; Zhang et al., 2006).

Kormanen et al. (1989) compared the photocatalytic activities of hematite colloids ($\alpha$-$Fe_2O_3$), ZnO and $TiO_2$ in the formation of $H_2O_2$ and their effects on the oxidation of chlorinated and carboxylic organic compounds under aerated conditions. They concluded that $TiO_2$ and ZnO appear to be more active photo-oxidation catalysts of most electron donor whereas $\alpha$-$Fe_2O_3$ particles appear to react only with a select set of molecules which are strong reducing agents and multidentate ligands. Under dark conditions hematite appeared to effectively oxidize sulfite or oxalate but showed little or no activity with respect to citrate, benzoate or cyanide and the presence of light increased the oxidation of the less reactive organic compounds (Kormanen et al., 1989).

Carboxylic compounds (e.g. oxalate, citrate) possess one of the most common

functional groups ($RCOO^-$) of dissolved organic compounds present in natural waters and form strong complexes with ferric iron (Deng et al., 1998). The photooxidation of these carboxylic acids could be sensitized by the presence of Fe(III) undergoing rapid photochemical reactions upon irradiation according to reaction 4.1 (Adamson et al., 1968). Deng et al. (1998) used Fe(III)-citrate complexes as a photochemical sensitization material to promote the discoloration of dyes forming more reactive species (e.g. $H_2O_2$ and $^{\cdot}OH$) compared to Fe(III)-hydroxyl and Fe(III)-oxalate complexes at acidic pH conditions. Deng et al. (1998) reported that at pH of 2 photodegradation rates of organic compounds increased for varying citrate to Fe(III) ratios in the order of 4:1>2:1>1:4>1:1>1:2. They also pointed out that at neutral to alkaline conditions Fe(III)-hydroxyl dominates the photoreactivity compared to Fe(III)-citrate complexes. Hydroxyl radicals produced in systems containing Fe(III)-ligands complexes could be responsible for the oxidation of organic compounds coexisting in aqueous solutions (Deng et al., 1998). Their study concluded that under near-UV light the efficiency of the Fe(III)-citrate complexes induced photoreduction reaction in aqueous solutions that depended on the pH and the initial citrate to Fe(III) ratio.

Wu and Deng (2000) reported that different organic compounds exhibit different photodegradation rates reflecting their differences in photo-degrabilities indicating the presence of several steps in the whole reaction of the photodegradation of organic compounds in aqueous solutions. According to their study several variables play a role in the observed differences including the photo-formation of $^{\cdot}OH$ radicals; $^{\cdot}OH$ radicals attacking target groups or bonds in the respective organic

compounds, and the latter might be a rate-controlling step in the photodegradation system. Wu and Deng (2000) concluded that the photochemical nature of organic compounds coexisting in photo-reactive complexes containing solutions is strongly influenced by the pH, Fe(III) concentration, wavelength and energy of irradiation source of the solution. This observation concurred with the observation made by Kormanen et al. (1989) that organic compounds dissolved in water with low concentration of ions do not get oxidized where as those dissolved solutions rich in ions easily get oxidized upon illumination.

Howsawkeng et al. (2001) studied the importance of simultaneous occurrence of microbially mediated degradation of oxalate and abiotic reduction of tetrachloroethene (PCE) in the presence of ferric iron at circum-neutral pH. They concluded that coexisting biotic-abiotic mechanisms in microbial-Fenton systems work synergistically in promoting enhanced mineralization of contaminants were potentially significant. Fenton-like mechanisms provide hydroxyl radical that could break the covalent bond of the recalcitrant PCE and make it bioavailable for further microbial metabolism mediated mineralization.

The main intent of the subsequent experiments in this part of the current research was to investigate the sources of carbon dioxide in the control samples of the microbial reduction of ferric iron research (See Chapter III). Understanding abiotically controlled electron transfer processes in laboratory based anaerobic system is the theme of our study. Literature review of such studies showed that photo assisted oxidation of polycarboxylic organic compounds (e.g. citrate, oxalate) and other natural and toxic organic contaminants in the presence of ferric iron, other

metals (Mn, Cd, and Ni) and semiconductors ($TiO_2$) is a well documented phenomenon (e.g. Abrahamson et al., 1994; Deng et al., 1998; Grundil and Sparks, 1998; Zhang et al., 2006). Most of these previous studies were done under acidic and aerobic conditions. Our study was completed under anaerobic conditions, in the presence or absence of light, and at varying pH (5 to 9) conditions.

In this research the oxidation of lactate and citrate with and without ferric iron was used to investigate the effect of (1) electron acceptor (ferric citrate vs. HFO) in the phosphate buffered system (2) media components (3) buffers under neutral pH condition (4) pH conditions and (5) fluorescent light. Most of these controlling factors have environmental implications in natural and engineered remediation strategies of contaminated sites. It will also be important in adding data to the exciting ongoing research in the abiotic degradation of organic pollutants. Moreover, to the best of our knowledge there are no reported abiotic studies on the oxidation of lactate. Here we report the possible mechanisms of the DIC produced during abiotic oxidation of lactate and citrate under strict anaerobic condition, circum neutral pH, and temperature of 30 °C. We also report carbon isotopic signatures associated with the abiotic electron transfer processes. The general schematic ferric iron sensitized photocatalytic processes in this study are represented by the reactions (4.2 for ferric citrate and 4.3 for HFO):

$$\underset{\text{(Citrate)}}{2FeC_6H_5O_7} + NaC_3H_5O_3 \xrightarrow{h\nu} \underset{\text{(Acetone)}}{C_3H_6O} + \underset{\text{(Lactate)}}{NaC_3H_5O_3} + 2Fe^{+2} + 3CO_2 + 2H^+ \qquad (4.2)$$

$$\underset{\text{(Lactate)}}{2NaC_3H_5O_3} + \underset{\text{(HFO)}}{2Fe(OH)_3} + H_2O \xrightarrow{h\nu} 6HCO_3^- + 2Fe^{2+} + 2Na^+ + 10H^+ + H_2O \qquad (4.3)$$

# Results

## Extent of Iron Reduction and Organic Compound Oxidation

The soluble iron and DIC measurements indicated that in all experimental conditions except when covered with aluminum foil (not exposed to fluorescent light), both the reduced form of iron and $CO_2$ yield increased as a function of the time of reaction as shown in Figures 4.1 and 4.2. Figure 4.1 shows the ferrous iron concentration of ferric citrate media exposed to fluorescent light at pH ~7 for both the bicarbonate and phosphate buffered systems. The DIC production, which is assumed to be a proxy for organic compound oxidation also increased with reaction time in all experiments except in the combined absence of light or Fe(III) containing compounds (ferric citrate or HFO) (Figure 4.2). Figure 4.3 is a cross plot of ferrous iron as a function of the DIC produced combined for both the bicarbonate and phosphate buffed conditions in the ferric citrate containing media. There is linear relationship between the concentrations of reduced form of iron and the production of carbon dioxide, consistent with a photo induced abiotic redox process. Low correlation between DIC and Fe(II) values ($R^2$=0.58) could be explained by the possible re-oxidation of ferrous to ferric iron via the Fenton-like reaction (Equation 4.4) with increased generation of hydrogen peroxide ($H_2O_2$) and ferrous iron (Deng et al., 1998).

$$H_2O_2 + Fe^{+2} \rightarrow Fe^{+3} + 2{\cdot}OH \qquad (4.4)$$

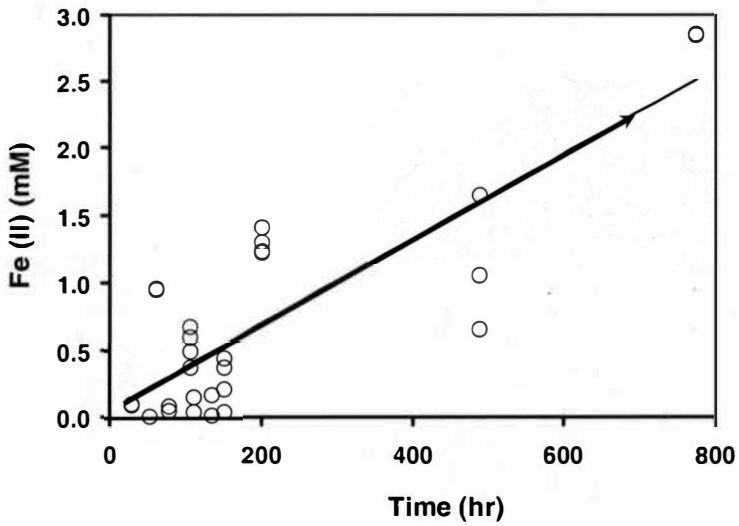


Figure 4.1 Graph showing the Fe(II) concentration for all fluorescent light exposed abiotic samples at neutral pH as a function of time.

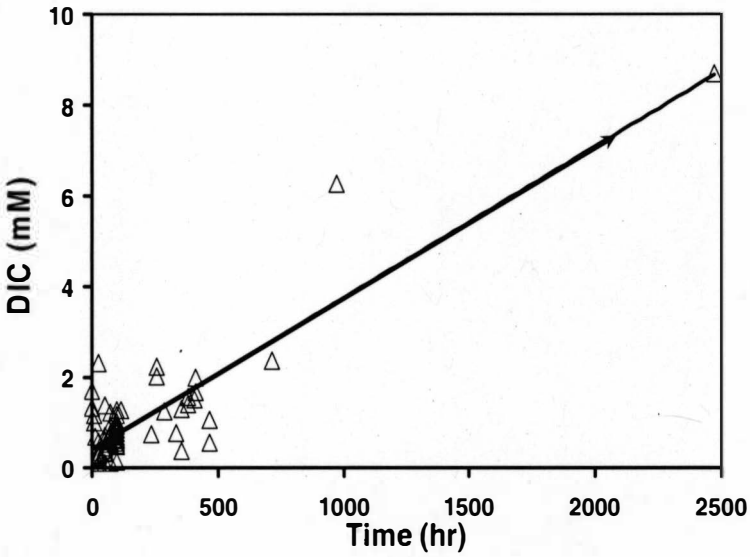


Figure 4.2 $CO_2$ yield from all abiotic samples exposed to fluorescent as a function of time.

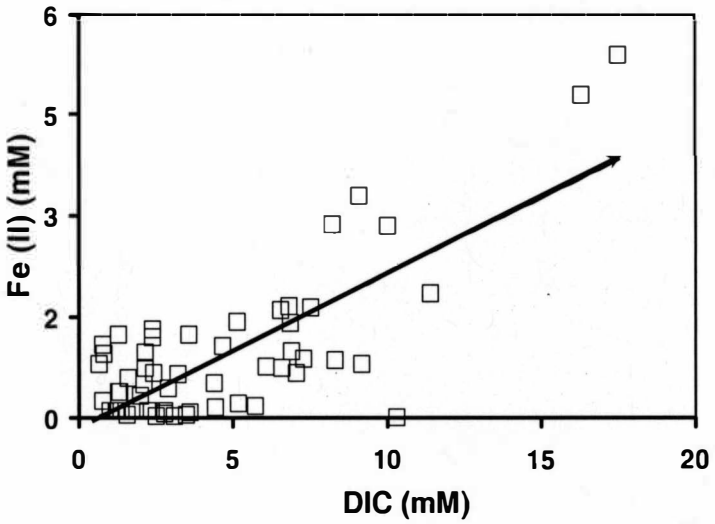


Figure 4.3 Fe(II) vs. DIC produced for all fluorescent light exposed abiotic samples at neutral pH in the presence of Fe (III).

Effects of Media Composition Figure 4.4 shows the results from a series of experiments with removal of one component per sample bottle. With time the DIC production increased in all experiments, but at different rates. The significant change occurred when ferric citrate was removed from the media (M-FC). The M-FC samples gave the least amount of DIC from the degradation of lactate, the only significant carbon containing organic compound. The amount of DIC in the M-FC samples was less by a factor of about 5 compared to the other set of samples in the current experimental setup. Interestingly, the media without lactate produced the highest DIC compared to the other set of samples and the reason for such observation is not clear (Figure 4.4). Generally, removal of media component in all the other set of samples is observed to have comparable carbon dioxide generation with time. The removal of Wolfe's minerals from the media also showed some effect on DIC

production (Figure 4.4). This could be attributed to the composition of the Wolfe's mineral listed in Appendix A.

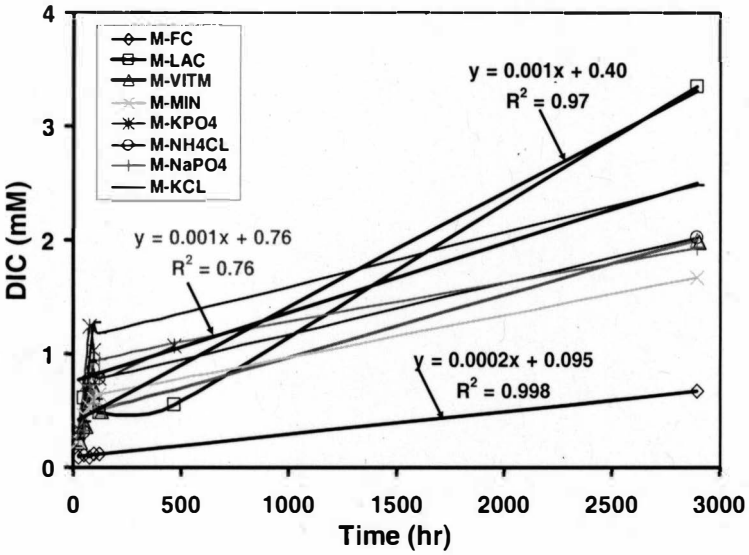


Figure 4.4 Plot showing the effect of media component omission on the oxidation of citrate, acetate and lactate for the phosphate buffering system as a function of time in a neutral pH and anaerobic conditions.

Effect of Fe (III) Containing Compounds Two sets of experiments with two different iron containing electron acceptors, ferric citrate and hydrous ferric oxide (HFO), were carried out to compare the importance of the form of ferric iron in organic carbon oxidation. As shown in Figure 4.5, HFO in the presence of lactate produced twice as much DIC compared to ferric citrate in the presence of lactate. This difference was observed to increase with time (Figure 4.5). The observed difference between the two sets of samples could be attributed to the efficiency of HFO in oxidizing organic compounds at near neutral pH condition compared to ferric

citrate (Kormanen et al., 1989; Deng et al., 1998).

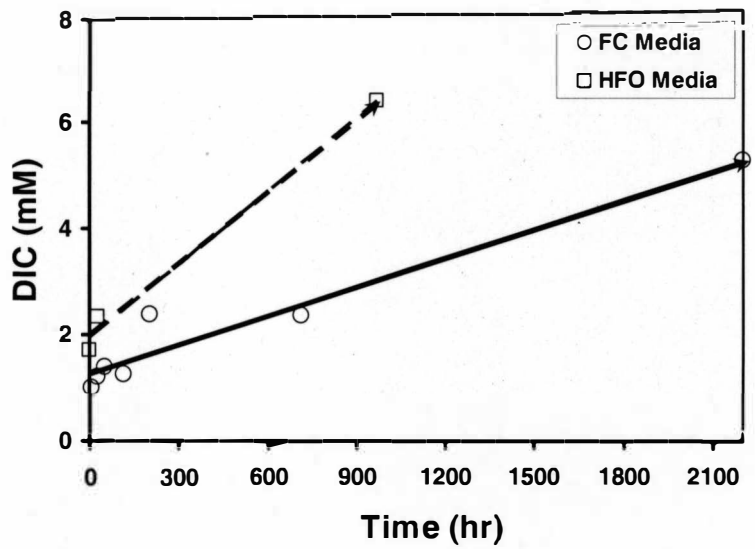


Figure 4.5 $CO_2$ yield in experiments with lactate containing media and ferric citrate compared to those with lactate containing media and HFO (hydrous ferric oxide) at pH 7 as a function of time.

Effect of Buffering Agent The DIC and Fe(II) generated from ferric citrate and lactate containing media using sodium bicarbonate or hydrous potassium phosphate as buffering agents are shown on Figures 4.6 and 4.7, respectively. These experiments were done to determine the effect of buffering agents on the abiotic process under fluorescent light at circum-neutral pH conditions. Graphical observation of the DIC results (Figure 4.6) show that phosphate had a slight enhancing effect compared to the bicarbonate buffer. However, Statistical analyses (F- and t-Test, $\alpha$=0.05, detail in Appendix E) showed that the two buffers have no significant difference in enhancing the redox process. The Fe(II) concentrations

measured for the two buffer systems are virtually identical (F- and t-Test, $\alpha$=0.05, detail in Appendix E) as shown on Figure 4.7. Both DIC and Fe(II) production suggest that the type of buffering agent does not affect the rates of Fe(III) reduction or organic matter oxidation. These observations showed that as long as the pH conditions are maintained, the type of buffering agent has little effect on the redox process.

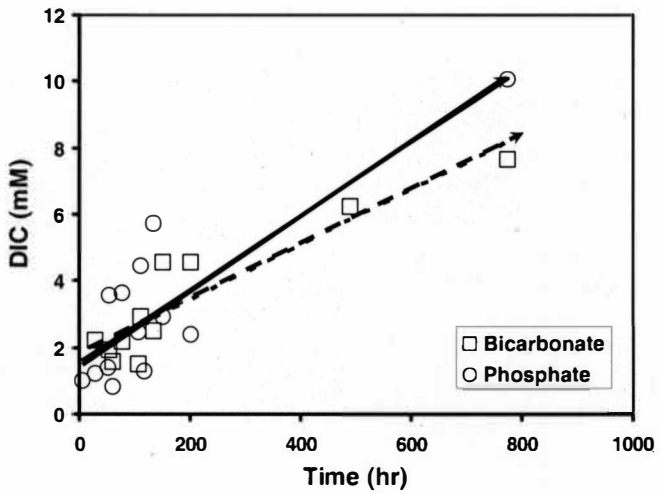


Figure 4.6 DIC production during the oxidation of organic compounds (citrate and lactate) mixed in the media under neutral pH condition with bicarbonate or phosphate buffer as a function of time.

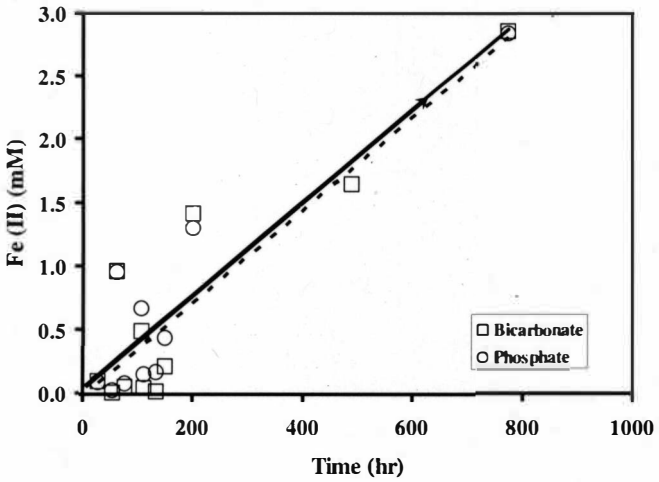


Figure 4.7 Fe(II) production during the oxidation of organic compounds (citrate and lactate) mixed in the media under neutral pH condition with bicarbonate or phosphate buffer as a function of time.

Effect of pH Effect of pH on the abiotic oxidation of organic compounds has been investigated by various researchers (e.g. Deng et al., 1998; Fischer et al., 2006; Meeroff et al., 2006; Minero et al., 2007). Most of these studies have been carried out at low pH conditions (<5). Here, our study reported the effects of pH, ranging from 5 to 9, on the redox process for both bicarbonate (Figures 4.8 and 4.9) and phosphate (Figures 4.10 and 4.11) buffered systems. Fe(II), Fe(III), pH and DIC were determined in each sample (see Appendix D: Table D7 and D8). Figure 4.8 shows the DIC as function of time for the acidic (pH = 5), neutral (pH = 7) and alkaline (pH =8 and 9) conditions. DIC production was the highest at acidic condition followed by the neutral and alkaline conditions respectively. Similarly, the highest Fe(II) accumulation was observed in the acidic condition compared to the neutral and alkaline pH conditions, respectively (Figure 4.9). Analogous relationships of pH

effect on DIC (Figure 4.10) and Fe (II) (Figure 4.11) were also observed in the phosphate buffered system with highest at pH 5 and lowest at alkaline pH values.

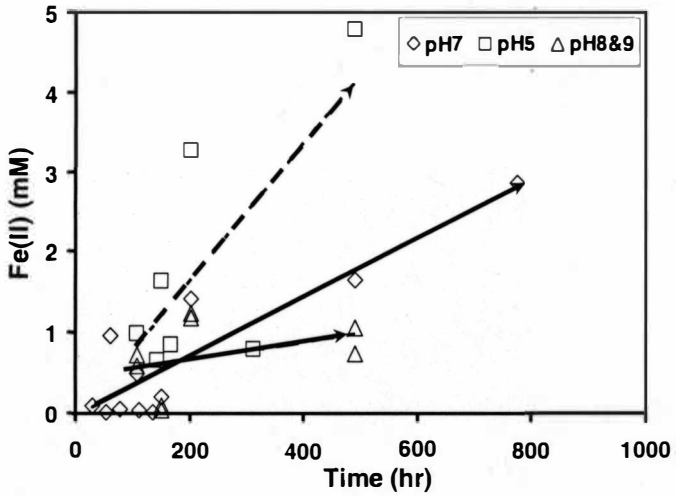


Figure 4.8 Comparison of DIC yield under different pH conditions (5, 7, or 8/ 9) in the bicarbonate buffered system as a function of time indicating increasing DIC production with lowering pH from 9 to 5.

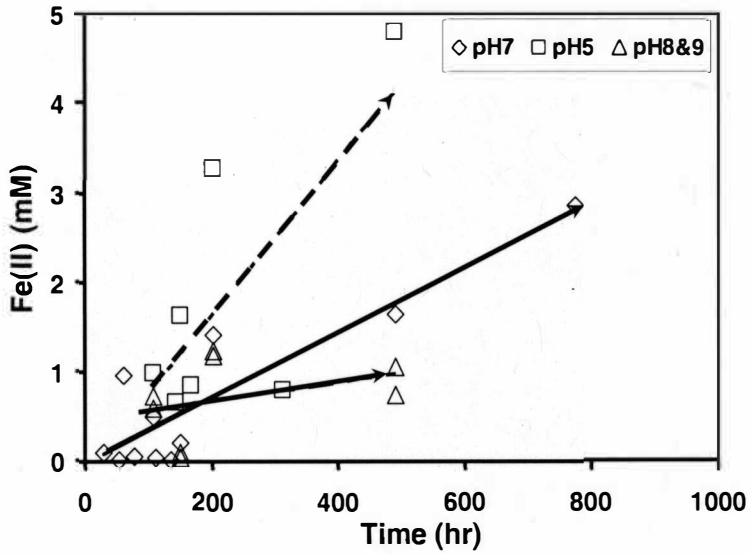


Figure 4.9 Ferrous iron accumulation at pH of 5, 7 or 8/9 in the bicarbonate buffered system as a function of time clearly indicating the lower the pH the higher the accumulation of Fe(II).

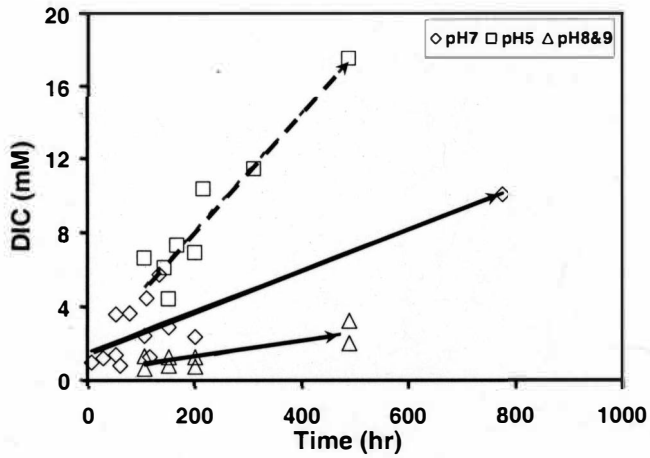


Figure 4.10 Comparison of DIC yield under different pH conditions (5, 7, or 8/ 9) in the phosphate buffered system as a function of time indicating increasing DIC production with lowering pH from 9 to 5.

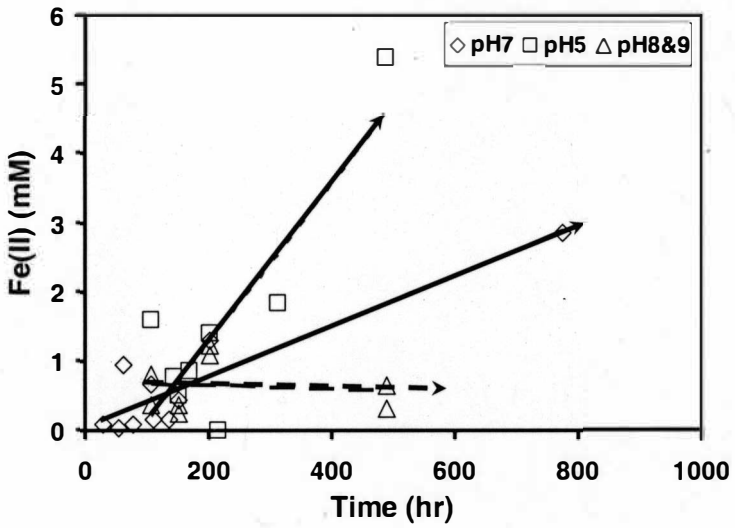


Figure 4.11 Ferrous iron accumulation at pH of 5, 7 or 8/9 in the phosphate buffered system as a function of time clearly indicating the lower the pH the higher the accumulation of Fe(II).

Effect of Light Under Acidic and Neutral Conditions These set of experiments were conducted to investigate the effect of light, pH and ferric iron. Experiments were carried out under fluorescent light and dark conditions, at acidic and neutral pH, and in the presence and absence of ferric iron. In the absence of ferric iron, no DIC generation occurred under any photo-exposure or different pH conditions. Figures 4.12 and 4.13 compare the effect of light and pH on the DIC and Fe(II) generations for the bicarbonate buffered condition respectively in the presence of ferric iron. Figures 4.14 and 4.15 showed the relative influence of light and pH on the oxidation of the organic compounds (citrate and lactate) and reduction of ferric iron for the phosphate buffered system. From Figures 4.12 - 4.15, we observed that under our experimental conditions fluorescent light had a greater effect on the redox process than pH in the presence of ferric iron. Regardless of the pH conditions, in the absence

of light or ferric iron both DIC and ferrous iron accumulate slowly or not at all, indicating the absence of organic compounds oxidation.

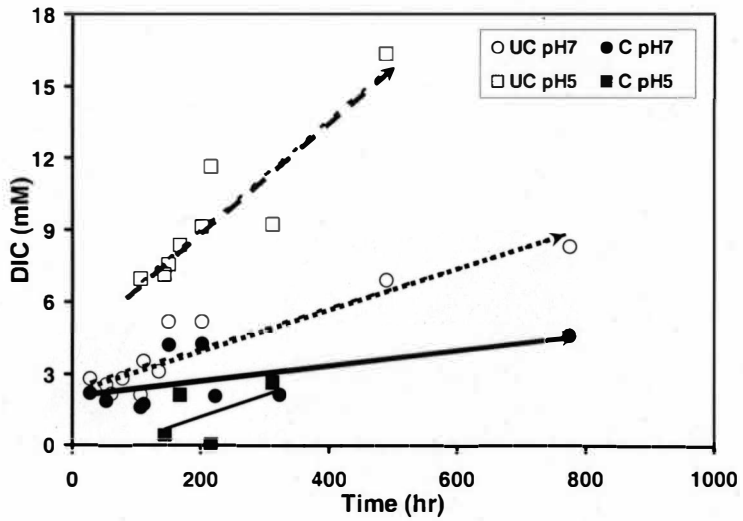


Figure 4.12 Influence of light under acidic and neutral conditions on DIC production in the bicarbonate buffered system. UC (open symbols) = uncovered, exposed to light; C (Filled symbols) = covered, dark.

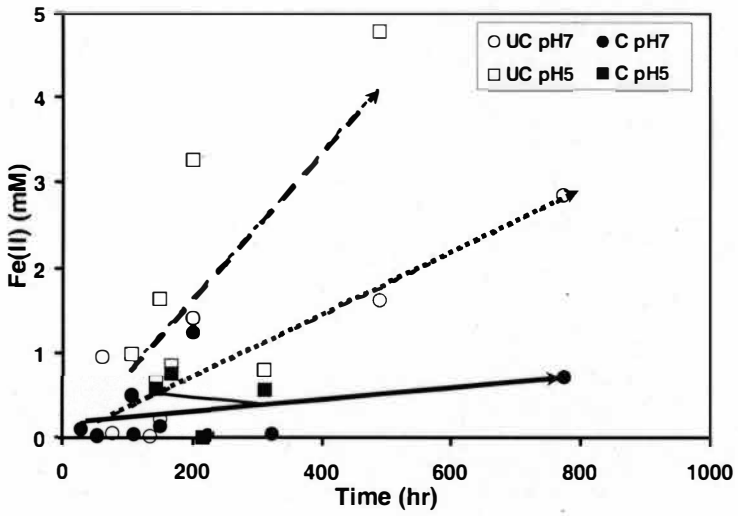


Figure 4.13 Ferrous iron productions in the bicarbonate buffering system in the presence or absence of light at pH 5 and 7 as a function of time. UC (open symbols) = uncovered, exposed to light; C (filled symbols) = covered, dark.

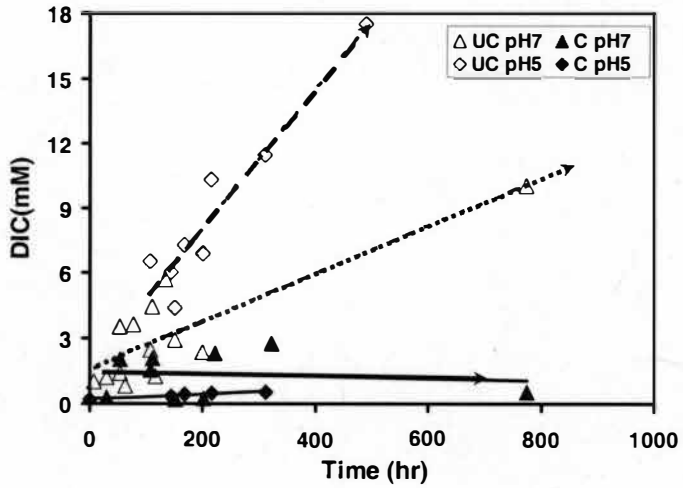


Figure 4.14 DIC productions in the phosphate buffered system in the presence or absence of light at pH 5 or 7. UC (open symbols) = uncovered, exposed to light; C (filled symbols) = covered, dark.

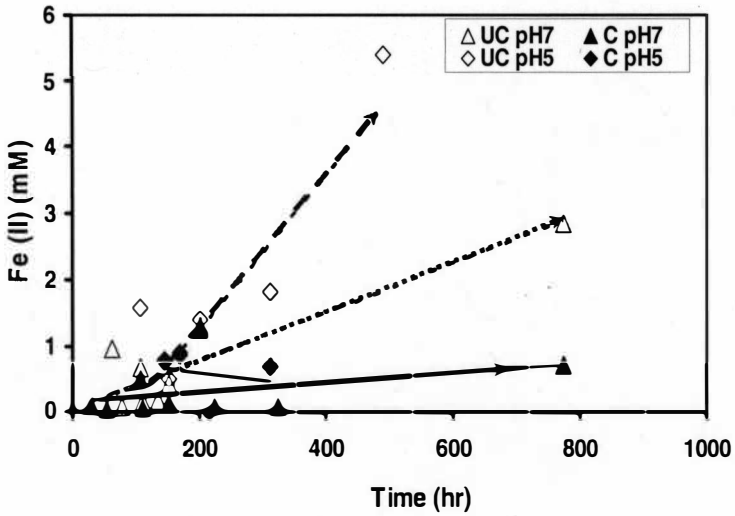


Figure 4.15 Ferrous iron production in the phosphate buffered system under light or dark conditions at pH 5 or 7 as a function of time. UC (open symbols) = uncovered, exposed to light; C (filled symbols) = covered, dark.

Stable Carbon Isotopes in Abiotic Systems

Results of isotopic analyses at neutral pH and anaerobic conditions of the extracted DIC are shown on Figures 4.16 - 4.18 both for bicarbonate- and phosphate-buffered systems, respectively.. Figure 4.16 shows plot of $\delta^{13}C_{DIC}$ as a function of total DIC in the bicarbonate system with out correcting for the initially added bicarbonate buffer. Solid line indicates the root mean square regression plots of the data points with three units forward and one unit backward forecasts of the trend. At lower pH conditions (pH ~5) there were no systematic relationship between the DIC and its respective carbon isotopic values. Figure 4.17 shows graph of the $\delta^{13}C_{DIC}$ values as a function of inverse of the total DIC in the bicarbonate system. Such plots are important in estimating the source of additional carbon dioxide produced from

oxidation of organic compounds.

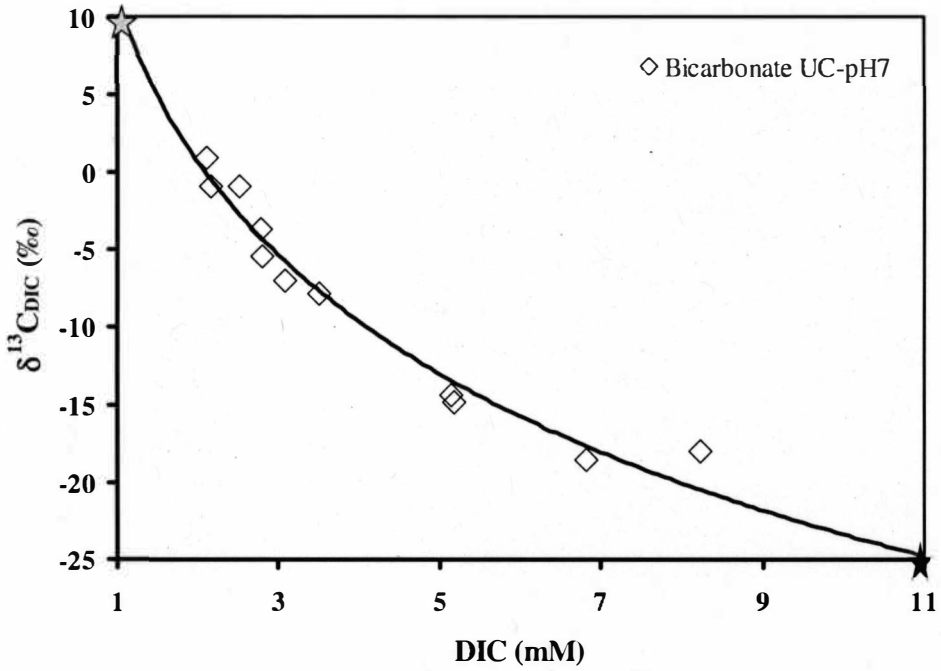


Figure 4.16 Carbon isotopic values of DIC vs. DIC concentration under neutral pH conditions in the bicarbonate buffered system as a function of total DIC. Gray and black stars indicate the initial $\delta^{13}C$ values of the bicarbonate and lactate/citrate, respectively. Line is showing the logarithmic trend line of the data with three units forward and one backward unit forecasts.

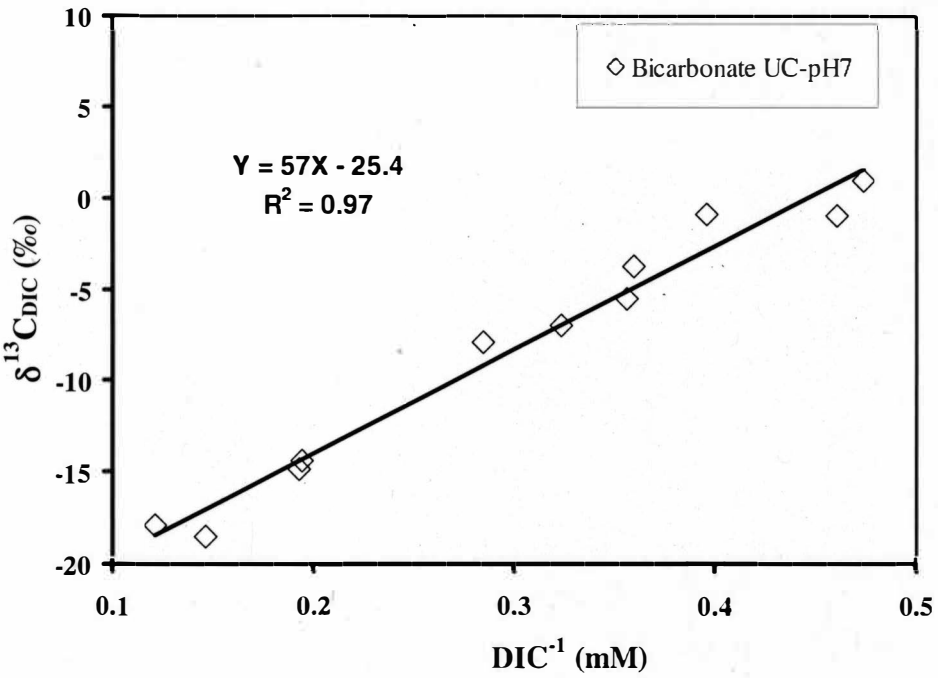


Figure 4.17 Carbon isotopic values of DIC vs. inverse of DIC concentration relationship of the bicarbonate buffered system under neutral pH conditions. The y-intercept of the regression of the line provides the estimate of the starting $\delta^{13}C$ value of the organic compound being oxidized in the bicarbonates system.

Figure 4.18 shows plot of $\delta^{13}C_{DIC}$ as a function of total DIC yield in the phosphate system at neutral pH and anaerobic conditions. Solid line indicates the root mean square regression plots of the data points with one unit forward and one unit backward forecast. Some data points were not used in the logarithmic trend analyses (black filled circles, Figure 4.18). At lower pH conditions (pH ~5) there were no systematic relationship between the DIC and its respective carbon.

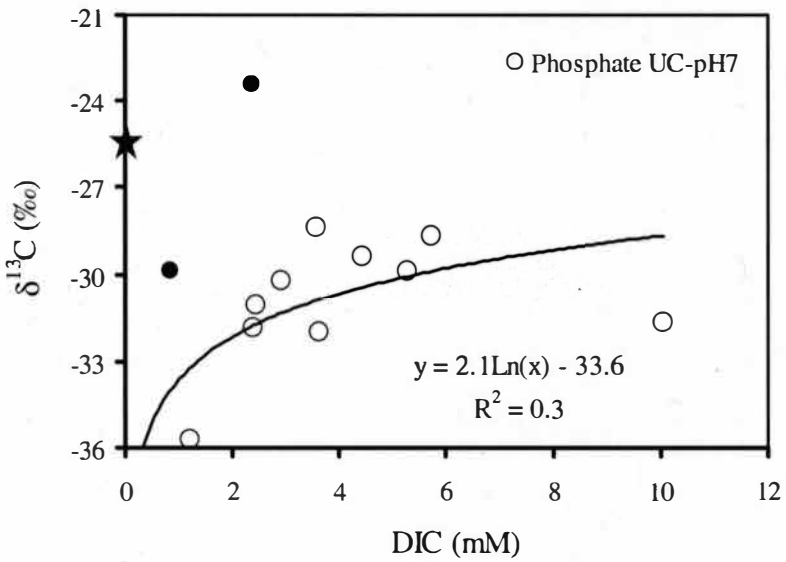


Figure 4.18 Carbon isotopic values DIC vs. DIC concentration under different pH conditions in the phosphate buffered system. Black star indicates the initial $\delta^{13}C$ values of the lactate/citrate. Logarithmic trend line is showing the successive enrichment of the $\delta^{13}C_{DIC}$ with increasing DIC concentration. Two samples (filled black circles) were not included in the trend line.

## Discussion

### Factors Controlling Redox Processes

Experiments were carried out in anaerobic conditions under different controlling factors. Our results agreed well with previous studies reporting the importance of pH, light and ferric iron for the abiotic oxidation of organic compounds coupled to metal reduction. In addition, the concentration of the ferric iron, wavelength and energy of irradiation source could influence the rate of redox processes (Wu and Deng, 2000). The type of photooxidizing catalysts, the strength of

the reducing agents and the presence of multidentate ligands also affect the rate of photo assisted redox processes (Kormanen et al., 1989). Moreover, different organic compounds exhibit different photodegradation rates involving several intermediate reactions in aqueous solutions (Deng et al., 1998; Wu and Deng, 2000). Our results could be affected by a combination of the multiple controlling factors mentioned above and by other researchers.

In the experimental setups containing all media components both Fe(II) and DIC increased with time. The rate of redox processes observed in our experimental conditions was slower compared to most of the previous studies both at acidic and neutral conditions (e.g. Deng et al., 1998; Northup and Cassidy, 2007). Deng et al. (1998) studied at lower pH (2) compared to our pH ranging from 5 to 9, considering the effectiveness of ferric citrate at lower pH could partially explain the observed discrepancies in the two studies. Northup and Cassidy, 2007 used modified Fenton mechanism using hydrogen peroxide at pH of 8. Such modification could explain faster rate observed in their study compared to our study. Moreover, in these two studies (Deng et al., 1998; Northup and Cassidy, 2007) the concentration of chloride ion is low compared to our experimental conditions, where we used KCl (1.4 mM) and $NH_4Cl$ (4.7 mM) in the media preparation. Recent studies (Calza et al., 2005; Vione et al., 2005) have shown that the presence of chloride ion in anaerobic conditions inhibit indirect photolysis by scavenging hydroxyl radicals in the systems. Hence, the chloride ions could be partially responsible for the slow rate of oxidation observed.

The HFO experiments (70 mM total Fe) generated more DIC than the ferric

citrate experiments (50 mM total Fe) showing the effect of concentration of initial Fe(III). The ratio of ligand to Fe(III) is also reported to influence the rate of photodegradation of organic compounds, at least at pH values less than 2 (Deng et al., 1998). In general, a larger ligand to sensitizing agent ratio results in a greater rate of organic compound photodegradation. In case of the two ligands (OH and citrate) containing electron acceptors used in our experiments the ligand to Fe(III) ratios are 3:1 in HFO compared to and 1:1 in HFO and ferric citrate respectively. This could also contribute to the difference in the rates of lactate/citrate oxidation observed for these two media compositions.

No measurable differences were observed when using either $KH_2PO_4$ or $NaHCO_3$ as buffering agents in the DIC or soluble ferrous iron production. These observations showed that as long as the pH conditions are maintained, the type of buffering agent has little effect on the redox process. This was contrary to our microbially mediated experiments discussed in Chapter III where bicarbonate clearly enhanced the oxidation and reduction process at near neutral pH. The complex enzymatic reactions in biotic systems could be responsible for the observed difference due to enhanced metabolism in the bicarbonate system. Whereas in abiotic systems, both bicarbonate and phosphate buffers affect the formation of $^{\cdot}OH$ radical at neutral pH equally enhancing the effect of Fenton mechanisms.

pH determines the dominance of different metal-ligand complexes influencing their photoreactivity and participation in redox reactions. Under acidic conditions, Fe(III)-citrate complexes photochemically produce more reactive species (e.g. $H_2O_2$ and $^{\cdot}OH$) compared to Fe(III)-hydroxyl and Fe(III)-oxalate complexes (Kormanen et

al., 1989; Deng et al., 1998; Deng and Wu, 2000). This observation could explain the greater DIC yield and ferrous iron production measured at pH of 5 compared to the neutral and alkaline pH conditions (Figures 4.8 – 4.11). At near neutral to alkaline conditions, Fe(III)-hydroxyl becomes more photoreactive than Fe(III)-citrate complex (Deng et al., 1998). Thus, the greater DIC production observed in HFO media compared to the ferric citrate media at near neutral pH conforms well to the observation of Deng et al. (1998).

The effects of light and sensitizing agents (Fe(III) and minor concentrations of transition metals in the Wolfe's minerals) were clearly demonstrated in our experimental conditions. In the absence of both Fe (III) and fluorescent light, minimal oxidation of lactate and citrate were observed indicating that in abiotic conditions these two organic compounds could only get oxidized via indirect (sensitized) photocatalytic processes. Omission of Wolfe's minerals from the media also affected DIC yield indicating the transition metals (e.g. Mn, Co, Zn, and Cu) might have some contribution in the oxidation of the organic compounds used.

Understanding the importance of microbially mediated and abiotic mechanisms such as the synergistic combination of microbial-Fenton systems (Fischer and Warneck, 1996; Howsawkeng et al, 2001; Northup and Cassidy, 2007) and sonochemical induced Fenton reaction (Minero et al. 2005) would help remediation of contaminants. These abiotic mechanisms could be important in the degradation of less microbially degradable compounds (e.g. PCE and TCE) by increasing production of $H_2O_2$ which in turn produces more hydroxyl radicals.

Stable Carbon Isotopes

The trend of isotopic values in Figure 4.16 indicated the presence of two isotopically distinct carbon sources (e.g. bicarbonate vs. organic compounds) and their sequential time dependent contribution of carbon indicating mixing of these isotopically distinct sources. As time progresses the isotopic contribution of the bicarbonate became less influential, where as the DIC coming from the oxidation of organic compounds increased.

Graph of the $\delta^{13}C_{DIC}$ of the samples as a function of the inverse of the total DIC ($DIC^{-1}$) is useful in the interpretation of the $\delta^{13}C_{DIC}$ – DIC relationship in the system (Not clear). The y-intercept of the regression line of this relationship provides clues to the isotopic value of the starting component (Nascimento et al., 1997 and references there in). Figure 4.17 showed clearly that the source of the starting component in the bicarbonate system to be either lactate or ferric citrate ($\delta^{13}C_{DIC}$ = -25.4 ‰). At lower pH conditions (pH ~5) there were no systematic relationship between the DIC and its respective carbon isotopic values.

The trend line on Figure 4.18 shows successive enrichment of the DIC produced from the oxidation of the organic compounds with increasing DIC concentration for the phosphate buffered system. Such systematic isotopic values observed with trend of the trend line appeared to show continuous consumption of the organic compounds via the Fe(III) sensitized photocatalytic oxidation approaching the initial $\delta^{13}C_{DIC}$ of these organic compounds. The heaviest $\delta^{13}C_{DIC}$ (-23.4 ‰) observed was slightly enriched compared to the starting carbon isotopic values for

citrate and lactate (≈-25.0‰).

In both bicarbonate and phosphate buffered systems, lower pH conditions (pH ≈5) did not show systematic relationship between the DIC and its respective carbon isotopic values. The reason for such observation in the lower pH conditions is unclear and seeks more quantitative work including the usage of isotopically tagged organic carbon compounds.

Rayleigh Fractionation Model for Abiotic Redox Processes

The carbon isotope values (Detail results in Appendix D, Table D9) were used to examine if the process of citrate and lactate oxidation was amenable to Rayleigh type modeling. In order to do this, we assumed that carbon came either from lactate or citrate oxidation. This assumption was based on the information that lactate and citrate are the dominant sources of carbon. Based on this observation, the isotopic fractionation in the bicarbonate- and phosphate-buffered systems was examined to check if the oxidation of lactate or citrate coupled with ferric iron reduction might follow Rayleigh distillation type fractionation. DIC was taken as a proxy for the oxidation of lactate and citrate. Detailed description of background of Rayleigh-type process is presented in Appendix B).

The isotopic value of the lactate remaining in solution at any time was calculated using equation 4.5 (The calculated values for each system is provided in Appendix D, Table D9) (Mariotti et al., 1981):

$$\delta_{react} = [\delta_{o\text{-}react} - ((1-f) * \delta_{prod\text{-}reservoir})]/f \qquad (4.5)$$

Where: $\delta_{react} = \delta^{13}C$ of lactate remaining at time t
$\delta_{o\text{-}react} = \delta^{13}C$ of initial lactate

$\delta_{product\text{-}reservoir}$= $\delta^{13}C$ of DIC produced at time t corrected for initial DIC and $\delta^{13}C$ of bicarbonate
f= fraction of lactate remaining at time t

Figure 4.19 shows the isotopic values of lactate as a function of remaining lactate fraction for both buffered systems assuming that citrate contributing negligible carbon to the system. Figure 4.20 shows the isotopic values of ferric citrate as a function of remaining citrate fraction for both buffered systems assuming lactate contributing negligible carbon to the system. The bicarbonate buffered systems were corrected for the initially added bicarbonate. In both cases (Figures 4.19 and 4.20), carbon isotopic values of the substrate (lactate or ferric citrate) tended to get isotopically heavier as it was consumed, although not as systematic as in the case of the microbially mediated processes discussed in Chapter III.

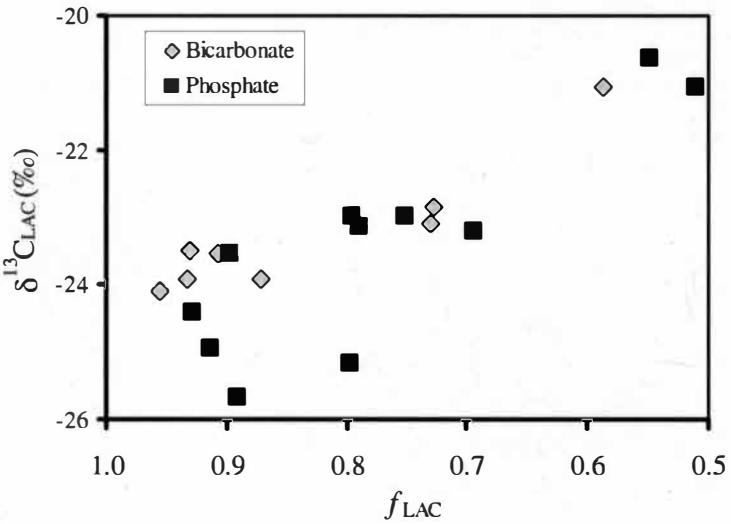


Figure 4.19 $\delta^{13}C$ values of remaining lactate as a function of remaining lactate fraction for the bicarbonate- (shaded diamond) and phosphate- (black squares) buffered systems.

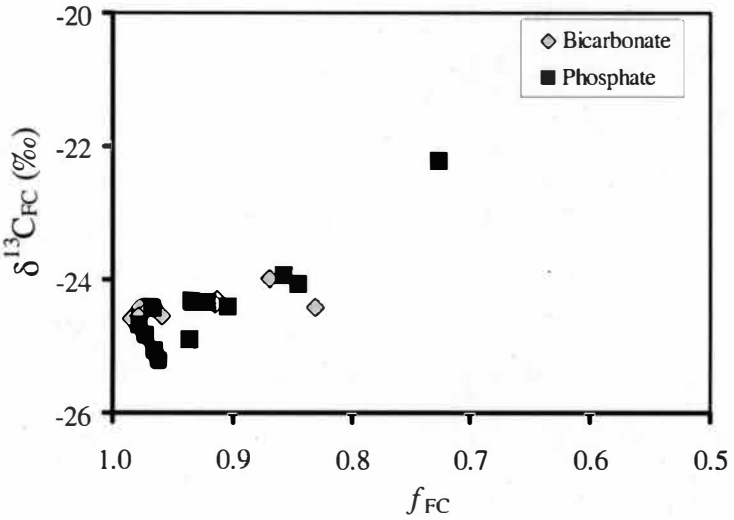


Figure 4.20 $\delta^{13}C$ values of remaining lactate as a function of remaining ferric citrate fraction for the bicarbonate- (shaded diamond) and phosphate- (black squares) buffered systems.

The fractionation factor for the two buffered systems during the reduction process could be estimated according to equation 4.6 (Mariotti et al., 1981, & Somsamak et al., 2006):

$$\delta_{react}=\delta_{o\text{-}react} + \varepsilon \ln f \qquad (4.6)$$

Where: $\delta_{react}$= $\delta^{13}C$ of lactate remaining at time t,
$\delta_{o\text{-}react}$= $\delta^{13}C$ of initial lactate,
ε= average equilibrium fractionation between lactate/citrate and DIC, which is related to α (fractionation factor) by: ε= (α-1)*1000
f= remaining fraction of lactate at time t

Figure 4.21 shows the $\delta^{13}C$ values vs. the natural logarithm of the remaining lactate fraction in the bicarbonate-buffered system and in the phosphate-buffered system. The slope of the regression line indicate an isotopic equilibrium fractionation (ε) between the lactate consumed and the produced carbon dioxide of ~-2.8 ‰ ($R^2$ =

0.6) in the bicarbonate buffered media and ~-7.4 ‰ ($R^2$ = 0.7) for the phosphate-buffered media. The difference in fractionation factors between the two buffered systems could be attributed to the differences in the magnitude of involvement of bicarbonate in scavenging the hydroxyl ions in the two systems. The mechanism for this difference and the effect of bicarbonate will be discussed below.

Figure 4.22 shows the $\delta^{13}C$ values vs. the natural logarithm of the remaining ferric citrate fraction in the bicarbonate-buffered system and in the phosphate-buffered system. The slopes of the regression lines indicate an isotopic equilibrium fractionation ($\varepsilon$) between the ferric citrate consumed and the carbon dioxide produced carbon dioxide of ~-1.9 ‰ ($R^2$ = 0.4) in the bicarbonate buffered media and ~-8.4 ‰ ($R^2$ = 0.9) for the phosphate-buffered media. The $R^2$ value of ~0.4 in the bicarbonate system indicates that there are processes that modify a strictly Rayleigh-type approximation. The y-intercept of the regression equations indicate that the average starting isotopic values to be -25.3 ‰ in the phosphate buffered system and -24.3 ‰ in the bicarbonate and which are close to the starting isotopic values of the citrate and lactate.

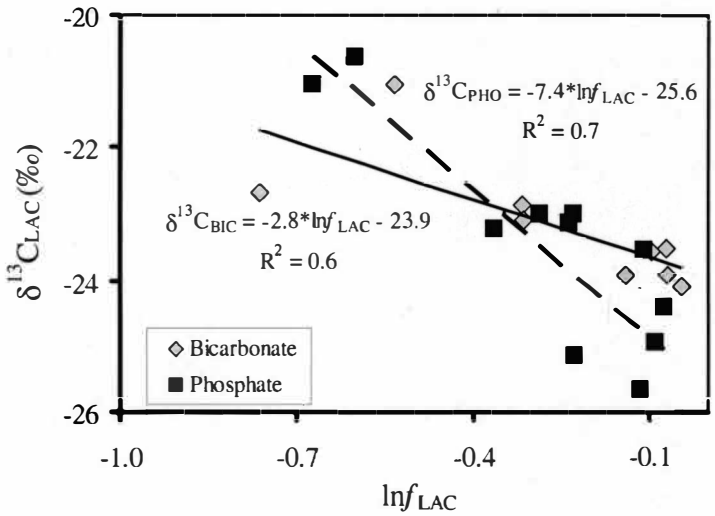


Figure 4.21 Semi-logarithmic plot of $\delta^{13}C$ values of the lactate as a function of remaining lactate fraction ($\ln f_{LAC}$) for bicarbonate- (shaded diamond) and phosphate- (black squares) buffered experiments. Slope of the regression lines were used to estimate equilibrium fractionation (ε).

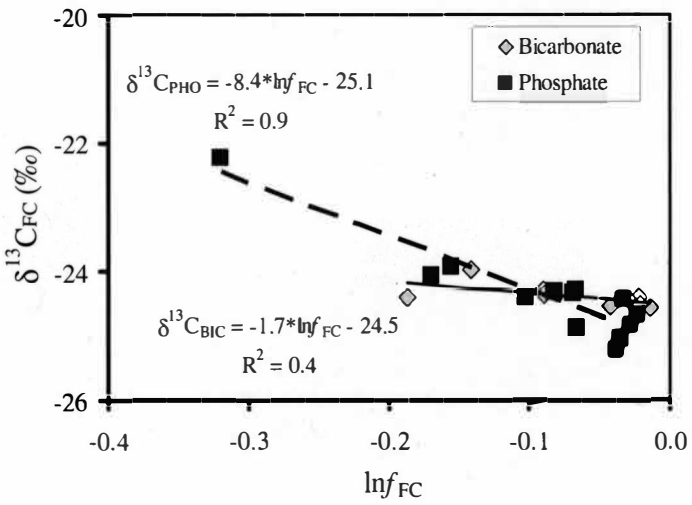


Figure 4.22 Semi-logarithmic plot of $\delta^{13}C$ values of the ferric citrate as a function of remaining ferric citrate fraction ($\ln f_{FC}$) for bicarbonate- (shaded diamond) and phosphate- (black squares) buffered experiments. Slope of the regression lines were used to estimate equilibrium fractionation (ε).

In the bicarbonate buffered systems Rayleigh type process was modified possibly by the role of bicarbonate in scavenging the hydroxyl radical during the oxidation of lactate/ferric citrate. Studies (e.g. Hoigne and Bader, 1978; Canonica et al., 2005; Busset et al., 2007) have shown that bicarbonate (at lower pH) and carbonate (at pH > 9) ions to have a scavenging effect on the hydroxyl radical. Media with high concentration of $HCO_3^-/CO_3^{-2}$ react with $^{\cdot}OH$ radical to form carbonate radical, which further attack the organic compounds (Canonica et al., 2005; Busset et al., 2007). Further oxidation of the organic compounds result in recycling of the bicarbonate ion and carbonate radical that could affect the isotopic systematics. Such usage of the initially added bicarbonate in the bicarbonate systems would alter the isotopic values of the bicarbonate from its initial value (~+9.3 ‰).

## Conclusions

Most previous studies have been conducted under aerobic and acidic conditions (pH=2-5), with a few under anaerobic conditions. Such acidic pH conditions are less likely in the natural environment due to the buffering capacity of soils in natural ecosystems. Here, this research reported results from experimental work done under circum-neutral and anaerobic conditions. The effects of light, Fe(III) presence and concentrations, ligand to Fe(III) ratio, and pH on the redox processes involving lactate and citrate as model organic compounds were observed in our study conforming previous observations made mostly under acidic and aerated conditions.

Both lactate and citrate undergo oxidation by indirect photolysis involving

sensitizing agents and modified Fenton reaction. Hydroxyl radicals play vital role in recycling the oxidized form of the sensitizing agents (e.g. Fe(III)) and could accelerate organic matter mineralization producing bioavailable intermediate products. The rate of oxidation of the organic compounds in our experimental condition was slowed down due to the presence of inhibiting ions such as chloride by the scavenging of the hydroxyl radical produced via Fenton-like mechanism.

Stable carbon isotopic signatures in both bicarbonate and phosphate buffered systems in neutral pH conditions were observed to approach $\delta^{13}C$ values of the lactate and citrate used (≈-25.0 ‰) with increasing DIC yield. The isotopic signatures in acidic conditions didn't show similar distinctive pattern to those observed in neutral pH conditions and need more quantitative work. The phosphate buffered system with the assumption of citrate as a sole source of DIC fit best with Rayleigh fractionation model with equilibrium fractionation (ε) of ~-8.4 ‰. The bicarbonate buffered conditions are affected by the involvement of bicarbonate in scavenging hydroxyl radical and produce carbonate radical that could possibly modify the Rayleigh fractionation process.

# CHAPTER V

## SUMMARY AND CONCLUSIONS

In this research, stable carbon isotopes combined with other chemical parameters were used to investigate both microbial (biotic) and abiotic redox processes in circum-neutral and anaerobic conditions.

The objectives of microbial iron reduction experiments were:

1. To compare the effect of two of the most commonly occurring buffering compounds (bicarbonate and phosphate) on the microbial reduction of iron and oxidation of lactate.
2. To characterize the iron reduction pathways based on the premise that DIC can be used a proxy for the reduction process.
3. To estimate carbon isotope fractionation between microbial biomass and respired carbon dioxide through the exponential growth stage of *Shewanella putrefaciens* strain 200R.
4. To propose a suitable model for iron reduction under the experimental conditions employed.

The main findings of the microbial based study were

1. Generally, both DIC and Fe(II) results indicated that bicarbonate buffered media tended to enhance the reduction process at least under our experimental conditions compared to the phosphate buffered system.

2. In both buffering systems the Fe(II)-DIC correlation was affected due to decrease in concentration of soluble iron .This can be due to post reduction processes causing the speciation of Fe(II) including formation ferrous iron compounds, adsorption onto microbial surfaces. These effects were more pronounced in the stationary phase of the growth curve with the precipitation of vivianite in the phosphate buffered system and increase in pH in the bicarbonate buffered system.
3. Bicarbonate appeared to induce a slightly larger fractionation between lactate and DIC compared to phosphate (6.6 ‰ vs. 4.6 ‰) which could be due to a reservoir effect.
4. The biomass (~ -27 ‰) was enriched by ~5 ‰ compared to the DIC. Based on this observation and the isotopic fractionation between DIC and gaseous $CO_2$, the biomass was estimated to be enriched by ~12 ‰ compared to the respired $CO_2$.
5. The incorporation of this isotopically light respired $CO_2$ (~ -39 ‰) might account for the isotopically depleted fatty acids in the serine pathway reported previously.

The objectives of the abiotic based experiments were:

1. To investigate the sources of $CO_2$ and ferrous iron in control samples.
2. To characterize effects of light, presence and concentrations of Fe(III), types of electron acceptors, types of buffer, and pH on the redox processes involving lactate and citrate as examples of organic

compounds.

3. Incorporation of stable carbon isotopes signatures to characterize and understand abiotic electron transferring processes.

The findings of the abiotic experiments in the current study were:

1. DIC and ferrous iron concentration increased with time both in the bicarbonate and phosphate systems indicating abiotic oxidation of organic compounds.
2. Sensitizing agents (e.g. Fe(III)) and pH play vital role in redox processes in the presence of light.
3. Hydroxyl radical showed an enhancing effect on photodegradation of the organic compounds used.
4. The presence of chloride ion in our experiments, in the form of KCl and $NH_4Cl$, slightly slowed the redox process, in agreement with previous observations by other researchers.
5. The requirement for light and sensitizing agents in the oxidation of lactate and citrate showed that these organic compounds belong to the sensitized photo-catalytically degraded group of organic compounds at least under our experimental conditions.
6. Isotopically, both bicarbonate and phosphate buffer systems showed progressive enrichment of $^{13}C_{DIC}$, with increasing DIC yield, approaching the starting $\delta^{13}C$ of lactate/citrate.
7. The source of the inorganic carbon added to the system was most likely lactate/citrate ($\delta^{13}C_{DIC} \approx$-25.0‰).

8. Average ε values of ~-7.9 ‰ and ~-2.4 ‰ were estimated between the consumed organic compounds and the produced DIC for the phosphate and bicarbonate buffered conditions. Rayleigh type process in the bicarbonate buffered abiotic systems could be possibly modified due to the scavenging effect of the bicarbonate on the hydroxyl radical as the initially added bicarbonate vary isotopically with time.

Overall implications of the current research:

- The coexistence of biotic-abiotic degradation mechanisms could promote enhanced treatment of *in situ* mineralization of organic and inorganic contaminants. Abiotic electron transfer processes could be not only useful but important in transforming microbially less degradable organic compounds (e.g. PCE and TCE) to bioavailable products.

# Appendix A

## Details of Media Components and Procedures

## Details of Media Components

In this research, both bicarbonate and phosphate buffered modified media were prepared and dispensed anaerobically (under an atmosphere of 95 % $N_2$, 5% $H_2$) according to Haas et al. (2001). The media were slightly modified in the phosphate buffered system. Autoclave the media at 121°C for 15 minutes and then added vitamins, minerals and the electron acceptors (HFO or Ferric Citrate prepared separately) sterilized, nitrogen-sparged stock solution prior to inoculation in the microbially mediated experiment and before starting the experiment in the abiotic systems. Final pH of medium was approximately 7 in all systems.

Components and Procedure 1

| Bicarbonate Media | Phosphate Media |
|---|---|
| $NH_4Cl$ .....0.25 g | $NH_4Cl$ .....0.25 g |
| $NaH_2PO_4.H_2O$ .....0.6 g | $NaH_2PO_4.H_2O$ .....0.6 g |
| KCl.....0.1 g | KCl.....0.1 g |
| $NaHCO_3$ .....2.5 g | $KH_2PO_4.3H_2O$ .....6.8 g |
| Na-Lactate.....5 ml | Na-Lactate.....5 ml |
| $QH_2O$ (R~17.6 MΩ cm).....1.0 L | $QH_2O$.....1.0 L |
| After Autoclaving: | After Autoclaving: |
| Ferric Citrate (50 mM) or HFO (70 mM) | Ferric Citrate (50 mM) or HFO (70 mM) |
| Wolfe's Vitamin Solution (see below).... 0.1 ml | Wolfe's Vitamin Solution....0.1 ml |
| Modified Wolfe's Minerals(see below)...1.0 ml | Modified Wolfe's Minerals...1.0 ml |

## Wolfe's Vitamin Solution:

This is available from ATCC™ (The Global Bioresource Center) as a sterile ready-to-use liquid (Vitamin Supplement, catalog no MD-VS) containing the following components:

Biotin.....2.0 mg

Folic acid.....2.0 mg

Pyridoxine hydrochloride....10.0 mg

Thiamine . HCl.....5.0 mg

Riboflavin.....5.0 m

Nicotinic acid.....5.0 mg

Calcium D-(+)-pantothenate...5.0 mg

Vitamin B12.....0.1 mg

p-Aminobenzoic acid.....5.0 mg

Thioctic acid.....5.0 mg

Distilled water.....1.0 L

## Modified Wolfe's Minerals:

$Na_2SeO_3$ .....10.0 mg

$NiCl_2$. $6H_2O$ .....10.0 mg

$Na_2WO4.2H_2O$.....10.0 mg

Wolfe's Mineral Solution (see below).....1.0 L

## Wolfe's Mineral Solution

It is Available from ATCC™ as a sterile ready-to-use liquid (Trace Mineral Supplement, catalog no. MD-TMS). And has the following components:

Nitrilotriacetic acid.....1.5 g

$MgSO_4$. $7H_2O$ .....3.0 g

$MnSO_4$. $H_2O$ .....0.5 g

NaCl.....1.0 g

$FeSO_4$. $7H_2O$ .....0.1 g

$CoCl_2$. $6H_2O$ .....0.1 g

$CaCl_2$ .....0.1 g

$ZnSO_4$. $7H_2O$ .....0.1 g

$CuSO_4$. $5H_2O$ .....0.01 g

$AlK(SO_4)_2$. $12H_2O$.....0.01 g

$H_3BO_3$ .....0.01 g

$Na_2MoO_4$. $2H_2O$.....0.01 g

Distilled water.....1.0 L

Table A1: Time (hr) series measurements of DIC (mM), pH, $\delta^{13}C_{DIC}$ (‰); and HPLC measurements of lactate, Acetate, Citrate, and butyrate (ppm) for the bicarbonate and phosphate-buffered condition. N = not measured, ND= Not detected

| Sample | Time | pH | DIC | $\delta^{13}C_{DIC}$ | Lactate | Acetate | Citrate | Butyrate |
|---|---|---|---|---|---|---|---|---|
| SPFe61 | 0 | 7.3 | 0.3 | -29.0 | 1334.97 | ND | 412.5 | ND |
| SPFe62 | 8 | 7.4 | 2.2 | -29.8 | N | N | N | N |
| SPFe63 | 16 | 7.5 | 4.6 | -28.5 | 936.1 | ND | 391.5 | ND |
| SPFe64 | 19 | 7.4 | 5.7 | -27.8 | N | N | N | N |
| SPFe65 | 22 | 8 | 7.2 | -27.3 | 895.7 | 81.5 | 476.6 | 21.5 |
| SPFe66 | 25 | 8 | 8.1 | -27.1 | N | N | N | N |
| SPFe67 | 28 | 7.9 | 10.1 | -27.0 | 2124.8 | 161.5 | 429.3 | 86.6 |
| SPFe68 | 31 | 7.9 | 9.9 | -27.2 | N | N | N | N |
| SPFe69 | 34 | 7.9 | 10.2 | -27.2 | 1110.6 | 418.9 | 535.4 | ND |
| SPFe70 | 40 | 7.9 | 12.2 | -26.4 | 1395.9 | 624.5 | 712.4 | ND |
| SPFe71 | 43 | 7.9 | 11.0 | -27.1 | N | N | N | N |
| SPFe72 | 46 | 7.9 | 11.8 | -26.7 | 245.0 | 6.8 | 526.8 | 21.4 |
| SPFe73 | 51 | 7.9 | 12.0 | -26.5 | 271.6 | 7.6 | 507.5 | N |

| | | | | | | | | |
|---|---|---|---|---|---|---|---|---|
| SPFe74 | 57 | 7.8 | 12.5 | -26.2 | N | N | N | N |
| SPFe75 | 70 | 7.9 | 12.5 | -26.4 | ND | 73.4 | 412.4 | ND |
| SPFe76 | 81 | 7.8 | 12.4 | -26.4 | ND | 46.3 | 441.7 | ND |
| SPFe77 | 93 | 7.9 | 12.6 | -26.4 | N | N | N | N |
| SPFe78 | 129 | 8 | 12.6 | -25.7 | 282.0 | 11.1 | 423.5 | ND |
| SPFe79 | 189 | 7.9 | 13.0 | -26.2 | ND | 82.4 | 510.1 | ND |
| SPFe80 | 273 | 8 | 11.9 | -26.9 | 291.4 | 14.2 | 604.7 | ND |
| SPFe81 | 351 | 8 | 12.4 | -26.6 | 315.0 | 10.9 | 413.1 | ND |
| SPFe211 | 25 | 7.7 | 6.04 | -27.3 | N | N | N | N |
| SPFe212 | 38 | 7.8 | 8.90 | -27.8 | N | N | N | N |
| SPFe213 | 48 | 8.3 | 9.39 | -28.2 | ND | ND | 5.1 | 84.9 |
| SPFe214 | 72 | 8.3 | 10.13 | -26.4 | 303.6 | 13.4 | 413.9 | ND |
| SPFe215 | 131 | 8.4 | 9.59 | -26.2 | 46.4 | ND | 0.5 | ND |
| SPFe82 | 0 | 7.1 | 0.3 | -32.5 | 3473.2 | ND | 505.8 | ND |
| SPFe83 | 8 | 7 | 1.8 | -29.5 | 3462.1 | ND | 542.1 | ND |
| SPFe84 | 16 | 7.1 | 3.0 | -28.0 | N | N | N | N |
| SPFe85 | 19 | 7.1 | 3.8 | -27.8 | N | N | N | N |
| SPFe86 | 22 | 7.1 | 1.3 | -26.6 | 2568.6 | ND | 485.4 | ND |
| SPFe87 | 25 | 7.1 | 4.8 | -26.9 | N | N | N | N |
| SPFe88 | 28 | 7.1 | 4.7 | -26.9 | ND | 6904.9 | 147.6 | ND |
| SPFe89 | 31 | 7.2 | 5.3 | -26.6 | N | N | N | N |
| SPFe90 | 34 | 7.1 | 5.6 | -27.1 | 453.7 | 4.6 | 386.5 | ND |
| SPFe91 | 40 | 7.2 | 6.8 | -26.8 | 314.8 | 11.1 | 344.5 | ND |
| SPFe92 | 43 | 7.2 | 6.0 | -27.0 | N | N | N | N |
| SPFe93 | 46 | 7.2 | 6.2 | -27.1 | 744.9 | 84.4 | 475.0 | ND |
| SPFe94 | 51 | 7.3 | 6.8 | -26.6 | 666.0 | 67.1 | 409.7 | ND |
| SPFe95 | 57 | 7.2 | 7.1 | -25.7 | 920.5 | 90.2 | 523.6 | ND |
| SPFe96 | 70 | 7.2 | 7.7 | -26.5 | 823.9 | 70.1 | 432.7 | ND |
| SPFe97 | 81 | 7.3 | 8.1 | -26.5 | 367.3 | 5.1 | 540.6 | ND |
| SPFe98 | 93 | 7.30 | 8.7 | -26.4 | 604.9 | 59.8 | 416.1 | 18.0 |
| SPFe99 | 129 | 7.4 | 9.3 | -26.6 | 356.3 | 8.6 | 508.3 | 25.0 |
| SPFe100 | 189 | 7.3 | 10.1 | -26.8 | 525.0 | 60.8 | 394.7 | ND |
| SPFe101 | 273 | 7.30 | 9.0 | -26.5 | 350.3 | 9.7 | 518.2 | 12.9 |

| | | | | | | | | |
|---|---|---|---|---|---|---|---|---|
| SPFe102 | 351 | 7.3 | 10.1 | -26.4 | 525.4 | 58.5 | 402.4 | 130.8 |
| SPFe221 | 25 | 7.1 | 3.32 | -28.1 | N | N | N | N |
| SPFe222 | 38 | 7.2 | 2.96 | -27.5 | N | N | N | N |
| SPFe223 | 48 | 7.1 | 5.28 | -27.4 | 504.7 | ND | 488.5 | ND |
| SPFe224 | 72 | 7.3 | 5.70 | -27.2 | 330.1 | 6.5 | 502.8 | ND |
| SPFe225 | 131 | 7.3 | 6.55 | -27.0 | 322.5 | 13.2 | 379.6 | ND |

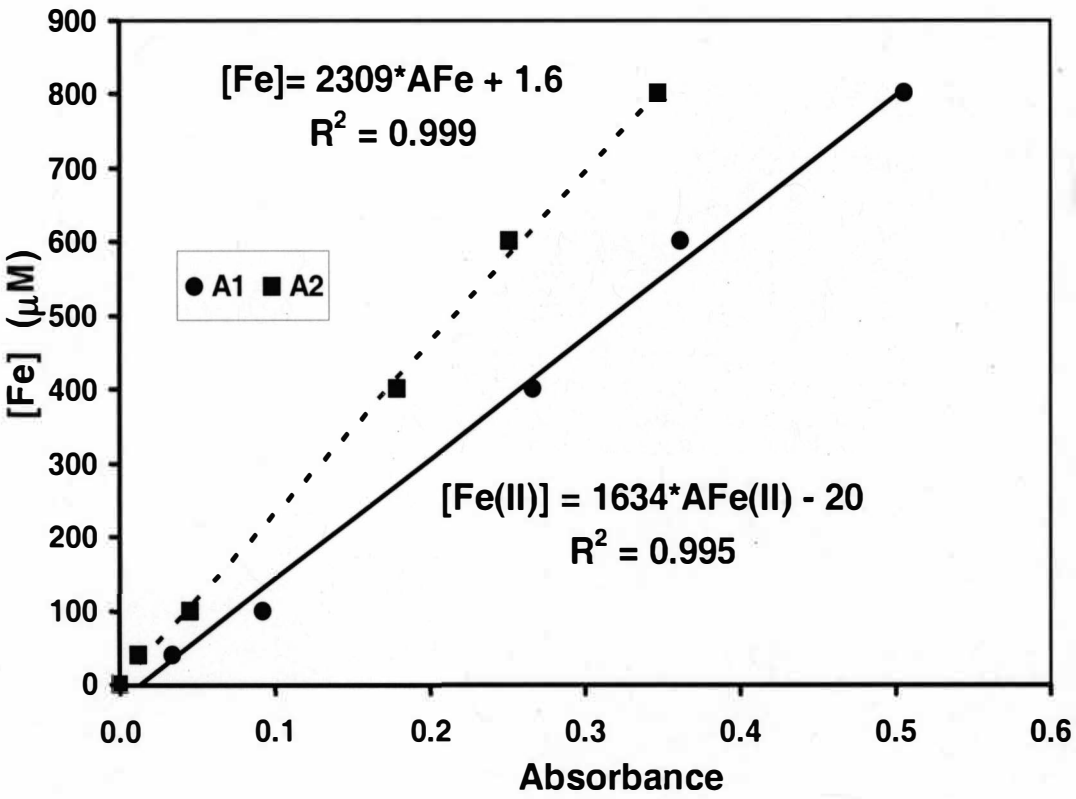


Figure A1 Typical calibration curve for spectrophotometric total iron and ferrous iron determinations according to the ferrozine method (Viollier et al., 2000).

# Appendix B

## Derivation of Rayleigh Type Process

## Derivation of Rayleigh Fractionation Equation

Understanding the variations in stable isotope abundance in any system requires a thorough knowledge of isotope fractionation taking place during physical, chemical or biochemical transformations involved in various processes. A number of these processes can be modeled using a Rayleigh type process. Two examples of Rayleigh processes in nature are the rainout process, and bacterial sulfate reduction. The Rayleigh equation (B1) was first introduced by Lord Rayleigh for characterizing fractional distillation of mixed liquids.

$$\frac{R_R}{R_{R0}} = f^{(\alpha_{P/R}-1)} \qquad \text{(B1)}$$

Where: $R_R$ = Isotope ratio of substrate at time t
$R_{R0}$ = Isotope ratio of initial substrate
$f$= Fraction of substrate remaining
$\alpha_{P/R}$= Fractionation factor

The Rayleigh model was later introduced to isotope geochemistry studies by Dansgaard (1964), in his study on stable isotope fractionation during precipitation.

Isotope ratios are measured using an Isotope Ratio Mass Spectrometer and the results are reported in a $\delta$ notation relative to an international standard (Vienna PeeDee Belemnite (V-PDB) for carbon and oxygen isotopes; SMOW for Oxygen and hydrogen isotopes, etc.):

$$\delta\,‰ = \left(\frac{R_{Sample}}{R_{S\,\mathrm{tan}\,dard}} - 1\right) * 1000 \qquad \text{(B2)}$$

Where: R= Isotope ratio of different elements (e.g. D/H, $^{13}C/^{12}C$; $^{18}O/^{16}O$); $R_{Sample}$ and $R_{Standard}$ represent the isotope ratio of the sample and standard respectively.

It can also be shown that (B3) relating $\alpha$ and $\delta$

$$\alpha_{P\text{-}R} = \left(\frac{1+\delta_P/1000}{1+\delta_R/1000}\right) = \left(\frac{1000+\delta_P}{1000+\delta_R}\right) \qquad \text{(B3)}$$

Here, the Raleigh equation will be derived step by step using carbon isotope partitioning between lactate and carbon dioxide as respective reactant and product for the unidirectional ( i.e. Kinetic reaction, a common case in most microbially mediated systems) transformation of lactate to carbon dioxide (B4).

$$\underset{\text{(Lactate)}}{\mathbf{NaC_3H_6O_3}} + 4FeC_6H_5O_7 + 2H_2O \rightarrow \underset{}{\mathbf{HCO_3^-}} + 4Fe^{2+} + \underset{\text{(Citrate)}}{4C_6H_5O_7^{-3}} + \underset{\text{(Acetate)}}{NaC_2H_3O_2} + 5H^+ \qquad \text{(B4)}$$

The Kinetic Fractionation Factor between the reactant lactate and the product DIC ($\alpha_{CO2/LAC}$) can be expressed as (B5):

$$\alpha_{CO2/LAC} = R_{CO2}/R_{LAC} = \frac{\left(d^{13}C_{CO_2}/d^{12}C_{CO_2}\right)}{\left(d^{13}C_{LAC}/d^{12}C_{LAC}\right)} \qquad \text{(B5)}$$

Where: $R_{CO2}$ is the isotope ratio of the increment of DIC at time t
$R_{LAC}$ is the isotope ratio of the lactate at the same time t,

Since $d^{13}C_{co_2} = -d^{13}C_{LAC}$ and $d^{12}C_{co_2} = -d^{12}C_{LAC}$, Equation B5 can be re-written as

$$\alpha_{co_2/LAC} = \frac{\left(d^{13}C_{LAC}/d^{13}C_{LAC}\right)}{\left(d^{12}C_{LAC}/d^{12}C_{LAC}\right)} \qquad \text{(B6)}$$

Considering $\alpha_{co_2/LAC}$ as a constant integration of equation B6 can be given as:

$$(\alpha_{co_2/LAC})\ \ln\left(\frac{d^{12}C_{LAC}}{d^{12}C_{LAC\,0}}\right) = \ln\left(\frac{d^{13}C_{LAC}}{d^{13}C_{LAC\,0}}\right) \qquad \text{(B7)}$$

$^{13}C_{LACo}$ and $^{12}C_{LACo}$ are the two isotopes of lactate at time zero

Let f be the remaining lactate fraction at any time t and $C_{LAC}$ the total quantity of carbon at time t ($C_{LAC}$= $^{13}C_{LAC}$ + $^{12}C_{LAC}$). Mathematically f can be expressed as:

$$f= C_{LAC}/C_{LACo}=\frac{\left(^{12}C_{LAC}+^{13}C_{LAC}\right)}{\left(^{12}C_{LAC\,O}+^{13}C_{LAC\,O}\right)} \qquad \text{(B8)}$$

In natural systems, the abundance of $^{13}C$ varies very little and $^{12}C+^{13}C\approx^{12}C$, so equation B8 can be simplified to f= $^{12}C_R/^{12}C_{Ro}$ and equation B7 can be re-written as:

$$(\alpha_{co_2/LAC})\ln f = \ln\left(\frac{d^{13}C_{LAC}}{d^{13}C_{LAC_0}}\right) = \ln\left(\frac{R_{LAC} * d^{12}C_{LAC}}{R_{LAC_0} d^{12}C_{LAC_0}}\right)$$

$$= \ln\left(\frac{R_{LAC}}{R_{LAC_0}}\right) * \left(\frac{R_{LAC} * d^{12}C_{LAC}}{R_{LAC_0} d^{12}C_{LAC_0}}\right)$$

$$= \ln\left(\frac{R_{LAC}}{R_{LAC_0}}\right) + \ln\left(\frac{d^{12}C_{LAC}}{d^{12}C_{LAC_0}}\right) = \ln\left(\frac{R_{LAC}}{R_{LAC_0}}\right) + \ln f$$

$$(\alpha_{co_2/LAC})\ln f - \ln f = \ln\left(\frac{R_{LAC}}{R_{LAC_0}}\right) = (\alpha_{co_2/LAC} - 1)\ln f \qquad \text{(B9)}$$

Equation B9 can also be expressed as $\frac{R_{LAC}}{R_{LAC_0}} = f^{\left(\alpha_{CO_2/LAC}-1\right)}$ (B10)

Equation B10 is a typical example of the Rayleigh Equation derived by Lord Rayleigh for characterizing fractional distillation of mixed liquids.

The fractionation factor for the isotope exchange between lactate and bicarbonate can be derived from the measured δ‰ values according to:

$$\alpha_{CO2\text{-}LAC} = \left(\frac{1+\delta_{CO_2}/1000}{1+\delta_{LAC}/1000}\right) = \left(\frac{1000+\delta_{CO_2}}{1000+\delta_{LAC}}\right) \qquad \text{(B11)}$$

The relationship of the fractionation factor to the per mil enrichment factor (ε), an estimation parameter used for the isotopic difference of lactate and bicarbonate in our experimental system will be demonstrated using the following equations. Using equation B9, it can be shown that:

$$(\alpha_{CO2/LAC} - 1) \ln f = \ln\left(\frac{10^{-3}\delta_{LAC}+1}{10^{-3}\delta_{LACo}+1}\right) \qquad \text{(B12)}$$

According to Mariotti et al. (1981), the fractionation factor generally differs by less than 5 % from unity, and it can be related to the per mil enrichment factor as:

$$\alpha_{CO_2/LAC} = 1 + 10^{-3} * \varepsilon_{CO_2/LAC} \qquad \text{(B13)}$$

Combining equations B12 and B13 we can get:

$$\varepsilon_{CO2/LAC} = \frac{10^3 * \ln\left(\frac{10^{-3}\delta_{LAC}+1}{10^{-3}\delta_{LACo}+1}\right)}{\ln f} \qquad \text{(B14)}$$

Since $\ln(1+X) \approx X$ when X is small relative to 1 and $\ln[(1+X)/(1+Y)] \approx X - Y$, when both X and Y are small relative to 1, and as a result equation B14 can be approximated as:

$$\varepsilon_{CO2/LAC} = \frac{\delta_{LAC} - \delta_{LACo}}{\ln f} \qquad \text{(B15)}$$

The following approach was used in the characterization of iron reduction process. Our batch experiments were treated as open or accumulated system. As shown in reaction B4 above, lactate ([C]= 30 mM, $\delta^{13}C$=-25.4 ‰) was the reactant in our system and the accumulated product treated for the isotopic study was bicarbonate. Each lactate molecule oxidizes to one molecule of bicarbonate and one molecule of acetate. Hence, the amount DIC measured was used as a proxy for the oxidized lactate and for calculating the fraction of lactate remaining in each batch sample analyzed (results are presented in Appendix C, Table C1). The equation used for calculating the remaining lactate fraction at any time t is given as B16:

$$f = [DIC]_t / [DIC]_{LAC} \qquad \text{(B16)}$$

Where: $[DIC]_t$ = measured DIC at any time t and
$[DIC]_{LAC}$ = stoichiometrically expected DIC when all lactate is oxidized

The isotopic value of the lactate remaining in solution at any time was calculated using equation B17 (Mariotti et al., 1981):

$$\delta_{react} = [\delta_{o-react} - ((1-f) * \delta_{prod-reservoir})]/f \qquad \text{(B17)}$$

Where: $\delta_{react}$= $\delta^{13}C$ of lactate remaining at time t
$\delta_{o-react}$= $\delta^{13}C$ of initial lactate
$\delta_{product-reservoir}$= $\delta^{13}C$ of DIC produced at time t corrected for initial DIC and $\delta^{13}C$ of bicarbonate
f= fraction of lactate remaining at time t

The fractionation factor for the two buffered systems representing the kinetically controlled phase of the reduction process could be estimated according to

equation B18, treating both systems as a closed system (Mariotti et al., 1981, & Somsamak et al., 2006):

$$\delta_{react} = \delta_{o-react} + \varepsilon \ln f \qquad \text{(B18)}$$

Where: $\delta_{react}$= $\delta^{13}C$ of lactate remaining at time t,

$\delta_{o-react}$= $\delta^{13}C$ of initial lactate,

$\varepsilon$= average equilibrium fractionation between lactate and DIC, which is related to $\alpha$ (fractionation factor) by: $\varepsilon = (\alpha - 1)*1000$

f= remaining fraction of lactate at time t

The slope of equation B18 in effect provides an estimate of the enrichment factor ($\varepsilon$) between the lactate and the product in our analyses

# Appendix C

## Chemical and Carbon Isotope Analyses of Biotic Study

Table C1: Time (hr) series measurements of pH, Fe (II), Fe(III) (mM), DIC (mM, mg C/l), & $\delta^{13}C_{DIC}$ (‰) for bicarbonate- & phosphate-buffered conditions. SPFe61: stands for SP (*S. putrefaciens*), Fe for iron reduction experiment and 61 time series sample number. This table was used for covered uncovered statistical comparison for the biotic experiments (see tables in Appendix E).

| Sample | Time | pH | Fe (II) | Fe (III) | DIC | DIC | $\delta^{13}C$ | Buffer | Remarks |
|---|---|---|---|---|---|---|---|---|---|
| SPFe61 | 0 | 7.3 | 1.8 | 10.4 | 0.3 | 4 | -30.5 | $NaHCO_3$ | UC |
| SPFe62 | 8 | 7.4 | 1.4 | 10.9 | 2.2 | 26 | -29.8 | $NaHCO_3$ | UC |
| SPFe63 | 16 | 7.5 | 4.6 | 7.6 | 4.6 | 55 | -28.5 | $NaHCO_3$ | UC |
| SPFe64 | 19 | 7.4 | 5.8 | 7.5 | 5.7 | 68 | -27.8 | $NaHCO_3$ | UC |
| SPFe65 | 22 | 8.0 | 6.9 | 5.6 | 7.2 | 87 | -27.3 | $NaHCO_3$ | UC |
| SPFe66 | 25 | 8.0 | 6.5 | 5.6 | 8.1 | 97 | -27.1 | $NaHCO_3$ | UC |
| SPFe67 | 28 | 7.9 | 6.4 | 5.9 | 10.1 | 121 | -27.0 | $NaHCO_3$ | UC |
| SPFe68 | 31 | 7.9 | 7.4 | 5.5 | 9.9 | 119 | -27.2 | $NaHCO_3$ | UC |
| SPFe69 | 34 | 7.9 | 6.6 | 4.5 | 10.2 | 123 | -27.2 | $NaHCO_3$ | UC |
| SPFe70 | 40 | 7.9 | 6.8 | 5.1 | 12.2 | 147 | -26.4 | $NaHCO_3$ | UC |
| SPFe71 | 43 | 7.9 | 6.7 | 4.9 | 11.0 | 132 | -27.1 | $NaHCO_3$ | UC |
| SPFe72 | 46 | 7.9 | 7.4 | 6.0 | 11.8 | 142 | -26.7 | $NaHCO_3$ | UC |
| SPFe73 | 51 | 7.9 | 5.6 | 0.5 | 12.0 | 144 | -26.5 | $NaHCO_3$ | UC |
| SPFe74 | 57 | 7.8 | 5.4 | 0.5 | 12.5 | 151 | -26.2 | $NaHCO_3$ | UC |
| SPFe75 | 70 | 7.9 | 7.0 | 0.6 | 12.5 | 151 | -26.4 | $NaHCO_3$ | UC |
| SPFe76 | 81 | 7.8 | 7.6 | 0.9 | 12.4 | 148 | -26.4 | $NaHCO_3$ | UC |
| SPFe77 | 93 | 7.9 | 4.9 | 0.1 | 12.6 | 152 | -26.4 | $NaHCO_3$ | UC |
| SPFe78 | 129 | 8.0 | 5.2 | 0.4 | 12.6 | 151 | -25.7 | $NaHCO_3$ | UC |
| SPFe79 | 189 | 7.9 | 7.0 | 0.8 | 13.0 | 156 | -26.2 | $NaHCO_3$ | UC |
| SPFe80 | 273 | 8.0 | 7.0 | 0.7 | 11.9 | 143 | -26.9 | $NaHCO_3$ | UC |
| SPFe81 | 351 | 8.0 | 8.0 | 0.7 | 12.4 | 149 | -26.6 | $NaHCO_3$ | UC |
| SPFe63B | 16 | 7.5 | 4.7 | 7.8 | 4.5 | 54 | -27.7 | $NaHCO_3$ | C |
| SPFe66B | 25 | 7.9 | 6.1 | 6.4 | 7.3 | 88 | -27.0 | $NaHCO_3$ | C |
| SPFe69B | 34 | 7.9 | 6.9 | 7.8 | 10.6 | 127 | -26.8 | $NaHCO_3$ | C |
| SPFe72B | 46 | 7.9 | 6.5 | 5.5 | 11.5 | 138 | -26.7 | $NaHCO_3$ | C |
| SPFe75B | 70 | 7.9 | 7.6 | 1.3 | 13.0 | 156 | -26.3 | $NaHCO_3$ | C |
| SPFe78B | 129 | 7.9 | 6.5 | 0.6 | 12.7 | 153 | -26.0 | $NaHCO_3$ | C |
| SPFe81B | 351 | 8.0 | 7.7 | 0.6 | 12.5 | 151 | -26.4 | $NaHCO_3$ | C |

| | | | | | | | | | |
|---|---|---|---|---|---|---|---|---|---|
| SPFe82 | 0 | 7.1 | 1.8 | 10.6 | 0.3 | 3 | -32.5 | $KH_2PO_4$ | UC |
| SPFe83 | 8 | 7.0 | 1.2 | 11.5 | 1.8 | 22 | -29.5 | $KH_2PO_4$ | UC |
| SPFe84 | 16 | 7.1 | 3.0 | 9.4 | 3.0 | 37 | -28.0 | $KH_2PO_4$ | UC |
| SPFe85 | 19 | 7.1 | 3.9 | 8.5 | 3.8 | 46 | -27.8 | $KH_2PO_4$ | UC |
| SPFe86 | 22 | 7.1 | 4.4 | 7.7 | 1.3 | 16 | -26.6 | $KH_2PO_4$ | UC |
| SPFe87 | 25 | 7.1 | 5.0 | 7.3 | 4.8 | 57 | -26.9 | $KH_2PO_4$ | UC |
| SPFe88 | 28 | 7.1 | 4.6 | 7.6 | 4.7 | 56 | -26.9 | $KH_2PO_4$ | UC |
| SPFe89 | 31 | 7.2 | 6.4 | 5.7 | 5.3 | 64 | -26.6 | $KH_2PO_4$ | UC |
| SPFe90 | 34 | 7.1 | 7.1 | 6.9 | 5.6 | 68 | -27.1 | $KH_2PO_4$ | UC |
| SPFe91 | 40 | 7.2 | 6.5 | 5.7 | 6.8 | 82 | -26.8 | $KH_2PO_4$ | UC |
| SPFe92 | 43 | 7.2 | 6.7 | 5.5 | 6.0 | 72 | -27.0 | $KH_2PO_4$ | UC |
| SPFe93 | 46 | 7.2 | 6.8 | 6.0 | 6.2 | 75 | -27.1 | $KH_2PO_4$ | UC |
| SPFe94 | 51 | 7.3 | 5.0 | 0.4 | 6.8 | 81 | -26.6 | $KH_2PO_4$ | UC |
| SPFe95 | 57 | 7.2 | 7.0 | 0.8 | 7.1 | 85 | -25.7 | $KH_2PO_4$ | UC |
| SPFe96 | 70 | 7.2 | 7.0 | 0.6 | 7.7 | 93 | -26.5 | $KH_2PO_4$ | UC |
| SPFe97 | 81 | 7.3 | 7.6 | 0.5 | 8.1 | 98 | -26.5 | $KH_2PO_4$ | UC |
| SPFe98 | 93 | 7.3 | 6.7 | 0.6 | 8.7 | 105 | -26.4 | $KH_2PO_4$ | UC |
| SPFe99 | 129 | 7.4 | 5.0 | 0.4 | 9.3 | 111 | -26.6 | $KH_2PO_4$ | UC |
| SPFe100 | 189 | 7.3 | 3.2 | 0.2 | 10.1 | 121 | -26.8 | $KH_2PO_4$ | UC |
| SPFe101 | 273 | 7.3 | 2.5 | 0.2 | 9.0 | 108 | -26.5 | $KH_2PO_4$ | UC |
| SPFe102 | 351 | 7.3 | 2.9 | 0.3 | 10.1 | 121 | -26.4 | $KH_2PO_4$ | UC |
| SPFe84B | 16 | 7.1 | 2.6 | 9.9 | 2.7 | 32 | -27.4 | $KH_2PO_4$ | C |
| SPFe87B | 25 | 7.1 | 4.2 | 8.0 | 4.0 | 48 | -27.2 | $KH_2PO_4$ | C |
| SPFe90B | 34 | 7.1 | 6.9 | 6.7 | 4.9 | 59 | -27.0 | $KH_2PO_4$ | C |
| SPFe93B | 46 | 7.2 | 6.8 | 5.9 | 6.2 | 74 | -26.7 | $KH_2PO_4$ | C |
| SPFe96B | 70 | 7.2 | 7.7 | 0.8 | 8.1 | 97 | -26.0 | $KH_2PO_4$ | C |
| SPFe99B | 129 | 7.2 | 3.1 | 0.5 | 10.1 | 121 | -26.5 | $KH_2PO_4$ | C |
| SPFe102B | 351 | 7.2 | 3.1 | 1.1 | 11.2 | 134 | -26.3 | $KH_2PO_4$ | C |

# Appendix D

## Chemical and Caron Isotope Analyses of Abiotic Study

Table D1: Time (hr) series measurements of DIC (mM, mg C/L), pH, Fe (II)(mM), Fe (III)(mM), and $\delta^{13}C_{DIC}$ (‰) for bicarbonate- & phosphate-buffered conditions. C22: C (Control sample), 22 sample number. Used to plot Figures 4.1 – 4.3, 4.16 – 4.18

| Sample | Time | DIC | DIC | $\delta^{13}C$ | pH | Fe(II) | Fe(III) | Buffer |
|---|---|---|---|---|---|---|---|---|
| C22 | 29 | 2.19 | 26.29 | -5.5 | 8.2 | 0.10 | 15.47 | $NaHCO_3$ |
| C23 | 54 | 1.91 | 22.93 | -0.9 | 8.2 | 0.01 | 14.24 | $NaHCO_3$ |
| C24 | 78 | 2.17 | 26.02 | -3.7 | 8.2 | 0.05 | 14.80 | $NaHCO_3$ |
| C25 | 111 | 2.89 | 34.76 | -7.9 | 8.1 | 0.04 | 14.52 | $NaHCO_3$ |
| C26 | 135 | 2.47 | 29.71 | -7.0 | 8.2 | 0.02 | 15.15 | $NaHCO_3$ |
| C51 | 62 | 1.56 | 26.1 | -0.95 | 7.4 | 1.0 | 1.6 | $NaHCO_3$ |
| C52 | 107 | 1.50 | 25.4 | 0.97 | 7.5 | 0.5 | 10.6 | $NaHCO_3$ |
| C54 | 151 | 4.56 | 62.1 | -14.81 | 7.5 | 0.2 | 10.9 | $NaHCO_3$ |
| C57 | 202 | 4.53 | 61.8 | -14.37 | 7.3 | 1.4 | 10.1 | $NaHCO_3$ |
| C59 | 490 | 6.21 | 82.0 | -18.56 | 7.4 | 1.6 | 13.9 | $NaHCO_3$ |
| C61 | 775 | 7.62 | 98.9 | -17.92 | 7.6 | 2.9 | 15.4 | $NaHCO_3$ |
| C107 | 107 | 0.98 | 11.83 | 0.44 | 8.2 | 0.59 | 11.5 | $NaHCO_3$ |
| C108 | 151 | 0.97 | 11.64 | 3.10 | 8.1 | 0.04 | 8.8 | $NaHCO_3$ |
| C109 | 202 | 2.95 | 35.48 | -13.84 | 8.1 | 1.24 | 7.2 | $NaHCO_3$ |
| C110 | 490 | 4.06 | 48.78 | -17.30 | 8.2 | 1.06 | 12.1 | $NaHCO_3$ |
| C32 | 29 | 1.20 | 14.45 | -35.7 | 6.7 | 0.1 | 15.9 | $KH_2PO_4$ |
| C34 | 78 | 3.62 | 43.53 | - | 6.9 | 0.1 | 14.6 | $KH_2PO_4$ |
| C35 | 111 | 4.45 | 53.40 | - | 6.9 | 0.1 | 15.1 | $KH_2PO_4$ |
| C36 | 135 | 5.72 | 68.70 | -28.7 | 6.9 | 0.2 | 15.4 | $KH_2PO_4$ |
| C63 | 62 | 0.83 | 9.98 | -29.9 | 7.0 | 0.9 | 2.6 | $KH_2PO_4$ |
| C64 | 107 | 2.45 | 29.45 | -31.0 | 7.1 | 0.7 | 9.4 | $KH_2PO_4$ |
| C66 | 151 | 2.90 | 34.87 | -30.2 | 7.0 | 0.4 | 9.1 | $KH_2PO_4$ |
| C70 | 202 | 2.39 | 28.69 | -31.8 | 7.0 | 1.3 | 9.4 | $KH_2PO_4$ |
| C73 | 775 | 10.05 | 120.65 | -31.6 | 7.1 | 2.8 | 17.9 | $KH_2PO_4$ |
| C127 | 107 | 1.3 | 15.9 | - | 7.6 | 0.4 | 13.1 | $KH_2PO_4$ |
| C128 | 151 | 1.3 | 15.5 | - | 7.9 | 0.4 | 9.5 | $KH_2PO_4$ |
| C129 | 202 | 1.3 | 15.6 | - | 7.8 | 1.2 | 7.5 | $KH_2PO_4$ |
| C130 | 490 | 3.2 | 38.8 | - | 7.9 | 0.7 | 17.5 | $KH_2PO_4$ |

Table D2: Time (hr) series measurements of DIC (mM, mg C/L), pH, Fe (II)(mM), Fe (III)(mM), and $\delta^{13}C_{DIC}$ (‰) for bicarbonate- and phosphate-buffered conditions. C22: stands for C (Control sample), 22 time series sample number

| Sample | Time | DIC | DIC | $\delta^{13}C$ | pH | Fe(II) | Fe(III) | Buffer | Remarks |
|---|---|---|---|---|---|---|---|---|---|
| C22 | 29 | 2.19 | 26.29 | -5.5 | 8 | 0.10 | 15.47 | $NaHCO_3$ | UC |
| C23 | 54 | 1.91 | 22.93 | -0.9 | 8.2 | 0.01 | 14.24 | $NaHCO_3$ | UC |
| C24 | 78 | 2.17 | 26.02 | -3.7 | 8.2 | 0.05 | 14.80 | $NaHCO_3$ | UC |
| C25 | 111 | 2.89 | 34.76 | -7.9 | 8.1 | 0.04 | 14.52 | $NaHCO_3$ | UC |
| C26 | 135 | 2.47 | 29.71 | -7.0 | 8.2 | 0.02 | 15.15 | $NaHCO_3$ | UC |
| C51 | 62 | 1.56 | 18.70 | -0.95 | 7.4 | 1.0 | 1.6 | $NaHCO_3$ | UC |
| C52 | 107 | 1.50 | 17.97 | 0.97 | 7.5 | 0.5 | 10.6 | $NaHCO_3$ | UC |
| C54 | 151 | 4.56 | 54.74 | - | 7.5 | 0.2 | 10.9 | $NaHCO_3$ | UC |
| C57 | 202 | 4.53 | 54.38 | - | 7.3 | 1.4 | 10.1 | $NaHCO_3$ | UC |
| C59 | 490 | 6.21 | 74.59 | - | 7.4 | 1.6 | 13.9 | $NaHCO_3$ | UC |
| C61 | 775 | 7.62 | 91.51 | - | 7.6 | 2.9 | 15.4 | $NaHCO_3$ | UC |
| C19 | 713 | 2.36 | 28.40 | -23.4 | 6.7 | - | - | $KH_2PO_4$ | UC |
| C32 | 29 | 1.20 | 14.45 | -35.7 | 6.7 | 0.1 | 15.9 | $KH_2PO_4$ | UC |
| C33 | 54 | 3.56 | 42.77 | -28.4 | 6.8 | 0.0 | 14.9 | $KH_2PO_4$ | UC |
| C34 | 78 | 3.62 | 43.53 | - | 6.9 | 0.1 | 14.6 | $KH_2PO_4$ | UC |
| C35 | 111 | 4.45 | 53.40 | - | 6.9 | 0.1 | 15.1 | $KH_2PO_4$ | UC |
| C36 | 135 | 5.72 | 68.70 | -28.7 | 6.9 | 0.2 | 15.4 | $KH_2PO_4$ | UC |
| C63 | 62 | 0.83 | 9.98 | -29.9 | 7.0 | 0.9 | 2.6 | $KH_2PO_4$ | UC |
| C64 | 107 | 2.45 | 29.45 | -31.0 | 7.1 | 0.7 | 9.4 | $KH_2PO_4$ | UC |
| C66 | 151 | 2.90 | 34.87 | -30.2 | 7.0 | 0.4 | 9.1 | $KH_2PO_4$ | UC |
| C70 | 202 | 2.39 | 28.69 | -31.8 | 7.0 | 1.3 | 9.4 | $KH_2PO_4$ | UC |
| C73 | 775 | 10.05 | 120.65 | -31.6 | 7.1 | 2.8 | 17.9 | $KH_2PO_4$ | UC |

Table D3: Time (hr) series measurements of DIC (mM, mg C/L) for phosphate-buffered condition for investigating sources of carbon in abiotic conditions. Data used for plotting Figure 4.4 and the sample descriptions are given below.

| Sample | Time | DIC | DIC |
|---|---|---|---|
| M-FC1 | 26 | 0.09 | 1.13 |
| M-FC2 | 50 | 0.11 | 1.37 |
| M-FC3 | 74 | 0.09 | 1.13 |
| M-FC4 | 98 | 0.12 | 1.50 |
| M-FC5 | 122 | 0.12 | 1.50 |
| M-FC7 | 2891 | 0.67 | 8.07 |
| M-LAC1 | 26 | 0.25 | 2.96 |
| M-LAC2 | 50 | 0.61 | 7.34 |
| M-LAC3 | 74 | 0.74 | 8.92 |
| M-LAC4 | 98 | 0.55 | 6.61 |
| M-LAC5 | 122 | 0.48 | 5.76 |
| M-LAC6 | 468 | 0.55 | 6.61 |
| M-LAC7 | 2891 | 3.36 | 40.34 |
| M-VITM1 | 26 | 0.25 | 2.96 |
| M-VITM2 | 50 | 0.39 | 4.66 |
| M-VITM3 | 74 | 0.58 | 6.97 |
| M-VITM4 | 98 | 0.68 | 8.19 |
| M-VITM5 | 122 | 0.51 | 6.12 |
| M-VITM7 | 2891 | 2.00 | 24.02 |
| M-MIN1 | 26 | 0.23 | 2.77 |
| M-MIN2 | 50 | 0.46 | 5.51 |
| M-MIN3 | 74 | 0.53 | 6.37 |
| M-MIN4 | 98 | 0.60 | 7.22 |
| M-MIN5 | 122 | 0.64 | 7.70 |
| M-MIN7 | 2891 | 1.66 | 19.96 |
| M-KPO41 | 26 | 0.34 | 4.12 |
| M-KPO42 | 50 | 0.71 | 8.55 |
| M-KPO43 | 74 | 1.24 | 14.89 |
| M-KPO44 | 98 | 1.03 | 12.32 |
| M-KPO45 | 122 | 0.78 | 9.40 |
| M-KPO46 | 468 | 1.07 | 12.82 |
| M-NH4Cl1 | 26 | 0.30 | 3.57 |

| Sample | Time | DIC | DIC |
|---|---|---|---|
| M-NaPO43 | 74 | 0.72 | 8.68 |
| M-NaPO44 | 98 | 0.56 | 6.73 |
| M-NaPO45 | 122 | 0.95 | 11.36 |
| M-NaPO46 | 2891 | 1.92 | 23.10 |
| M-KCl1 | 26 | 0.26 | 3.09 |
| M-KCl2 | 50 | 0.40 | 4.79 |
| M-KCl3 | 74 | 0.94 | 11.23 |
| M-KCl4 | 98 | 1.27 | 15.26 |
| M-KCl5 | 122 | 1.18 | 14.15 |
| M-KCl7 | 2891 | 2.48 | 29.75 |
| M-MNH1 | 175 | 2.75 | 33.06 |
| M-MNH2 | 223 | 2.12 | 25.44 |
| M-MNH4 | 343 | 3.11 | 37.32 |
| M-VMNH1 | 175 | 2.25 | 26.98 |
| M-VMNH2 | 223 | 0.54 | 6.47 |
| M-VMNH4 | 343 | 1.83 | 21.99 |
| DIFC1 | 175 | 21.72 | 260.89 |
| DIFC2 | 223 | 10.49 | 126.01 |
| DIFC3 | 295 | 13.19 | 158.44 |
| DIFC4 | 343 | 13.29 | 159.64 |
| DIFC5 | 391 | 7.72 | 92.75 |
| DILC3 | 295 | 0.22 | 2.59 |
| DILC4 | 343 | 0.20 | 2.40 |
| DICT3 | 295 | 0.42 | 4.99 |
| DICT4 | 343 | 0.26 | 3.14 |

**Legend**

| | |
|---|---|
| M-FC | Media - Ferric Citrate |
| M-LAC | Media - Sodium Lactate |
| M-VITM | Media - Wolfe's Vitamins |
| M-MIN | Media - Wolfe's Minerals |
| M-KPO4 | Media - Potassium Phosphate |
| M-NH4Cl | Media - Ammonium Chloride |

| | | | | | |
|---|---|---|---|---|---|
| M-NH4Cl2 | 50 | 0.32 | 3.81 | M-NaPO4 | Media - Sodium Phosphate |
| M-NH4Cl3 | 74 | 0.77 | 9.28 | M-KCl | Media - Potassium Chloride |
| M-NH4Cl4 | 98 | 0.86 | 10.38 | M-MNH | Media - Minerals & $NH_4Cl$ |
| M-NH4Cl5 | 122 | 0.78 | 9.40 | M-VMNH | Media - Vitamins & $NH_4Cl$ |
| M-NH4Cl7 | 2891 | 2.02 | 24.20 | DIFC | DDI water with Ferric Citrate |
| M-NaPO41 | 26 | 0.27 | 3.20 | DILC | DDI water with Sodium Lactate |
| M-NaPO42 | 50 | 0.34 | 4.05 | DICT | DDI water with Citric acid |

Table D4: Time (hr) series measurements of DIC (mM, mg C/L) and $\delta^{13}C_{DIC}$ (‰) for phosphate-buffered condition. C12: stands for C (Control sample), 12 time series sample number. Used for plotting Figure 4.5

| Sample | Time | DIC | DIC | $\delta^{13}C_{DIC}$ | Fe(III) CPD D |
|---|---|---|---|---|---|
| C12 | 7 | 1.01 | 12.12 | -22.5 | Ferric Citrate |
| C13 | 53 | 1.38 | 16.63 | -13.4 | Ferric Citrate |
| C14 | 117 | 1.27 | 15.24 | -17.0 | Ferric Citrate |
| C19 | 713 | 2.36 | 28.40 | -23.4 | Ferric Citrate |
| C21 | 2199 | 5.28 | 63.36 | -29.9 | Ferric Citrate |
| C32 | 29 | 1.20 | 14.45 | -35.7 | Ferric Citrate |
| C70 | 202 | 2.39 | 28.69 | -31.8 | Ferric Citrate |
| C9 | 1 | 1.71 | 20.53 | -24.3 | HFO |
| C10 | 26 | 2.33 | 27.96 | -11.4 | HFO |
| C11 | 970 | 6.40 | 76.90 | -30.9 | HFO |

Table D5: Time (hr) series measurements of DIC (mM, mg C/L), pH, Fe (II)(mM), Fe (III)(mM), and $\delta^{13}C_{DIC}$ (‰) for bicarbonate-buffered conditions. C22: stands for C (Control sample), 22 time series sample number. Used for Figures 4.12 and 4.13

| Sample | Time | DIC | $DIC^{-1}$ | DIC | $\delta^{13}C$ | pH | Fe(II) | Fe(III) | Buffer | Remarks |
|---|---|---|---|---|---|---|---|---|---|---|
| C22 | 29 | 2.80 | 0.36 | 33.68 | -5.5 | 8.2 | 0.10 | 15.5 | $NaHCO_3$ | UC |
| C23 | 54 | 2.52 | 0.40 | 30.32 | -0.9 | 8.2 | 0.01 | 14.2 | $NaHCO_3$ | UC |
| C24 | 78 | 2.78 | 0.36 | 33.41 | -3.7 | 8.2 | 0.05 | 14.8 | $NaHCO_3$ | UC |
| C25 | 111 | 3.51 | 0.28 | 42.15 | -7.9 | 8.1 | 0.04 | 14.5 | $NaHCO_3$ | UC |
| C26 | 135 | 3.09 | 0.32 | 37.10 | -7.0 | 8.2 | 0.02 | 15.1 | $NaHCO_3$ | UC |

| | | | | | | | | | | |
|---|---|---|---|---|---|---|---|---|---|---|
| C51 | 62 | 2.17 | 0.46 | 26.1 | -0.95 | 7.4 | 0.96 | 1.6 | $NaHCO_3$ | UC |
| C52 | 107 | 2.11 | 0.47 | 25.4 | 0.97 | 7.5 | 0.49 | 10.6 | $NaHCO_3$ | UC |
| C54 | 151 | 5.17 | 0.19 | 62.1 | -14.8 | 7.5 | 0.21 | 10.9 | $NaHCO_3$ | UC |
| C57 | 202 | 5.14 | 0.19 | 61.8 | -14.4 | 7.3 | 1.41 | 10.1 | $NaHCO_3$ | UC |
| C59 | 490 | 6.83 | 0.15 | 82.0 | -18.6 | 7.4 | 1.64 | 13.9 | $NaHCO_3$ | UC |
| C61 | 775 | 8.24 | 0.12 | 98.9 | -17.9 | 7.6 | 2.86 | 15.4 | $NaHCO_3$ | UC |
| C55 | 144 | 7.08 | 0.14 | 85.02 | -29.5 | 5.0 | 0.65 | 18.8 | $NaHCO_3$ | UC |
| C60 | 168 | 8.34 | 0.12 | 100.12 | -31.0 | 5.0 | 0.85 | 18.9 | $NaHCO_3$ | UC |
| C67 | 216 | 11.62 | 0.09 | 139.57 | -36.7 | 5.0 | - | - | $NaHCO_3$ | UC |
| C68 | 312 | 9.21 | 0.11 | 110.59 | -37.9 | 5.0 | 0.80 | 18.1 | $NaHCO_3$ | UC |
| C99 | 107 | 6.92 | 0.14 | 83.15 | -20.6 | 6.4 | 0.99 | 9.4 | $NaHCO_3$ | UC |
| C100 | 151 | 7.53 | 0.13 | 90.44 | -21.5 | 6.4 | 1.64 | 8.3 | $NaHCO_3$ | UC |
| C101 | 202 | 9.10 | 0.11 | 109.29 | -22.3 | 6.5 | 3.27 | 6.5 | $NaHCO_3$ | UC |
| C102 | 490 | 16.35 | 0.06 | 196.41 | -27.0 | 6.6 | 4.79 | 11.3 | $NaHCO_3$ | UC |
| C27 | 29 | 2.20 | 0.45 | 26.42 | 6.3 | 8.1 | 0.09 | 15.2 | $NaHCO_3$ | C |
| C28 | 54 | 1.86 | 0.54 | 22.38 | 7.9 | 8.2 | 0.02 | 13.2 | $NaHCO_3$ | C |
| C29 | 111 | 1.72 | 0.58 | 20.69 | 8.1 | 8.1 | 0.04 | 14.0 | $NaHCO_3$ | C |
| C30 | 223 | 2.08 | 0.48 | 25.02 | 7.9 | 8.2 | 0.03 | 18.0 | $NaHCO_3$ | C |
| C31 | 323 | 2.11 | 0.47 | 25.31 | 9.1 | 8.2 | 0.04 | 15.3 | $NaHCO_3$ | C |
| C53 | 107 | 1.63 | 0.61 | 19.53 | 8.2 | 7.6 | 0.5 | 11.4 | $NaHCO_3$ | C |
| C56 | 151 | 4.18 | 0.24 | 50.15 | -12.9 | 7.5 | 0.1 | 8.5 | $NaHCO_3$ | C |
| C58 | 202 | 4.21 | 0.24 | 50.57 | -12.6 | 7.4 | 1.2 | 6.5 | $NaHCO_3$ | C |
| C62 | 775 | 4.58 | 0.22 | 55.01 | -13.0 | 7.8 | 0.7 | 16.8 | $NaHCO_3$ | C |
| C55B | 144 | 0.44 | 2.28 | 5.27 | -6.8 | 5.0 | 0.6 | 18.7 | $NaHCO_3$ | C |
| C60B | 168 | 2.11 | 0.47 | 25.33 | - | 5.0 | 0.8 | 20.6 | $NaHCO_3$ | C |
| C67B | 216 | 0.05 | 19.70 | 0.61 | - | 5.0 | - | - | $NaHCO_3$ | C |
| C68B | 312 | 2.62 | 0.38 | 31.41 | - | 5.0 | 0.6 | 18.8 | $NaHCO_3$ | C |

Table D6: Time (hr) series measurements of DIC (mM, mg C/L), pH, Fe (II)(mM), Fe (III)(mM), and $\delta^{13}C_{DIC}$ (‰) for phosphate-buffered condition. C12: stands for C (Control sample), 12 time series sample number. Used for Figures 4.14 and 4.15

| Sample | Time | DIC | $DIC^{-1}$ | DIC | $\delta^{13}C$ | Fe(II) | Fe(III) | pH | buffer | Remarks |
|---|---|---|---|---|---|---|---|---|---|---|
| C12 | 7 | 1.01 | 0.99 | 12.12 | -23.3 | - | - | 6.7 | $KH_2PO_4$ | UC |

| | | | | | | | | | | |
|---|---|---|---|---|---|---|---|---|---|---|
| C13 | 53 | 1.38 | 0.72 | 16.63 | -14.0 | - | - | 6.7 | $KH_2PO_4$ | UC |
| C14 | 117 | 1.27 | 0.79 | 15.24 | -17.7 | - | - | 6.7 | $KH_2PO_4$ | UC |
| C19 | 713 | 2.36 | 0.42 | 28.40 | -23.4 | - | - | 6.7 | $KH_2PO_4$ | UC |
| C21 | 2199 | 5.28 | 0.19 | 63.36 | -29.9 | - | - | 6.7 | $KH_2PO_4$ | UC |
| C32 | 29 | 1.20 | 0.83 | 14.45 | -35.7 | 0.1 | 15.9 | 6.7 | $KH_2PO_4$ | UC |
| C33 | 54 | 3.56 | 0.28 | 42.77 | -28.4 | 0.0 | 14.9 | 6.8 | $KH_2PO_4$ | UC |
| C34 | 78 | 3.62 | 0.28 | 43.53 | - | 0.1 | 14.6 | 6.9 | $KH_2PO_4$ | UC |
| C35 | 111 | 4.45 | 0.22 | 53.40 | - | 0.1 | 15.1 | 6.9 | $KH_2PO_4$ | UC |
| C36 | 135 | 5.72 | 0.17 | 68.70 | -28.7 | 0.2 | 15.4 | 6.9 | $KH_2PO_4$ | UC |
| C63 | 62 | 0.83 | 1.20 | 9.98 | -29.9 | 0.9 | 2.6 | 7.0 | $KH_2PO_4$ | UC |
| C64 | 107 | 2.45 | 0.41 | 29.45 | -31.0 | 0.7 | 9.4 | 7.1 | $KH_2PO_4$ | UC |
| C66 | 151 | 2.90 | 0.34 | 34.87 | -30.2 | 0.4 | 9.1 | 7.0 | $KH_2PO_4$ | UC |
| C70 | 202 | 2.39 | 0.42 | 28.69 | -31.8 | 1.3 | 9.4 | 7.0 | $KH_2PO_4$ | UC |
| C73 | 775 | 10.05 | 0.10 | 120.7 | -31.6 | 2.8 | 17.9 | 7.1 | $KH_2PO_4$ | UC |
| C103 | 144 | 6.09 | 0.16 | 73.09 | -32.1 | 0.8 | 18.0 | 5.4 | $KH_2PO_4$ | UC |
| C104 | 168 | 7.29 | 0.14 | 87.58 | 33.0 | 0.9 | 19.2 | 5.6 | $KH_2PO_4$ | UC |
| C105 | 216 | 10.33 | 0.10 | 124.1 | -39.9 | 0.0 | 0.0 | 5.7 | $KH_2PO_4$ | UC |
| C106 | 312 | 11.44 | 0.09 | 137.4 | -41.3 | 1.8 | 17.2 | 5.3 | $KH_2PO_4$ | UC |
| C119 | 107 | 6.57 | 0.15 | 78.90 | 32.1 | 1.6 | 10.1 | 5.8 | $KH_2PO_4$ | UC |
| C120 | 151 | 4.42 | 0.23 | 53.03 | -32.1 | 0.5 | 9.7 | 5.6 | $KH_2PO_4$ | UC |
| C121 | 202 | 6.89 | 0.15 | 82.78 | -30.9 | 1.4 | 10.4 | 5.7 | $KH_2PO_4$ | UC |
| C122 | 490 | 17.54 | 0.06 | 210.6 | -30.2 | 5.4 | 9.0 | 5.7 | $KH_2PO_4$ | UC |
| C37 | 29 | 0.31 | 3.22 | 3.73 | - | 0.1 | 17.6 | 6.7 | $KH_2PO_4$ | C |
| C38 | 54 | 2.02 | 0.49 | 24.30 | -29.4 | 0.0 | 15.0 | 6.7 | $KH_2PO_4$ | C |
| C39 | 111 | 2.11 | 0.47 | 25.31 | -25.8 | 0.1 | 14.2 | 6.8 | $KH_2PO_4$ | C |
| C40 | 223 | 2.34 | 0.43 | 28.08 | -29.1 | 0.1 | 17.2 | 7.0 | $KH_2PO_4$ | C |
| C41 | 323 | 2.80 | 0.36 | 33.63 | -31.5 | 0.1 | 18.5 | 6.9 | $KH_2PO_4$ | C |
| C65 | 107 | 1.53 | 0.65 | 18.38 | -28.3 | 0.5 | 11.4 | 7.0 | $KH_2PO_4$ | C |
| C69 | 151 | 0.21 | 4.74 | 2.53 | -31.4 | 0.1 | 8.5 | 7.0 | $KH_2PO_4$ | C |
| C71 | 202 | 0.24 | 4.22 | 2.85 | -37.9 | 1.2 | 6.5 | 7.0 | $KH_2PO_4$ | C |
| C74 | 775 | 0.53 | 1.88 | 6.37 | -32.1 | 0.7 | 16.8 | 7.1 | $KH_2PO_4$ | C |
| $H2PO4^0$ | 0 | 0.22 | 4.64 | 2.59 | - | - | - | 7.0 | $KH_2PO_4$ | |
| C103B | 144 | 0.35 | 2.88 | 4.18 | - | 0.8 | 19.4 | 5.4 | $KH_2PO_4$ | C |

| | | | | | | | | | | |
|---|---|---|---|---|---|---|---|---|---|---|
| C104B | 168 | 0.45 | 2.23 | 5.40 | - | 0.9 | 18.4 | 5.2 | $KH_2PO_4$ | C |
| C105B | 216 | 0.50 | 2.00 | 6.01 | - | 0.0 | 0.0 | 5.3 | $KH_2PO_4$ | C |
| C106B | 312 | 0.54 | 1.85 | 6.50 | - | 0.7 | 19.1 | 5.1 | $KH_2PO_4$ | C |

Table D7: Time (hr) series measurements of DIC (mM, mg C/L), pH, Fe (II)(mM), Fe (III)(mM), and $\delta^{13}C_{DIC}$ (‰) for bicarbonate-buffered conditions. C22: stands for C (Control sample), 22 time series sample number. Used for Figures 4.8 and 4.9

| Sample | Time | DIC | DIC | $\delta^{13}C$ | pH | Fe(II) | Fe(III) | buffer | Remarks |
|---|---|---|---|---|---|---|---|---|---|
| C22 | 29 | 2.19 | 26.3 | -5.50 | 7.9 | 0.10 | 15.5 | $NaHCO_3$ | UC |
| C23 | 54 | 1.91 | 22.9 | -0.90 | 7.7 | 0.01 | 14.2 | $NaHCO_3$ | UC |
| C24 | 78 | 2.17 | 26.0 | -3.70 | 7.8 | 0.05 | 14.8 | $NaHCO_3$ | UC |
| C25 | 111 | 2.89 | 34.8 | -7.90 | 7.6 | 0.04 | 14.5 | $NaHCO_3$ | UC |
| C26 | 135 | 2.47 | 29.7 | -7.00 | 7.5 | 0.02 | 15.1 | $NaHCO_3$ | UC |
| C51 | 62 | 1.56 | 26.1 | -0.95 | 7.4 | 0.96 | 1.6 | $NaHCO_3$ | UC |
| C52 | 107 | 1.50 | 25.4 | 0.97 | 7.5 | 0.49 | 10.6 | $NaHCO_3$ | UC |
| C54 | 151 | 4.56 | 62.1 | -14.8 | 7.5 | 0.21 | 10.9 | $NaHCO_3$ | UC |
| C57 | 202 | 4.53 | 61.8 | -14.4 | 7.3 | 1.41 | 10.1 | $NaHCO_3$ | UC |
| C59 | 490 | 6.21 | 82.0 | -18.6 | 7.4 | 1.64 | 13.9 | $NaHCO_3$ | UC |
| C61 | 775 | 7.62 | 98.9 | -17.9 | 7.6 | 2.86 | 15.4 | $NaHCO_3$ | UC |
| C55 | 144 | 7.08 | 85.0 | -29.5 | 5.4 | 0.65 | 18.8 | $NaHCO_3$ | UC |
| C60 | 168 | 8.34 | 100.1 | -31.0 | 5.5 | 0.85 | 18.9 | $NaHCO_3$ | UC |
| C67 | 216 | 11.62 | 139.6 | -36.6 | 5.3 | - | - | $NaHCO_3$ | UC |
| C68 | 312 | 9.21 | 110.6 | -37.9 | 5.6 | 0.80 | 18.1 | $NaHCO_3$ | UC |
| C99 | 107 | 6.92 | 83.1 | -20.6 | 6.4 | 0.99 | 9.4 | $NaHCO_3$ | UC |
| C100 | 151 | 7.53 | 90.4 | -21.5 | 6.4 | 1.64 | 8.3 | $NaHCO_3$ | UC |
| C101 | 202 | 9.10 | 109.3 | -22.3 | 6.5 | 3.27 | 6.5 | $NaHCO_3$ | UC |
| C102 | 490 | 16.35 | 196.4 | -27.0 | 6.6 | 4.79 | 11.3 | $NaHCO_3$ | UC |
| C107 | 107 | 1.60 | 19.2 | 0.44 | 8.2 | 0.59 | 11.5 | $NaHCO_3$ | UC |
| C108 | 151 | 1.58 | 19.0 | 3.10 | 8.1 | 0.04 | 8.8 | $NaHCO_3$ | UC |
| C109 | 202 | 3.57 | 42.9 | -13.8 | 8.1 | 1.24 | 7.2 | $NaHCO_3$ | UC |
| C110 | 490 | 4.68 | 56.2 | -17.3 | 8.2 | 1.06 | 12.1 | $NaHCO_3$ | UC |
| C115 | 107 | 2.17 | 26.1 | 1.36 | 8.6 | 0.73 | 11.0 | $NaHCO_3$ | UC |
| C116 | 151 | 2.23 | 26.8 | 3.36 | 8.6 | 0.09 | 8.5 | $NaHCO_3$ | UC |

| | | | | | | | | | |
|---|---|---|---|---|---|---|---|---|---|
| C117 | 202 | 2.42 | 29.0 | 0.02 | 8.6 | 1.19 | 9.3 | $NaHCO_3$ | UC |
| C118 | 490 | 6.60 | 79.3 | -16.4 | 8.5 | 0.74 | 16.4 | $NaHCO_3$ | UC |

Table D8: Time (hr) series measurements of DIC (mM, mg C/L), pH, Fe (II)(mM), Fe (III)(mM), and $\delta^{13}C_{DIC}$ (‰) for phosphate-buffered condition. C12: stands for C (Control sample), 12 time series sample number. Used for Figures 4.10 and 4.11

| Sample | Time | DIC | DIC | $\delta^{13}C$ | Fe(II) | Fe(III) | pH | buffer | Remarks |
|---|---|---|---|---|---|---|---|---|---|
| C12 | 7 | 1.0 | 12.1 | -23.3 | - | - | 6.7 | $KH_2PO_4$ | UC |
| C13 | 53 | 1.4 | 16.6 | -14.0 | - | - | 6.7 | $KH_2PO_4$ | UC |
| C14 | 117 | 1.3 | 15.2 | -17.7 | - | - | 6.7 | $KH_2PO_4$ | UC |
| C32 | 29 | 1.2 | 14.4 | -35.7 | 0.1 | 15.9 | 6.7 | $KH_2PO_4$ | UC |
| C33 | 54 | 3.6 | 42.8 | -28.4 | 0.0 | 14.9 | 6.8 | $KH_2PO_4$ | UC |
| C34 | 78 | 3.6 | 43.5 | - | 0.1 | 14.6 | 6.9 | $KH_2PO_4$ | UC |
| C35 | 111 | 4.4 | 53.4 | - | 0.1 | 15.1 | 6.9 | $KH_2PO_4$ | UC |
| C36 | 135 | 5.7 | 68.7 | -28.7 | 0.2 | 15.4 | 6.9 | $KH_2PO_4$ | UC |
| C63 | 62 | 0.8 | 10.0 | -29.9 | 0.9 | 2.6 | 7.0 | $KH_2PO_4$ | UC |
| C64 | 107 | 2.5 | 29.5 | -31.0 | 0.7 | 9.4 | 7.1 | $KH_2PO_4$ | UC |
| C66 | 151 | 2.9 | 34.9 | -30.2 | 0.4 | 9.1 | 7.0 | $KH_2PO_4$ | UC |
| C70 | 202 | 2.4 | 28.7 | -31.8 | 1.3 | 9.4 | 7.0 | $KH_2PO_4$ | UC |
| C73 | 775 | 10.0 | 120.7 | -31.6 | 2.8 | 17.9 | 7.1 | $KH_2PO_4$ | UC |
| C103 | 144 | 6.1 | 73.1 | -32.1 | 0.8 | 18.0 | 5.4 | $KH_2PO_4$ | UC |
| C104 | 168 | 7.3 | 87.6 | 33.0 | 0.9 | 19.2 | 5.6 | $KH_2PO_4$ | UC |
| C105 | 216 | 10.3 | 124.1 | -39.9 | 0.0 | 0.0 | 5.7 | $KH_2PO_4$ | UC |
| C106 | 312 | 11.4 | 137.4 | -41.3 | 1.8 | 17.2 | 5.3 | $KH_2PO_4$ | UC |
| C119 | 107 | 6.6 | 78.9 | 32.1 | 1.6 | 10.1 | 5.8 | $KH_2PO_4$ | UC |
| C120 | 151 | 4.4 | 53.0 | -32.1 | 0.5 | 9.7 | 5.6 | $KH_2PO_4$ | UC |
| C121 | 202 | 6.9 | 82.8 | -30.9 | 1.4 | 10.4 | 5.7 | $KH_2PO_4$ | UC |
| C122 | 490 | 17.5 | 210.6 | -30.2 | 5.4 | 9.0 | 5.7 | $KH_2PO_4$ | UC |
| C127 | 107 | 1.3 | 15.9 | - | 0.4 | 13.1 | 7.6 | $KH_2PO_4$ | UC |
| C128 | 151 | 1.3 | 15.5 | - | 0.4 | 9.5 | 7.9 | $KH_2PO_4$ | UC |
| C129 | 202 | 1.3 | 15.6 | - | 1.2 | 7.5 | 7.8 | $KH_2PO_4$ | UC |
| C130 | 490 | 3.2 | 38.8 | - | 0.7 | 17.5 | 7.9 | $KH_2PO_4$ | UC |
| C135 | 107 | 0.7 | 7.9 | - | 0.8 | 18.2 | 8.4 | $KH_2PO_4$ | UC |

| | | | | | | | | | |
|---|---|---|---|---|---|---|---|---|---|
| C136 | 151 | 0.8 | 9.7 | - | 0.3 | 9.8 | 8.5 | $KH_2PO_4$ | UC |
| C137 | 202 | 0.8 | 9.3 | - | 1.1 | 9.8 | 8.5 | $KH_2PO_4$ | UC |
| C138 | 490 | 2.0 | 24.3 | - | 0.3 | 26.2 | 8.5 | $KH_2PO_4$ | UC |

Table D9: Time (hr) series measurements of DIC (mM, mg C/L), pH, Fe (II)(mM), Fe (III)(mM), and $\delta^{13}C_{DIC}$ (‰) (C➔ corrected in the bicarbonate, RL➔ Remaining lactate, RF➔ Remaining ferric citrate, *f*➔ fraction remaining) for bicarbonate and phosphate-buffered conditions. C12➔ C (Control sample), 12 ➔ sample number. Used for isotopic mass balance and Rayleigh type model. Representative plots are shown in Figures 4.19 – 4.22.

| Sample | Time | DIC | $DIC_C$ | $DIC^{-1}$ | DIC | $f_{LAC}$ | $f_{FC}$ | $\ln f_{LAC}$ | $\ln f_{FC}$ | $\delta^{13}C$ | $\delta^{13}C_C$ | $\delta^{13}C_{BL}$ | $\delta^{13}C_{RF}$ | pH | Fe(II) | Fe(III) | Buffer | Remarks |
|---|---|---|---|---|---|---|---|---|---|---|---|---|---|---|---|---|---|---|
| $NaHCO_3$ | 0 | 2.00 | | | | | | | | 9.3 | | | | | | | | |
| C22 | 29 | 2.80 | 0.80 | 0.36 | 33.68 | 0.93 | 0.98 | -0.07 | -0.02 | -5.5 | -42.3 | -23.50 | -24.41 | 8.2 | 0.10 | 15.47 | $NaHCO_3$ | UC |
| C23 | 54 | 2.52 | 0.52 | 0.40 | 30.32 | 0.96 | 0.99 | -0.05 | -0.01 | -0.9 | -39.8 | -24.09 | -24.58 | 8.2 | 0.01 | 14.24 | $NaHCO_3$ | UC |
| C24 | 78 | 2.78 | 0.78 | 0.36 | 33.41 | 0.93 | 0.98 | -0.07 | -0.02 | -3.7 | -37.0 | -23.93 | -24.54 | 8.2 | 0.05 | 14.80 | $NaHCO_3$ | UC |
| C25 | 111 | 3.51 | 1.51 | 0.28 | 42.15 | 0.87 | 0.96 | -0.14 | -0.04 | -7.9 | -30.7 | -23.92 | -24.55 | 8.1 | 0.04 | 14.52 | $NaHCO_3$ | UC |
| C26 | 135 | 3.09 | 1.09 | 0.32 | 37.10 | 0.91 | 0.97 | -0.10 | -0.03 | -7.0 | -36.9 | -23.55 | -24.43 | 8.2 | 0.02 | 15.15 | $NaHCO_3$ | UC |
| C54 | 151 | 5.17 | 3.17 | 0.19 | 62.1 | 0.73 | 0.91 | -0.32 | -0.09 | -14.8 | -30.0 | -22.86 | -24.31 | 7.5 | 0.2 | 10.9 | $NaHCO_3$ | UC |
| C57 | 202 | 5.14 | 3.14 | 0.19 | 61.8 | 0.73 | 0.91 | -0.31 | -0.09 | -14.4 | -29.4 | -23.09 | -24.37 | 7.3 | 1.4 | 10.1 | $NaHCO_3$ | UC |
| C59 | 490 | 6.83 | 4.83 | 0.15 | 82.0 | 0.59 | 0.87 | -0.53 | -0.14 | -18.6 | -30.1 | -21.06 | -24.00 | 7.4 | 1.6 | 13.9 | $NaHCO_3$ | UC |
| C61 | 775 | 8.24 | 6.24 | 0.12 | 98.9 | 0.47 | 0.83 | -0.76 | -0.19 | -17.9 | -26.7 | -22.68 | -24.42 | 7.6 | 2.9 | 15.4 | $NaHCO_3$ | UC |
| C12 | 7 | 1.01 | | 0.99 | 12.12 | 0.91 | 0.97 | -0.09 | -0.03 | -23.3 | | -24.94 | -24.84 | 6.7 | - | - | $KH_2PO_4$ | UC |
| C13 | 53 | 1.38 | | 0.72 | 16.63 | 0.88 | 0.96 | -0.13 | -0.04 | -14.0 | | -26.25 | -25.22 | 6.7 | - | - | $KH_2PO_4$ | UC |
| C14 | 117 | 1.27 | | 0.79 | 15.24 | 0.89 | 0.97 | -0.12 | -0.04 | -17.7 | | -25.66 | -25.05 | 6.7 | - | - | $KH_2PO_4$ | UC |
| C19 | 713 | 2.36 | | 0.42 | 28.40 | 0.80 | 0.94 | -0.23 | -0.07 | -23.4 | | -25.16 | -24.90 | 6.7 | - | - | $KH_2PO_4$ | UC |
| C21 | 2199 | 5.28 | | 0.19 | 63.36 | 0.55 | 0.86 | -0.60 | -0.16 | -29.9 | | -20.62 | -23.95 | 6.7 | - | - | $KH_2PO_4$ | UC |
| C32 | 29 | 1.20 | | 0.83 | 14.45 | 0.90 | 0.97 | -0.11 | -0.03 | -35.7 | | -23.55 | -24.43 | 6.7 | 0.1 | 15.9 | $KH_2PO_4$ | UC |

| | | | | | | | | | | | | | | | | |
|---|---|---|---|---|---|---|---|---|---|---|---|---|---|---|---|---|
| C33 | 54 | 3.56 | 0.28 | 42.77 | 0.69 | 0.90 | -0.36 | -0.10 | -28.4 | -23.2 | -24.41 | 6.8 | 0.0 | 14.9 | $KH_2PO_4$ | UC |
| C36 | 135 | 5.72 | 0.17 | 68.70 | 0.51 | 0.84 | -0.67 | -0.17 | -28.7 | -21.05 | -24.08 | 6.9 | 0.2 | 15.4 | $KH_2PO_4$ | UC |
| C63 | 62 | 0.83 | 1.20 | 9.98 | 0.93 | 0.98 | -0.07 | -0.02 | -29.9 | -24.41 | -24.68 | 7.0 | 0.9 | 2.6 | $KH_2PO_4$ | UC |
| C64 | 107 | 2.45 | 0.41 | 29.45 | 0.79 | 0.93 | -0.24 | -0.07 | -31.0 | -23.14 | -24.35 | 0.7 | 9.4 | 7.1 | $KH_2PO_4$ | UC |
| C66 | 151 | 2.90 | 0.34 | 34.87 | 0.75 | 0.92 | -0.29 | -0.08 | -30.2 | -23.00 | -24.33 | 0.4 | 9.1 | 7.0 | $KH_2PO_4$ | UC |
| C70 | 202 | 2.39 | 0.42 | 28.69 | 0.80 | 0.93 | -0.23 | -0.07 | -31.8 | -22.99 | -24.31 | 1.3 | 9.4 | 7.0 | $KH_2PO_4$ | UC |
| C73 | 775 | 10.05 | 0.10 | 120.7 | 0.14 | 0.73 | -1.97 | -0.32 | -31.6 | 17.52 | -22.22 | 2.8 | 17.9 | 7.1 | $KH_2PO_4$ | UC |

| | |
|---|---|
| DIC expected of Lactate(mM) | 11.7 |
| DIC expected of Citrate (mM) | 25 |
| DIC expected of Lactate + Citrate(mM) | 36.7 |
| Starting $\delta^{13}C$ (‰) | -25 |

# Appendix E

## Statistical Analyses of Selected Experimental Data Both for Biotic and Abiotic Studies

## Statistical Analyses of Selected Experimental Data

Both microbially mediated and abiotic experimental samples were treated statistically to compare the effect of light for both bicarbonate and phosphate buffered at neutral pH. F-test and student t-test were used for comparing variances and means of the samples. Detailed of each analyses are given in the subsequent tables associated with null hypothesis testing in each case.

F-Test: This test is used to test the equality of variances based on a probability distribution of two samples by randomly sampling a normal population and calculating the ratio of sample variances. Both Fe(II) and DIC were compared. Here the hypothesis to be tested is:

$H_0$: $\sigma^2_C = \sigma^2_{UC}$

$H_1$: $\sigma^2_C \neq \sigma^2_{UC}$

The null hypothesis states that the parent populations of the two samples have equal variances; the alternative hypothesis states that they do not. The degrees of freedom associated with this test are $(n_C - 1)$ for $\nu_C$ and $(n_{UC} - 1)$ for $\nu_{UC}$. The critical values of F associated with each degree of freedom and level of significance of 5% ($\alpha$=0.05) can be found from any F-distribution tables. In each case, if the F critical is less than the calculated values, the null hypothesis will be rejected and can be concluded that the variation in results from the two experimental set ups are not the same. If the calculated value is less than the F critical, we would have no evidence for concluding that the variances are different.

If the variances are not significantly different, the next step in the procedure is to test the equality of means. The appropriate test is the student t-test and the level of significance attached to this test should not be higher than the significance attached to the test of equality of variances. Tests called the t-test and based on the probability distribution, are useful for testing hypotheses about the equivalency of two samples (covered vs. uncovered) with regard to [Fe(II)] and DIC. The appropriate hypothesis and alternative tests are:

$$H_0: \mu^2_C = \mu^2_{UC}$$

$$H_1: \mu^2_C \neq \mu^2_{UC}$$

If the hypothesis rejects for the equality of variances, there is no need to test for t-test with the assumption of equality of variance. So, the appropriate test for the equality of means would be assuming the inequality of variances.

1. Microbial mediated experiments on comparison of effect of light for both bicarbonate and phosphate systems at circum-neutral pH conditions. The following tables represent the analyses of the two systems using both F-test and student t-test methods (Data table is shown in Appendix C: table C1).

Table E1 F-Test Two-Sample for Variances Fe(II) Bicarbonate

| | ***Uncovered*** | ***Covered*** |
|---|---|---|
| Mean | 5.99 | 6.57 |
| Variance | 2.92 | 1.02 |
| Observations | 21 | 7 |
| df | 20 | 6 |

| | |
|---|---|
| F | 2.85 |
| P(F<=f) one-tail | 0.10 |
| F Critical one-tail | 3.87 |

Here in the above table it is shown that $F_{Calc} < F_{Crit}$ ➔ The null hypothesis does not reject the equivalence of the variances

Table E2 t-Test: Two-Sample Assuming Equal Variances Fe (II) Bicarbonate

| | ***Uncovered*** | ***Covered*** |
|---|---|---|
| Mean | 5.993 | 6.567 |
| Variance | 2.917 | 1.023 |
| Observations | 21 | 7 |
| Pooled Variance | 2.480 | |
| Hypothesized Mean Difference | 0 | |
| df | 26 | |
| t Stat | -0.835 | |
| P(T<=t) one-tail | 0.206 | |
| t Critical one-tail | 1.706 | |
| P(T<=t) two-tail | 0.411 | |
| t Critical two-tail | 2.056 | |

Here in the above table it is shown that $t_{Calc} < t_{Crit}$ ➔ The null hypothesis is accepted and the two sample (covered and uncovered) are not significantly different at significance level of 5% with respect to ferrous iron

Table E3 F-Test Two-Sample for Variances in DIC Bicarbonate

| | ***Uncovered*** | ***Covered*** |
|---|---|---|
| Mean | 9.774 | 10.303 |
| Variance | 13.845 | 10.340 |
| Observations | 21 | 7 |
| df | 20 | 6 |
| F | 1.339 | |
| P(F<=f) one-tail | 0.381 | |

| F Critical one-tail | 3.874 |
|---|---|

Here in the above table it is shown that $F_{Calc} < F_{Crit}$ ➔ The null hypothesis does not reject the equivalence of the variances

Table E4 t-Test: Two-Sample Assuming Equal Variances DIC Bicarbonate

| | ***Uncovered*** | ***Covered*** |
|---|---|---|
| Mean | 9.774 | 10.303 |
| Variance | 13.845 | 10.340 |
| Observations | 21 | 7 |
| Pooled Variance | 13.036 | |
| Hypothesized Mean Difference | 0 | |
| df | 26 | |
| t Stat | -0.336 | |
| P(T<=t) one-tail | 0.370 | |
| t Critical one-tail | 1.706 | |
| P(T<=t) two-tail | 0.740 | |
| t Critical two-tail | 2.056 | |

Here in the above table it is shown that $t_{Calc} < t_{Crit}$ ➔ The null hypothesis is accepted and the two sample (covered and uncovered) are not significantly different at significance level of 5% with respect to DIC

Table E5 F-Test Two-Sample for Variances of Fe(II) (Phosphate)

| | ***Uncovered*** | ***Covered*** |
|---|---|---|
| Mean | 4.962 | 4.923 |
| Variance | 3.885 | 4.707 |
| Observations | 21 | 7 |
| df | 20 | 6 |
| F | 0.825 | |
| P(F<=f) one-tail | 0.341 | |
| F Critical one-tail | 0.385 | |

Here in the above table it is shown that $F_{Calc} < F_{Crit}$ ➔ The null hypothesis does not reject the equivalence of the variances

Table E6 t-Test: Two-Sample Assuming Unequal Variances Fe(II) Phosphate

| | ***Uncovered*** | ***Covered*** |
|---|---|---|
| Mean | 4.962 | 4.923 |
| Variance | 3.885 | 4.707 |
| Observations | 21 | 7 |
| Hypothesized Mean Difference | 0 | |
| df | 10 | |
| t Stat | 0.042 | |
| P(T<=t) one-tail | 0.484 | |
| t Critical one-tail | 1.812 | |
| P(T<=t) two-tail | 0.967 | |
| t Critical two-tail | 2.228 | |

Here in the above table it is shown that $t_{Calc} < t_{Crit}$ ➔ The null hypothesis is accepted and the two sample (covered and uncovered) are not significantly different at significance level of 5% with respect to ferrous iron

Table E7 F-Test Two-Sample for Variances of DIC (Phosphate)

| | ***Uncovered*** | ***Covered*** |
|---|---|---|
| Mean | 6.026 | 6.737 |
| Variance | 7.961 | 10.014 |
| Observations | 21 | 7 |
| df | 20 | 6 |
| F | 0.795 | |
| P(F<=f) one-tail | 0.320 | |
| F Critical one-tail | 0.385 | |

Here in the above table it is shown that $F_{Calc} > F_{Crit}$ ➔ The null hypothesis rejects the equivalence of the variances

Table E8 t-Test: Two-Sample Assuming Unequal Variances-Phosphate DIC

| | ***Uncovered*** | ***Covered*** |
|---|---|---|
| Mean | 6.026 | 6.737 |
| Variance | 7.961 | 10.014 |
| Observations | 21 | 7 |
| Hypothesized Mean Difference | 0 | |
| df | 9 | |
| t Stat | -0.528 | |
| P(T<=t) one-tail | 0.305 | |
| t Critical one-tail | 1.833 | |
| P(T<=t) two-tail | 0.610 | |
| t Critical two-tail | 2.262 | |

Here in the above table it is shown that $t_{Calc} < t_{Crit}$ ➔ The null hypothesis is accepted and the two sample (covered and uncovered) are not significantly different at significance level of 5% with respect to DIC

Table E9 F-Test Two-Sample for Variances Fe(II)
(Phosphate and Bicarbonate Combined)

| | ***Uncovered*** | ***Covered*** |
|---|---|---|
| Mean | 5.478 | 5.745 |
| Variance | 3.590 | 3.373 |
| Observations | 42 | 14 |
| df | 41 | 13 |
| F | 1.064 | |
| P(F<=f) one-tail | 0.477 | |
| F Critical one-tail | 2.336 | |

Here in the above table it is shown that $F_{Calc} < F_{Crit}$ ➔ The null hypothesis is accepted and the two variances (covered and uncovered) are not significantly different at significance level of 5% with respect to ferrous iron

Table E10 t-Test: Two-Sample Assuming Equal Variances Fe(II)
(Combined Bicarbonate and Phosphate)

| | ***Uncovered*** | ***Covered*** |
|---|---|---|
| Mean | 5.478 | 5.745 |
| Variance | 3.590 | 3.373 |
| Observations | 42 | 14 |
| Pooled Variance | 3.538 | |
| Hypothesized Mean Difference | 0 | |
| df | 54 | |
| t Stat | -0.461 | |
| P(T<=t) one-tail | 0.323 | |
| t Critical one-tail | 1.674 | |
| P(T<=t) two-tail | 0.647 | |
| t Critical two-tail | 2.005 | |

Here in the above table it is shown that $t_{Calc} < t_{Crit}$ ➔ The null hypothesis is accepted and the two sample (covered and uncovered) are not significantly different at significance level of 5% with respect to ferrous iron

Table E11 F-Test Two-Sample for Variances DIC
(Phosphate and Bicarbonate Combined)

| | ***Uncovered*** | ***Covered*** |
|---|---|---|
| Mean | 7.900 | 8.520 |
| Variance | 14.236 | 12.819 |
| Observations | 42 | 14 |
| df | 41 | 13 |
| F | 1.111 | |
| P(F<=f) one-tail | 0.440 | |
| F Critical one-tail | 2.336 | |

Here in the above table it is shown that $F_{Calc} < F_{Crit}$ ➔ The null hypothesis is accepted and the two variances (covered and uncovered) are not significantly different at significance level of 5% with respect to DIC

Table E12 t-Test: Two-Sample Assuming Equal Variances DIC (Combined Bicarbonate and Phosphate)

| | ***Uncovered*** | ***Covered*** |
|---|---|---|
| Mean | 7.900 | 8.520 |
| Variance | 14.236 | 12.819 |
| Observations | 42 | 14 |
| Pooled Variance | 13.895 | |
| Hypothesized Mean Difference | 0 | |
| df | 54 | |
| t Stat | -0.539 | |
| P(T<=t) one-tail | 0.296 | |
| t Critical one-tail | 1.674 | |
| P(T<=t) two-tail | 0.592 | |
| t Critical two-tail | 2.005 | |

Here in the above table it is shown that $t_{Calc} < t_{Crit}$ ➔ The null hypothesis is accepted and the two sample (covered and uncovered) are not significantly different at significance level of 5% with respect to DIC

2. Abiotic statistical analyses were done to compare effect of buffer condition at neutral pH conditions. The above principles F- and t- test distributions studies were used in the comparison.

Table E13 F-Test Two-Sample for Variances for DIC

| | ***Bicarbonate*** | ***Phosphate*** |
|---|---|---|
| Mean | 3.42 | 3.23 |
| Variance | 4.166 | 5.915 |
| Observations | 11 | 15 |
| df | 10 | 14 |

| | |
|---|---|
| F | 0.70439 |
| P(F<=f) one-tail | 0.29249 |
| F Critical one-tail | 0.34907 |

$\alpha = 0.05$

Here in the above table it is shown that $F_{Calc} < F_{Crit}$ ➔ The null hypothesis is accepted and the two variances (covered and uncovered) are not significantly different at significance level of 5% with respect to DIC

Table E14 t-Test: Two-Sample Assuming Unequal Variances for DIC

| | ***Bicarbonate*** | ***Phosphate*** |
|---|---|---|
| Mean | 3.418 | 3.232 |
| Variance | 4.1661 | 5.9145 |
| Observations | 11.000 | 15 |
| Hypothesized Mean Difference | 0 | |
| df | 23 | |
| t Stat | 0.212 | |
| P(T<=t) one-tail | 0.417 | |
| t Critical one-tail | 1.714 | |
| P(T<=t) two-tail | 0.834 | |
| t Critical two-tail | 2.069 | |

$\alpha = 0.05$

Here in the above table it is shown that $t_{Calc} < t_{Crit}$ ➔ The null hypothesis is accepted and the two sample (Bicarbonate and Phosphate) are not significantly different at significance level of 5% with respect to DIC

Table E15 F-Test Two-Sample for Variances Fe(II)

| | ***Bicarbonate*** | ***Phosphate*** |
|---|---|---|
| Mean | 0.769 | 0.736 |
| Variance | 0.907 | 0.812 |
| Observations | 10 | 9 |
| df | 9 | 8 |

| | |
|---|---|
| F | 1.117 |
| P(F<=f) one-tail | 0.444 |
| F Critical one-tail | 3.388 |

$\alpha = 0.05$

Here in the above table it is shown that $F_{Calc} < F_{Crit}$ ➔ The null hypothesis is accepted and the two variances (Bicarbonate and Phosphate) are not significantly different at significance level of 5% with respect to ferrous iron

Table E16 t-Test: Two-Sample Assuming Equal Variances Fe(II)

| | ***Bicarbonate*** | ***Phosphate*** |
|---|---|---|
| Mean | 0.77 | 0.74 |
| Variance | 0.9069 | 0.8122 |
| Observations | 10 | 9 |
| Pooled Variance | 0.8624 | |
| Hypothesized Mean Difference | 0 | |
| df | 17 | |
| t Stat | 0.07860 | |
| P(T<=t) one-tail | 0.46913 | |
| t Critical one-tail | 1.73961 | |
| P(T<=t) two-tail | 0.93827 | |
| t Critical two-tail | 2.10982 | |

$\alpha = 0.05$

Here in the above table it is shown that $t_{Calc} < t_{Crit}$ ➔ The null hypothesis is accepted and the two sample (Bicarbonate and Phosphate) are not significantly different at significance level of 5% with respect to ferrous iron

# BIBLIOGRAPHY

Abrahamson HB, Rezvani AB, Brushmiller JG (1994): Photochemical and spectroscopic studies of complexes of iron(III) with citric acid and other carboxylic acids, *Inorganic Chimica Acta* **226**, 117–127

Adamson AW, Waltz WL, Zinato E, Watts DW, Fleischauer PD, Lindholm R D (1968) Photochemistry of transition-metal coordination compounds, *Chemical Review* **68**, 541-543

Atekwana EA, Krishnamurthy RV (1998) Investigations of inorganic carbon cycling of some natural waters using a modified gas evolution technique, *Journal of Hydrology* **205**, 265-278

Busset C, Mazellier P, Sarakha M, De Laat J (2007) Photochemical generation of carbonate radicals and their reactivity with phenol, *Journal of Photochemistry and Photobiology A: Chemistry*, **185**, 127–132

Calza P, Maurino V, Minero C, Pelizzetti E, Sega M, Vincenti M (2005) Photoinduced halophenol formation in the presence of iron(III) species or cadmium sulfide, *Journal of Photochemistry and Photobiology A, Chemistry* **170**, 61–67

Chatterjee D and Dasgupta S (2005), Review: Visible light induced photocatalytic degradation of organic pollutants, *Journal of Photochemistry and Photobiology C: Photochemistry Reviews* **6**, 186–205

Chiron S, Minero C, Vione DE (2006) Photodegradation Processes of the Antiepileptic Drug Carbamazepine Relevant To Estuarine Waters, *Environmental Science & Technology* **40**, 5977–5983

Canonica S, Kohn T, Mac M, Real FJ, Wirz J, von Gunten U (2005) Photosensitizer Method to Determine Rate Constants for the Reaction of Carbonate Radical with Organic Compounds, *Environmental Science & Technology* **39**, 9182–9188

Dansgaard W (1964) Stable isotopes in precipitation, *Tellus*, **XVI**: 436–468.

Deng NS, Wu F, Luo F, Xiao M (1998) Ferric citrate induced photodegradation of dyes in aqueous solutions, *Chemosphere* **36**, 3101–3112

DiChristina TJ, DeLong EF (1994) Isolation of anaerobic respiratory, Mutants of *Shewanella putrefaciens* and genetic analysis of mutants deficient in anaerobic growth on Fe (III), *Journal of Bacteriology* **176,** 1468–1474.

DiChristina TJ, Moore CM, Haller CA (2002) Dissimilatory Fe(III) and Mn(IV) reduction by *Shewanella putrefaciens* requires ferE, a homolog of the pulE (gspE) type II protein secretion gene, *Journal of Bacteriology* **184**, 142– 151.

Fischer M, Warneck P, (1996) Photodecomposition of nitrite and undissociated nitrous acid in aqueous solution, *Journal of Physical Chemistry* **100**, 18749–18756

Fredrickson JK, Zachara JM, Kennedy DW, Dong H, Onstott TC, Hinman NW (1998) Biogenic iron mineralization accompanying the dissimilatory reduction of hydrous ferric oxide by a groundwater bacterium, *Geochimica et Cosmochimica Act* **62**, 3239–3257.

Fredrickson JK, Kota S, Kukkadapu RK, Liu C, Zachara JM (2003) Influence of electron donor/acceptor concentrations on hydrous ferric oxide (HFO) Bioreduction, *Biodegradation **14***, 91-103.

Grundl TJ, Sparks DL, (1998) Kinetics and mechanisms of reactions at the mineral–water interface: an overview. In: Sparks DL, Grundl TJ (eds) Mineral–water interfacial reactions: kinetics and mechamisms. *American Chemical Society*, Washington, District of Columbia, 2–13

Haas JR, DiChristina, TJ, Wade Jr. R (2001) Thermodynamics of U(VI) sorption onto *Shewanella putrefaciens*, *Chemical Geology* **180**, 33–54.

Haas JR, DiChristina, TJ (2002) Effects of Fe(III) chemical speciation on Dissimilatory Fe(III) reduction by *Shewanella putrefaciens, Environmental Science and Technology* **36**, 373-380.

Hansel C, Benner S, Nico P, Fendorf S (2004) Structural constraints of ferric (hydr) oxides on dissimilatory iron reduction and the fate of Fe (II). *Geochimica et Cosmochimica. Acta* **68**, 3217-3229.

Hoigne J, Bader H (1978), Ozonation of Water: Kinetics of Oxidation of Ammonia by Ozone and Hydroxyl Radicals, *Environmental Science and Technology* **12**(1), 79-

84.

Howsawkeng J, Watts R, Washington D, Teel A, Hess T, Crawford R (2001) Evidence for simultaneous abiotic-biotic oxidations in a microbial-Fenton's system, *Environmental Science & Technology* **35**, 2961-2966

Kappler A, Straub KL (2005) Geomicrobiological Cycling of Iron, *Reviews in Mineralogy and Geochemistry* **59,** 85-108

Kormann C, Bahnemann DW, Hoffamnn MR (1989) Environmental photochemistry: is iron oxide (Hematite) an active photocatalyst? A Comparative study: $\alpha$-$Fe_2O_3$, ZnO, $TiO_2$, *Journal of Photochemistry and Photobiology A, Chemistry* **48**, 161-169

Krishnamurthy RV, Atekwana EA, Guha H (1997) A simple, Inexpensive Carbonate-Phosphoric Acid Reaction Method for the Analysis of Carbon and Oxygen Isotopes of Carbonates, *Analytical Chemistry* **69**, 4256-4258

Li F, Chen J, Liu C, Dong J, Liu T (2006) Original paper: Effect of iron oxides and carboxylic acids on photochemical degradation of bisphenol A, *Biol Fertil Soils* **42**, 409–417

Liu C, Zachara J, Gorby Y, Szecsody J, Brown C (2001) Microbial reduction of Fe (III) and sorption/precipitation of Fe (II) on *Shewanella putrefaciens* strain CN32, *Environmental Science and Technology* **35**, 1385-1393.

Lovley DR, Phillips EJ (1988) Novel mode of microbial energy metabolism: organic carbon oxidation coupled to dissimilatory reduction of iron and manganese, *Applied Environmental Microbiology* **54,** 1472–1480.

Lovley DR (1991) Dissimilatory Fe (III) and Mn (IV) reduction, *Microbiology Review* **55,** 259–287

Lovley DR (1993) Dissimilatory metal reduction, *Annual Reviews in Microbiology* **47,** 263–290

Mariotti A, Germon JC, Hubert P, Kaiser P, Letolle T, Tardieux A, Tardieux P (1981) Experimental determination of nitrogen kinetic isotope fractionation: some principles; illustration for the denitrification and nitrification processes, *Plant and Soil* **62,** 413–430.

Meeroff DE, Englehardt JD, Echegoyen LA and Shibata T (2006) Iron-Mediated Aeration: Evaluation of Energy-Assisted Enhancement for In Situ Subsurface Remediation, *Journal of Environmental Engineering* **132**, 747 - 757

Minero C, Lucchiari M, Vione D, Maurino V (2005) "Fe III-Enhanced Sonochemical Degradation of Methylene Blue in Aqueous Solution, *Environ Sci. Technol* **39**(22), 8936–8942

Minero C, Bono F, Rubertelli F, Pavino D, Maurino V, Pelizzetti E, Vione D (2007) On the effect of pH in aromatic photonitration upon nitrate photolysis, *Chemosphere* **66**, 650–656

Mook WG, Bommerson JC, Staverman WH (1974) Carbon isotope fractionation between dissolved bicarbonate and gaseous carbon dioxide, *Earth and Planetary Science Lett*er **22**, 169–176.

Myers CR, Myers JM (1997) Outer membrane cytochromes of *Shewanella putrefaciens* MR-1: spectral analysis, and purification of the 83-kDa *c*-type cytochromes, *Biochimica et Biophysica Acta* **1326,** 307–318.

Nascimento C, Atekwana EA, Krishnamurthy RV (1997) Concentrations and isotopes of dissolved inorganic carbon in denitrifying environments, *Geophysical Research Letters* **24** (12), 1511 – 1514

Nealson KH, Belz A, McKee B (2002) breathing metals as a way of life: geobiology in action, *Antonie van Leeuwenhoek* **81**, 215–222.

Northup A, Cassidy D (2007) Evidence for the production of surfactants accompanying the chemical oxidation of hydrocarbons in soils, *Journal of Advanced Oxidation Technologies* **10**(1), 137 – 143

Ndjou'ou AC, Cassidy D (2006) Surfactant production accompanying the modified Fenton oxidation of hydrocarbons in soil, Chemosphere **65**, 1611 – 1615

Penning H, Tyler SC, Conard R (2006) Determination of isotope fractionation factors and quantification of carbon flow by stable carbon isotope signatures in a methanogenic rice root model system *Geobiology* **4**, 109–121.

Penning H, Conrad R (2006) Carbon isotope effects associated with mixed-acid fermentation of saccharides by Clostridium papyrosolvens, *Geochimica et Cosmochimica Acta* **70**, 2283-2297

Pignatello JJ, Oliveros E, Mackay A (2006) Advanced Oxidation Processes for Organic Contaminant Destruction Based on the Fenton Reaction and Related Chemistry, *Critical Reviews in Environmental Science and Technology* **36**, 1-84

Roden EE (2003) Fe(III) oxide reactivity toward biological versus chemical reduction, *Environmental Science and Technology* **37**, 1319-1324.

Roden EE, Wetzel RG (2003) Competition between Fe(III)-reducing and methanogenic bacteria for acetate in iron-rich freshwater sediments, *Microbial Ecology* **45**, 252 – 258

Roden EE (2004) Analysis of long-term bacterial vs. chemical Fe(III) oxide reduction kinetics, *Geochimica et Cosmochimica Acta* **68**, 3205-3216.

Romanek CS, Zhang CL, Li, Hornito J, Vail H, Cole DR, Phelps TJ (2003) Carbon and hydrogen isotope fractionations associated with dissimilatory iron-reducing bacteria, *Chemical Geology* **195**, 5 – 16.

Schwertmann U, Cornell RM (2000) Iron Oxides in the Laboratory, Preparation and characterization. Wiley-VCH, Weinheim, 188p

Sokolov I, Smith DS, Henderson GS, Gorby YA, Ferris FG (2001) Cell Surface Electrochemical Heterogeneity of the Fe (III)-Reducing Bacteria *Shewanella putrefaciens, Environmental Science and Technology* **35**, 341-347.

Somsamak P, Richnow HH, Haggblom MM (2006) Carbon Isotope Fractionation during Anaerobic Degradation of Methyl *tert*-Butyl Ether under Sulfate-Reducing and Methanogenic Conditions, *Applied and Environmental Microbiology* **72**, 1157–1163.

Spence MJ, Bottrell SH, Thornton SF, Richnow HH, Spence KH (2005) Hydrochemical and isotopic effects associated with petroleum fuel biodegradation pathways in a chalk aquifer, *Journal of Contaminant Hydrology* **79**, 67– 88.

Straub KL, Benz M, Schink B (2001) Iron metabolism in anoxic environments at near neutral pH: *FEMS Microbiology Ecology* **34**, 181-186.

Teece MA, Fogel ML, Dollhopf ME, Nealson KH (1999) Isotopic fractionation associated with biosynthesis of fatty acids by a marine bacterium under oxic and anoxic conditions, *Organic Geochemistry* **30**, 1571– 1579.

Viollier E, Inglett PW, Hunter K, Roychoudhury AN, Van Cappellen P (2000) The ferrozine method revisited: Fe(II)/Fe(III) determination in natural waters, *Applied Geochemistry* **15**, 785-790

Vione D, Maurino V, Minero C, Calza P, Pelizzetti E (2005) Phenol chlorination and photochlorination in the presence of chloride ions in homogeneous aqueous solution, *Environmental Science & Technology* **39**, 5066–5075

Vione D, Maurino V, Minero C, Pelizzetti E, Harrison MAJ, Olariu RI, Arsene C (2006) Photochemical reactions in the tropospheric aqueous phase and on particulate matter, *Chemical Society Reviews* **35**, 441 – 453

Warren LA, Haack EA (2001) Biogeochemical controls on metal behavior in freshwater environments, *Earth-science reviews* **54**, 261 – 320

Watts RJ, Dilly SE (1996) Evaluation iron catalysts for the Fenton-like Remediation of Diesel-contaminated soils, *Journal of Hazardous Materials* **51,** 109 – 124

Wu F, Deng NS (2000) Photochemistry of hydrolytic iron (III) species and photoinduced degradation of organic compounds, A mini-review, *Chemosphere* **41**, 1137–1147

Zachara J, Fredrickson J, Li S, Kennedy D, Smith S, Gassman P (1998) Bacterial reduction of crystalline $Fe^{3+}$ oxides in single phase suspensions and subsurface materials, *American Mineralogist* **83**, 1426-1443.

Zachara J, Kukkadapu R, Fredrickson J, Gorby Y, Smith S (2002) Biomineralization of poorly crystalline Fe(III) oxides by dissimilatory metal reducing bacteria (DMRB)., *Geomicrobiological Journal* ***19***, 179-207.

Zhang CL, Hornito J, Cole DR, Zhou J, Lovely DR, Phelps TJ (2001) Temperature - dependent oxygen and carbon isotope fractionations of biogenic siderite, *Geochimica et Cosmochimica Acta* **65**, 2257–2271.

Zhang CL, Li Y, Ye Q, Fong J, Peacock AD, Blunt E, Fang J, Lovely DR, White DC (2003) Carbon isotope signatures of fatty acids in Geobacter metallireducens and Shewanella algae, *Chemical Geology* **195**, 17– 28.

Zhang C, Wang L, Wu F, Deng N (2006) Quantitation of Hydroxyl Radicals from Photolysis of Fe(III)-Citrate Complexes in Aerobic Water, *Environ Science & Pollution Research* **13** (3), 156 – 160